UTRECHT UNIVERSITY,
FACULTY OF GEOSCIENCES

MSC THESIS EARTH SURFACE AND WATER

Effects of mud, *Spartina anglica* and *Zostera marina* on large scale morphodynamics in a tide-dominated estuary

Author:
I.R. Lokhorst

Student ID:
3711064

Email:
i.r.lokhorst@uu.nl

Supervisors:
Prof. Dr. M.G. Kleinhans (UU)
Dr. S. Selakovic (UU)

Final version: 16-11-2016

Preface

This thesis ”Effects of mud, *Spartina anglica*, and *Zostera marina* on large scale morphodynamics in a tide-dominated estuary” has been written as final assignment to fulfil the graduation requirements of my masters program Earth Surface and Water. The thesis was written at Utrecht University from July till December 2016.

The thesis was undertaken in the larger context of the research on biomorphodynamics by the group of Maarten Kleinhans. Together with Maarten Kleinhans I formulated the research question and objectives which were later on refined with help from Sanja Selakovic. The research learned me to use Delft3D modelling and to work with the state of the art vegetation model by Mijke van Oorschot.

I would like to thank my supervisors Maarten Kleinhans and Sanja Selakovic for their help with my research and the fruitful discussions. Also I would like to thank Mijke van Oorschot and Lisanne Braat for their help with the models I used.

I would like to thank my fellow MSc students Steven Weisscher, Erik van Onselen and especially Bente de Vries for the useful discussions about my research and the GEO ICT support for helping me with malfunctioning computers. A huge thank you goes to my father for proof-reading my thesis twice. Finally I would like to thank my room-mates who helped to cheer me up when I was stuck.

I truly hope you enjoy the read.

Ivar Lokhorst

Utrecht, November 16, 2016

Abstract

Estuaries are morphodynamically active regions where tidal and river currents together with (cohesive) sediment and vegetation create patterns of channels, shoals, mud flats and salt marshes. The effects of mud and vegetation have mainly been studied on a local scale and their effects on the large scale morphological development of estuaries on the long term is unknown. Classic numerical models are unable to produce realistic vegetation patterns and cannot take into account their influence on estuary morphodynamics. Recent advances in modelling, however, made it possible to integrate dynamic vegetation models with advanced numerical morphodynamic models. The objective of this study is to use a computer model to assess effects of mud and vegetation on estuary hydro-morphodynamics.

A numerical model which combines dynamic intertidal and submerged vegetation with morphodynamics is developed. The dynamic vegetation module incorporates vegetation colonization, mortality due to scour, uprooting, burial, dessication, flooding and light attenuation and it adjusts the hydrodynamics through flow resistance and thus affects morphodynamics as well. The development of two vegetation species, *Spartina anglica* and *Zostera marina*, and their effect on estuary morphodynamics, has been modelled for 50 years in a hypothetical tide-dominated estuary with sand and mud.

When mud is modelled without vegetation it accumulates predominantly on the edges of the estuary. Due to its cohesiveness it limits channel movements and decreases the braiding index in the estuary.

Spartina anglica colonizes shoals and the intertidal area on the edges of the estuary, where it drives rapid sedimentation. Because *Spartina* increases the flow resistance in the intertidal area it decreases flow velocity and stabilizes the intertidal area if it is naturally prone to erosion. When the intertidal area is not prone to erosion, however, *Spartina* might actually cause erosion of the intertidal area because it increases the flow velocity on its patch edges. The decreased flow velocity in the *Spartina* marshes causes an increase in flow velocity in the deeper parts of the estuary. Dependent on the initial estuary bathymetry the increased flow velocity in the deeper parts of the estuary might drive channel deepening.

Zostera marina is difficult to model properly due to its flexible nature and the need for a specific colonization module. Advances have been made in modelling *Zostera* but it has to be tested comprehensively. The first results indicate that *Zostera* might deepen channels and that it does not elevate subtidal areas into the intertidal regime.

Spartina enhances the deposition of mud and redistributes the mud over the estuary. The mud accumulation pattern follows the vegetation distribution and through this *Spartina* elevates itself into a higher part of the intertidal zone. Through elevating itself *Spartina* decreases its physical stress and *Spartina* concentrations in the estuary increase. The enhanced sedimentation of predominantly mud under influence of *Spartina* enhances the morphological development induced by *Spartina*. In the future this knowledge of the interaction between *Spartina* and mud might be used in managing hyper-turbid estuaries like the Ems-Dollard.

Key words: estuary; river; vegetation; morphology; cohesive sediment; *Spartina anglica*; *Zostera marina*; Eco-engineering;

Contents

List of Figures

List of Tables

1 Introduction

1.1 Problem definition

Estuaries contain unique ecosystems (Davidson et al., 1991), with submerged and intertidal vegetation and usually a very high biomass (Meire et al., 2005). Vegetation is known to exert significant influence on hydromorphodynamics and is therefore likely to affect estuary morphology (Oorschot et al., 2015; Corenblit et al., 2009). It influences morphology through eco-engineering: *"organisms that create, modify and maintain habitats by causing the physical state changes in biotic and abiotic materials"* (Jones et al., 1994). Though the interest in eco-engineering is increasing rapidly there is little knowledge of large scale effects of vegetation on estuary morphodynamics. The effect of vegetation on morphodynamics has been studied on the patch scale in nature and in experiments (Järvelä, 2002; Siniscalchi et al., 2012). This results in knowledge of the processes at work within a vegetation patch, but the effects when it is up-scaled are less well known.

Recent advances in modelling riparian vegetation in a realistic dynamic way open up possibilities to investigate the effects of vegetation on estuary morphodynamics. For rivers a model with mortality due to flooding, dessication, scour, uprooting and burial is able to predict realistic vegetation patterns (Oorschot et al., 2015). In a model with submerged vegetation a sixth important variable is light availability as a function of sediment concentration and waterdepth (Davidson et al., 1991).

An extensive combination of computer and analogue modelling, and field research will have to be performed to get a thorough understanding of the feedbacks and interplay between vegetation, sediment transport, hydrodynamics and morphodynamics on estuary scale. The scope of this research is to make a first assessment of the possible effects of vegetation and mud on large scale estuary morphodynamics on engineering timescale (0-100 years). *Zostera marina* and *Spartina anglica*, two common species in estuaries, have been studied as subtidal and intertidal vegetation species and increasing mud concentrations have been investigated. This leads to the main aim of this thesis:

- To assess effects of dynamic vegetation and mud compared to estuaries with only sand on the hydromorphological development of entire estuaries on an engineering timescale.

1.2 Objectives of this study

There are a lot of difficulties in researching real estuaries. It is not possible to influence sediment concentrations, discharge, tidal conditions and vegetation growth and changes occur over tenths of years. Thus far analogue estuary models with real vegetation have not been made. Therefore an attempt is made to create a realistic integrated computer model which includes hydrodynamics, morphodynamics, dynamic vegetation and mud characteristics to investigate their effects on morphodynamics. The inclusion of vegetation in estuary morphodynamic models is one of the three biggest challenges to overcome shortcomings in current models (Coco et al., 2013). To reach the main aim and make a first assessment of the reliability, the results are compared with available field data. The main part of the research consists of creating and modelling a hypothetical, simplified estuary. No attempt was made to model a real estuary for the aim is to distinguish the general effects of including several variables and not their precise influence in a specific setting. This study thus has three objectives:

- To couple a hydro-morphodynamic Delft3D model with cohesive sediment and a model for dynamic vegetation which is modified to simulate intertidal and subtidal vegetation. This model should be able to simulate morphodynamic development on estuary spatial- and engineering time-scale.
- To assess effects of cohesive sediment, *Z. marina* and *S. anglica* vegetation on estuary morphodynamics.

- To compare the emergent patterns in vegetation spreading with available field data

1.3 Relevance

Estuaries are found throughout the world and are important providers of both economical and ecosystem services. The unique variability in hydrodynamics and salinity conditions causes an unique flora and fauna to develop throughout estuaries (Davidson et al., 1991).

Large parts of the world population live, or have moved to coastal areas and estuaries over the last decades (Small and Nicholls, 2003). Anthropogenic activities can severely alter the sedimentary and hydrodynamical conditions in the estuary (Monge-Ganuzas et al., 2013; Dias and Picado, 2011). For example dredging and dumping and construction trigger the import of sediment, which disrupts the equilibrium within estuaries and damages ecosystems (Monge-Ganuzas et al., 2013; Coco et al., 2013). The negative effects of human interference with the natural system have increased interest in eco-engineering over the last decade to understand how present estuary shapes and patterns are influenced by the species that live there.

Eco-engineering is the principle that organisms create, modify and maintain habitats by causing the physical state changes in biotic and abiotic materials (Jones et al., 1994). To predict the effects of the disappearance of species or to restore natural patterns we need to have a better understanding of the interaction between the biological and physical processes in estuaries. Though the interest in eco-engineering is rapidly increasing, and it offers many opportunities, there are quite some limitations when applied to estuaries. The effects of mud and vegetation in estuaries on the morphodynamics is only limitedly understood, especially on a longer timescale. To be able to restore natural estuary dynamics and to predict the effect of alterations in the ecosystems, we need a better understanding of the interactions at work.

Concluding there is ecological, economical and scientific relevance in understanding large scale estuary morphodynamics under influence of vegetation development.

1.4 Definitions

In scientific literature different terms are used for estuarine elements. This section gives the definitions of important terms used in this thesis in bold face. Some of these terms are also visualized in figure 1. In this research the used definition of an **estuary** is a '*body of water that is either permanently or periodically open to the sea and which receives at least periodic discharge from a river(s)*' (Potter et al., 2010). This does not define the upstream boundary of the estuary, but this research takes some distance beyond the tidal limit as maximum upstream extend. The **tidal limit** is the maximum distance upstream which is affected by the tidal wave. The **tidal amplitude** is the difference between high and low tide and the **tidal flow velocity** is the flow velocity caused by the tidal wave. These features, together with the river discharge, make up the **hydrodynamics**. Under influence of this hydrodynamics the estuary develops channels, salt marshes, shoals, and mud flats, which together make up the **morphology** of the estuary.

Vegetation which grows between the low and high tide boundary is called **intertidal vegetation** and aquatic vegetation is referred to as **submerged vegetation**. The intertidal vegetation species in the models is *Spartina anglica*, often abbreviated as ***Spartina***. The submerged vegetation does not necessarily remain submerged permanently, but dependent on its dessication resistance might emerge during a small part of the day. In this research *Zostera marina* is included as submerged vegetation, and it is often abbreviated as ***Zostera***. The vegetation in the **supratidal zone**, the zone above the high tide level, is called **riparian vegetation**.

In the research **mud** is used for the sediment fraction < 0.063 mm which acts **cohesively**, which means that it limits erosion because it strengthens bottoms.

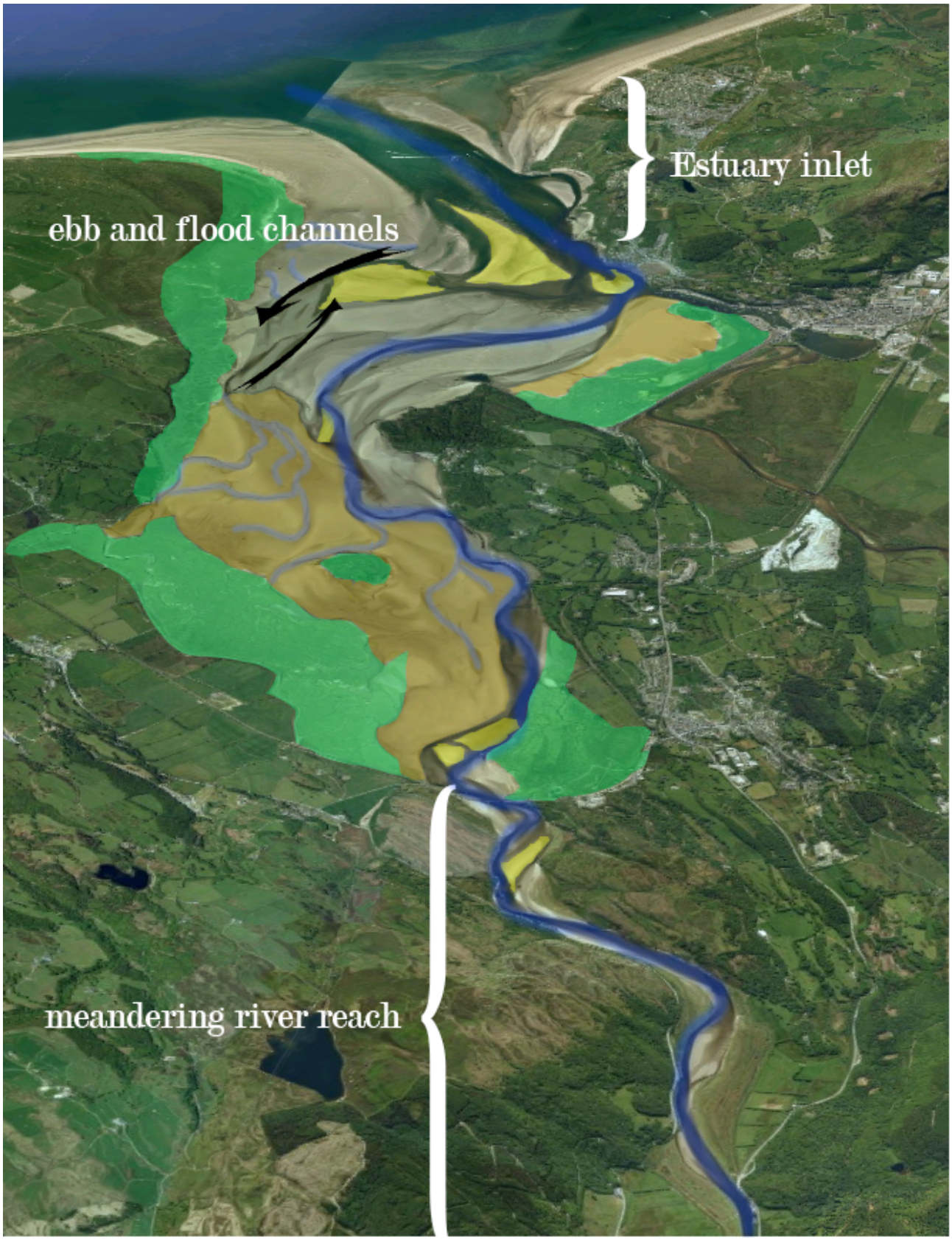

Figure 1: Important morphodynamic features in estuaries, here portrayed on the Afon Dwyryd estuary in Wales. Green areas are salt marshes, brown areas sand or mudflats, yellow areas (tidal) bars, dark blue the main river and purple are tidal creeks.

1.5 Structure of this thesis

First a thorough literature review on estuary morphodynamics, cohesive sediment dynamics and vegetation interaction with morphodynamics is presented (section 2). This is the basis for the integrated model (section 3). A presentation and interpretation of the results in terms of estuary evolution is presented (section 4). The results are discussed and compared with field data (section 5), followed by conclusions of the research (section 6). The last part consists of suggestions for future research (section 7).

2 Theoretical Background

This literature review starts with with an introduction on the different types of estuaries and their morphological and hydrodynamical characteristics. It will be followed by sections about cohesive sediment dynamics and estuarine vegetation and the interaction of vegetation with morphology. These theoretical and scientific insights are integrated into the research model that is used to investigate the effect of mud and vegetation on the morphodynamics in a tide-dominated estuary. The final part of this section contains the hypotheses to the aims based on the literature study.

2.1 Estuaries, an introduction

Estuaries are common coastal features around the world and are important areas in terms of biodiversity and providing services to humans, for example fishing and shipping. Most estuaries developed due to the last postglacial marine transgression which flooded coastal river valleys (Masselink et al., 2014). Sea level rise decreased 6000 BP and since this moment most estuaries have slowly been infilling (Masselink et al., 2014). Estuaries receive sediment from both the river and sea which causes them to slowly infill and, if sedimentation rates are to high, transform into prograding delta's. Estuaries consist of embayments where the sea intrudes the coastline, unlike delta's which are extending the coastline. The large amount of fluvial, marine, gravitational (Hansen and Rattray, 1966) and biological processes in an estuary make that the behaviour and development of these areas is only limitedly understood (Coco et al., 2013). In the following paragraphs estuary morphodynamics and their driving hydrodynamics will be discussed.

2.2 Estuarine morphology

2.2.1 Large scale morphology

Estuaries consist of three zones, distinguished by the main energy source, morphology and sediment characteristics (Dalrymple et al., 1992). At the upstream boundary the river is the main hydrodynamic energy source, but its importance decreases in seaward direction. For marine processes the opposite holds, tidal and wave energy are largest at the seaward boundary and decrease in upstream direction (Dalrymple et al., 1992). This leads to the classification by Dalrymple et al. (1992) of an inner, river dominated, outer, marine dominated, and central, mixed, zone. The inner zone transports sediment in the seaward direction and the outer zone usually transports sediment in the upstream direction. This results in a net sediment accumulation in estuaries. The central part of the estuary where energy is lowest tends to be dominated by relatively fine material (see also subsection 2.4), while the outer and inner zone are usually more coarse.

Estuary classification

Estuaries differ in hydrodynamics dependent on infilling, width/depth ratio and inlet morphology. There are two end-member estuary types: tide- and wave-dominated estuaries, with both distinct characteristics (Dalrymple et al., 1992). This research deals with tide-dominated estuaries, but a short background on wave-dominated estuaries will be provided as well.

Wave-dominated estuaries contain a barrier at the estuary inlet and a tidal inlet (Figure 2B). This tidal inlet develops an ebb-tide and flood-tide delta at the outer and inner part of the barrier respectively (Hayes, 1980). The barrier and small tidal inlet cause significant wave breaking and energy dissipation of both the waves and tide. Because of this the central zone of the estuary is very low in energy and there are large mud accumulations, salt flats and salt marshes (Donaldson, 1970). The river builds out a bay-head delta, because it enters a low energy water body (Donaldson, 1970). The hydrodynamic conditions in a wave dominated estuary differ significantly from these in a tide dominated estuary due to the barrier and therefore the results from this research are unlikely to hold for wave dominated estuaries.

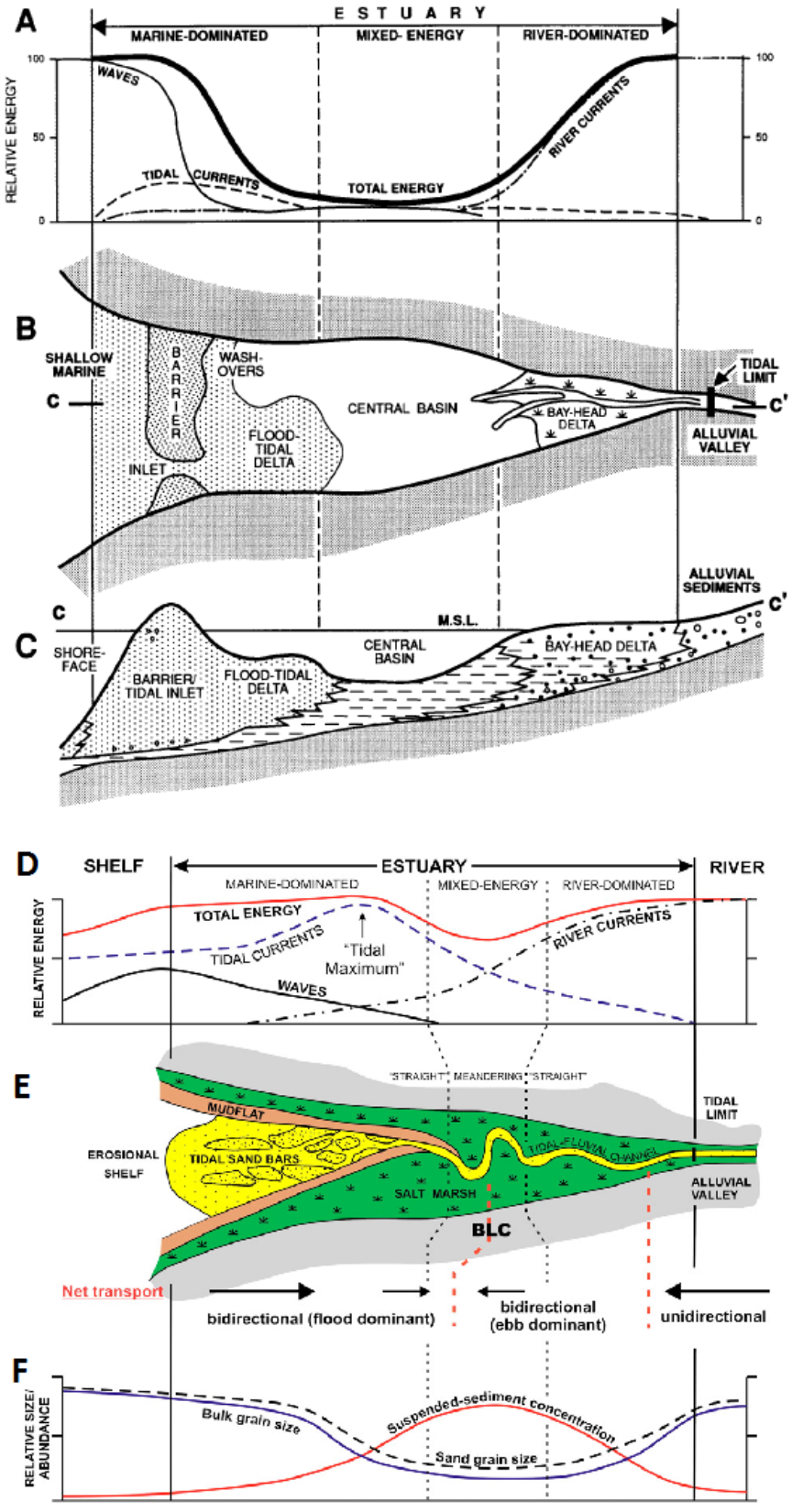

Figure 2: Schematic overview of a wave (ABC) and tide (DEF) dominated estuary. A shows the rapid decrease in wave and tidal energy at the seaward end and the strong decrease in river current at the upstream end. B shows the classic morphology which consists of a barrier at the inlet with a small tidal channel and ebb and flood delta, a central basin with mud accumulation (C) and a bay-head delta (Dalrymple et al., 1992). D shows the change from tide dominance to river dominance along the estuary, E shows the classic morphology with linear tidal bars in the outer zone and a strongly meandering channel in the central zone and F shows the distribution of grainsize over the estuary.

Tide-dominated estuaries are channelized with ebb and flood channels and the outer zone is characterized by linear sand bars which form due to these channels (Hayes et al., 1975) (Figure 2E). Though tidal energy is the dominant process in the outer zone of the tide-dominated estuary, wave energy in the central part of the estuary might actually increase compared to the situation in a wave dominated estuary. Waves are able to prograde further into the estuary because the inlet is not as protected as in a wave dominated estuary. The tidal energy in the outer part and channels of the estuary is relatively large and therefore the sediment transported consists mainly of sand (Woodroffe et al., 1989). Most of the tidal channels appear to be somewhat curved similar to meandering rivers. The multiple channels in the outer zone turn to a single meandering channel with pointbar deposits in the central zone (Barwis, 1977). This transition to a single channel occurs when the tide loses too much energy to scour flood channels (Van den Berg et al., 2007). The central part of the estuary consists of an interaction between river and tidal processes. This area is characterized by a dominant ebb current because the river flow adds to the ebb current and counteracts the flood current. The tidal processes create a temporarily submerged, intertidal, area which contains salt marshes (or mangroves in tropical regions) and which will be discussed in more detail below.

tidal zones

The different tidal zones are characteristic and of great morphological importance in tide-dominated estuaries. Estuaries contain a subtidal zone, which is almost continuously submerged, an intertidal zone which is between the mean low and mean high water and the supratidal zone which lies above the mean high water level (Reineck and Singh, 1980). These three zones are a sequence from the mid of the estuary (the tidal channel) towards the estuarine margins. The subtidal zone is the highest energy environment because water depth is largest here and thus the currents as well (Reineck and Singh, 1980). This part of the estuary conveys water at all tidal stages as well and is therefore most prone to sediment transport. The intertidal zone is submerged during part of the tidal cycle with energy levels decreasing with a decreasing submergence time. As maximum tidal velocity (in general) occurs at mid tide, areas above the mean water level are not exposed to strong currents. The supratidal zone is submerged during springtide only and is therefore a very low energy environment.

2.2.2 Small scale morphology

On a smaller scale it is important to understand patterns in estuarine morphology as well as the interaction of channels and shoals has large influence on estuary morphology. Estuaries have channels which are predominantly used by either the ebb or flood flow (van Veen et al., 2005). These channels form characteristic patters and the areas in between ebb and flood channels form shoals (Figure 3). These patterns have significant effects on the estuary, because they determine the main channel depth, braiding index and extent of the intertidal areas. Schramkowski et al. (2004) have shown some relation between channel width, tidal excursion length and equilibrium channel shoal configurations but it is still unknown what process drives the formation of this channel pattern.

2.3 Estuarine hydrodynamics

The previous subsection considered the different types of estuaries and the zones in there. This subsection will deal with the hydrodynamics of the estuary and how channel morphology interacts with tidal flow.

Estuary hydrodynamics consist of four components, wave action, tidal currents, river currents and density currents, driven by the gradient in salinity due to the mixing of salt sea water and fresh river water. Salinity patterns will, however, not be discussed because these are not included as a current driving component in this research. A well mixed estuary is assumed. This choice is made because salinity distribution is not fully understood yet which makes it difficult to model it reliably. This might affect the mud distribution as the density driven current can have significant effects on the turbidity

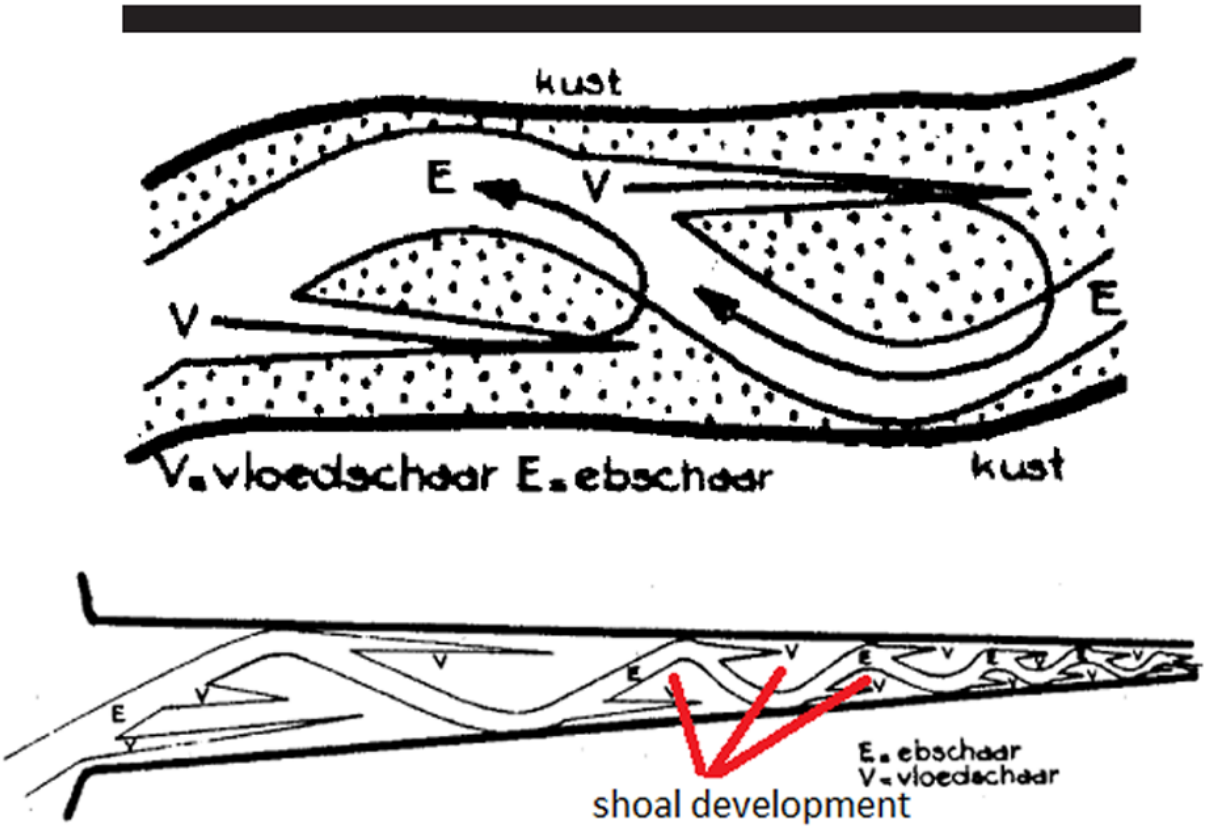

Figure 3: A schematic estuary with ebb and flood channels which cause shoals to develop (van Veen et al., 2005). E stands for ebb channel and V for flood channel.

maximum zone (section 2.4.1), therefore there is uncertainty whether the results hold for stratified estuaries as well.

2.3.1 River currents

River currents are the main source of energy in the inner part of the estuary (Dalrymple et al., 1992). The main reason that their energy decreases in a seaward direction is twofold. First of all estuaries are widening with usually multiple channels in the downstream reach which decrease the strength of the river in the individual channel (Dalrymple and Choi, 2007). Secondly the gradient of the river diminishes when it reaches its seaward end which also decreases its strength.

2.3.2 Tidal currents

Tidal waves enter estuaries from their seaward boundary, resulting in an alternating landward (flood) and seaward (ebb) directed current. The water level rises and falls with the passing wave which creates the subtidal, intertidal and supratidal zones. When the flow reverses from ebb to flood or the other way around flow velocity becomes zero. This is called slack water. The progradation of the tidal wave is described by the celerity equation for shallow-water waves (Masselink et al., 2014). This equation holds because the tidal wavelength is so large that it always behaves as a shallow-water wave in the coastal region.

$$C = \sqrt{gh} \tag{1}$$

In which C is the wave celerity or tidal speed, g is the gravitational acceleration (9.81 m/s) and h is the water depth. The tidal wavelength (L) can be calculated with the tidal period (12.4 hours for the

M2 tide):

$$L = T\sqrt{gh} = TC \tag{2}$$

In which T is the tidal period. It is the tidal wavelength which determines whether the tide behaves as a progressive or standing tide. A progressive tide occurs when the tidal wavelength fits multiple times within an estuary, which results in a different timing of high and low water along the estuary. A progressive tide has its maximum flood velocity at high water and its maximum ebb velocity at low water while a standing tide has a 90° phase difference between maximum water level and flow velocity (Figure 4).

There are two factors which influence the tidal range over the estuary: reflection of the tidal wave and estuary convergence. When the tidal wave reflects on channel bends or the river boundary a standing tide might develop (Figure 4A). A standing tide has in general a node at the estuary entrance and an antinode at the river boundary. This occurs when the estuary length is a multiple of a quarter of the tidal wavelength (Masselink et al., 2014). The tidal range at the antinode(s) in the estuary will be twice the tidal range outside the estuary in the case of a perfect standing tide. The phase difference between the maximum water elevation and the maximum flood velocity of 90°, results in maximum flood (and ebb) velocities at mid tide. Standing tides are important hydrodynamic factors for estuaries as they are responsible for the typical funnel shape of estuaries (Figure 5) (Wright et al., 1973).

To create a stable system the sediment transport should be constant throughout the estuary, which requires an increasing tidal range at the river boundary, which is what happens under a standing tide (Wright et al., 1973).

The second factor which influences the tidal range is the shape and depth of the estuary (Dyer, 1995). The ratio between convergence and friction determines whether the tidal range increases or decreases along an estuary. The continuously shrinking cross sectional area in the estuary where the tidal wave passes through forces the water level to increase (convergence) and thus causes an increase

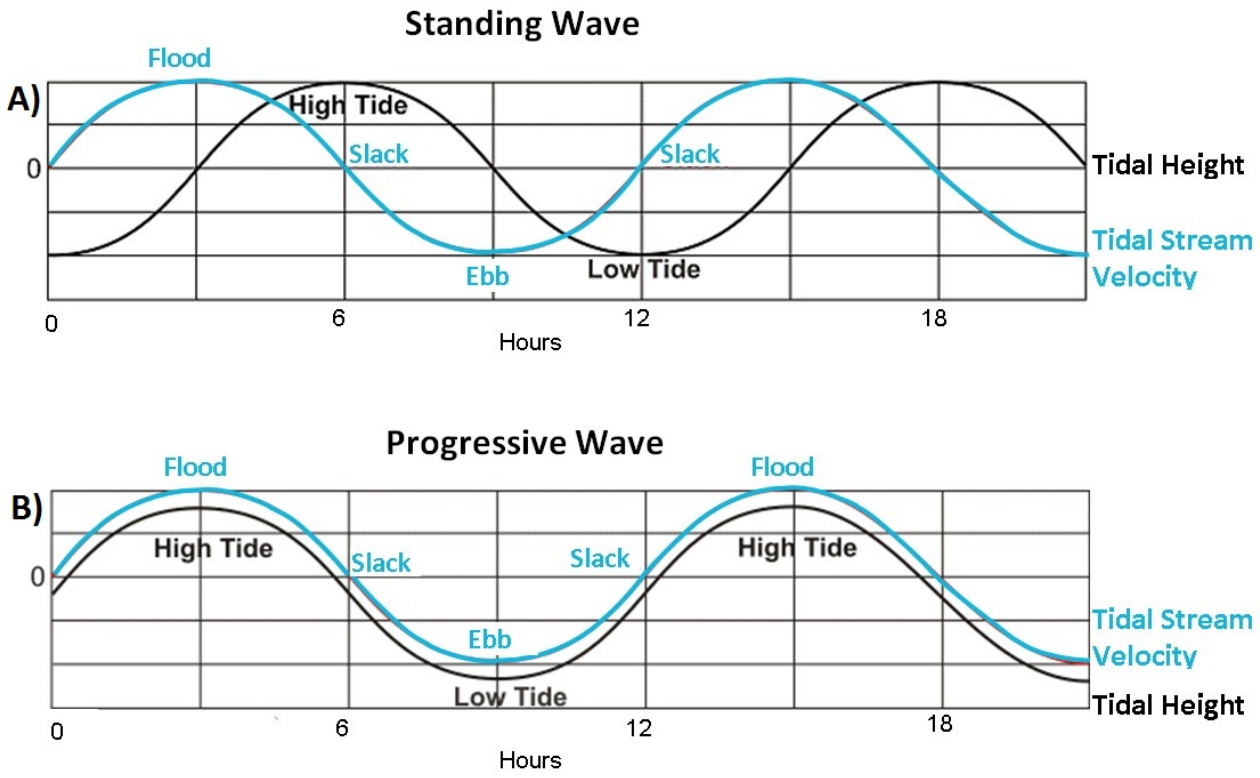

Figure 4: The two main types of tidal waves. A) standing wave which occurs when the tide is reflecting in the estuary, which results in a phase difference between the maximum flood velocity and high water. B) progressive wave with maximum flood velocities during high tide and maximum ebb velocities during low tide (University of Strathclyde).

Figure 5: The Fly River estuary in Papua New Guinea, clearly shows a funnel shape and transition from meandering towards multiple channels with bars when going in seaward direction.

in tidal range. The friction does, however, increase simultaneously due to a decrease in waterdepth and this decreases the tidal range. The balance between friction and convergence can result in three types of estuaries: synchronous, hyposynchronous and hypersynchronous (Figure 6) (Dyer, 1995). These types of estuaries all have their maximum amplitude and current velocity at a different position in the estuary.

When it comes to net sediment transport in a tidal environment tidal asymmetry or tidal distortion becomes of importance. Tidal asymmetry means that the duration of either the flood or the ebb flow lasts longer than the other.

Flood-dominance can be explained with the wave celerity (Eq. 1). The wave celerity depends on the water depth, and the water depth is dependent on the tidal wave motion. In shallow water the tidal amplitude starts to exert a significant influence on the water height in the equation and thus on celerity ($C = \sqrt{g(h \pm tidalamplitude)}$). The equation shows that the velocity of the wave crest (largest water depth) is significantly larger than the velocity of the trough (smallest water depth) and this results in a shorter flood duration than ebb duration. This means that the flood velocity must be of a larger magnitude when mass is conserved, as is the case in an estuary. This velocity asymmetry results in a relatively large sediment transport in the flood direction (onshore) (Dalrymple and Choi, 2007).

Ebb-dominance is the opposite type of velocity asymmetry which might develop when the cross sectional area of the ebb and flood flow differ significantly (Friedrichs and Aubrey, 1988). Due to the intertidal areas in an estuary the flow cross sectional area might differ significantly over the tidal cycle. When the intertidal area floods, the cross sectional area increases. Flow is most efficient when roughness is small and thus it is more efficient when flowing through the estuarine channels than over the shoals and marshes. This causes the ebb flow, which is concentrated in the estuarine channels, to

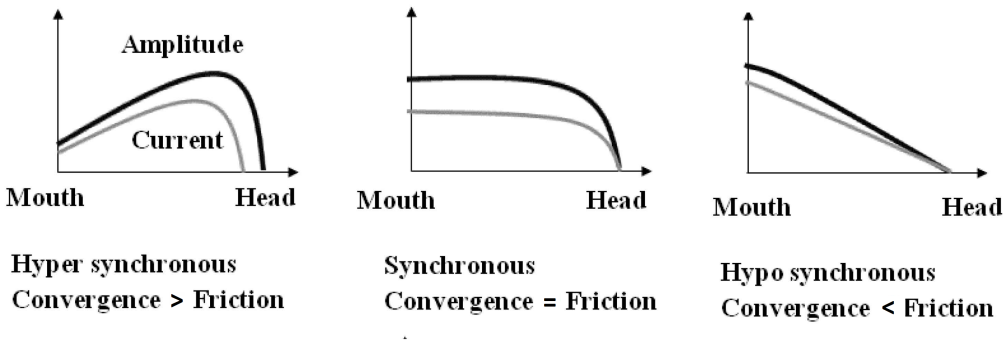

Figure 6: The tidal amplitude and tidal current development for different types of estuaries based on the ratio between friction and convergence in the estuary.

be hydraulically more efficient and have a larger velocity magnitude. An estuary where ebb flow is more efficient than flood flow due to concentration in the channels tends to have a tidal net sediment transport offshore. A clear example of an ebb-dominant estuary is the Dyfi estuary in Wales (Brown and Davies, 2010).

2.3.3 Wave action

Wave action is mainly of importance at the seaward end of the estuary. Since most estuaries have their seaward end at the sea, or ocean, the waves are likely to have a large fetch and therefore they are able to build up a significant energy dependent on wind conditions. Waves are likely to reach their maximum energy at the coastline after which their energy will dissipate due to friction as the estuary becomes more shallow (Dalrymple and Choi, 2007). Because waves are significantly altered by the tidal elevation they are computationally demanding and are left out of the model.

Cohesive sediment is known to have its own very unique dynamics within estuaries and it is assumed to have a significant influence on estuarine morphodynamics. Therefore the following subsection discusses cohesive sediment dynamics before vegetation is introduced.

2.4 Cohesive sediment dynamics

Mud is the mixture of silt (0.004-0.063 mm) and clay (<0.004 mm) particles, which differs from sand because it acts cohesively and is transported predominantly in suspension. Mud transport and its sedimentation or erosion have major influence on channel siltation, and vegetation zonation. It is important to understand mud dynamics because:

- Siltation of shipping channels and harbours is a major and expensive problem which we do not yet know how to solve properly.
- High concentrations of suspended sediment, mostly mud, may significantly decrease light penetration in the water column and so affect primary production in the estuary (Heip et al., 1995).
- Mud content in the soil is one of the main controlling factors of the vegetation distribution (Mackin and Kennish, 1988).

First the turbidity maximum zone will be discussed and after that the transport characteristics of mud because these are both relevant for modelling the effects of mud on estuary morphodynamics.

2.4.1 Turbidity maximum zone

Some estuaries contain a distinct turbidity maximum zone (TMZ), an area where the suspended sediment concentration is significantly higher than more seaward or landward parts of the estuary. The TMZ occurs where the net current becomes zero. In the case of a symmetrical tide this is the point where the gravitational estuarine circulation equals river flow in magnitude, the so called null point. In nature the TMZ is an area with roughly the tidal excursion length around this null point. In the case of an asymmetrical, flood-dominant, tide the TMZ occurs where the tidal flood current equals the river current in magnitude. Here both currents have lost significant amounts of energy and therefore they mainly transport fine suspended matter. As the net flow velocity becomes approximately 0 m/s during flood, mud deposition is large here. The TMZ is therefore the part of the estuary where the influence of mud on morphodynamics will likely be the largest.

2.4.2 Transport and sedimentation characteristics

Van Ledden et al. (2004) performed research on mud morphodynamics in a short tidal basin. Tidal basins have some similarities with estuaries, but differ in the sense that the energy of the system

dampens when moving further inshore because there is no river. An important characteristic of mud is its cohesiveness. Clay particles which have a negative charge tend to adhere to each other and significantly affect settling velocity through flocculation and strongly increase bed strength. The relative abundance of clay determines whether the mud behaves cohesive or not (Dyer, 1986). The boundary between cohesive and non-cohesive sediment beds is found at a 5-10% clay content. If the clay/silt ratio is known it becomes possible to determine the critical mud content ($p_{m,cr}$) in the system. Dependent on whether the mud content does exceed the critical value or not two different equations apply to the vertical sediment fluxes. The equations below describe the sand flux (F_s) and the mud flux (F_m) near the bed surface (Van Ledden et al., 2004). A positive value means net erosion and a negative value means deposition.

$$F_s = w_s(c_a - c_s) \qquad p_m \leq p_{m,cr} \tag{3}$$

$$F_s = (1-p_m)M(\frac{\tau_b}{\tau_e} - 1)H((\frac{\tau_b}{\tau_e} - 1) - w_s c_s \qquad p_m > p_{m,cr} \tag{4}$$

$$F_m = p_m M(\frac{\tau_b}{\tau_e} - 1)H((\frac{\tau_b}{\tau_e} - 1) - w_m c_m(1 - \frac{\tau_b}{\tau_d})H(1 - \frac{\tau_b}{\tau_d}) \qquad 0 \leq p_m \leq 1 \tag{5}$$

In these equations w_s is the sand settling velocity, c_a a reference sand concentration, c_s the sand concentration near the bed. p_m is the mud content which is compared to $p_{m,cr}$ to determine whether the bed behaves cohesive or not. M is an erosion coefficient, τ_b is the bed shear stress, and τ_e the critical shear stress for mud erosion. H is the Heaviside function, which is 1 if the argument is true and 0 when it is false, this is to incorporate the equations in Delft3D models. The mud settling velocity is given by w_m and c_m is the mud concentration. Last, τ_d is the critical shear stress for mud deposition. Equation 4 shows that for a cohesive sediment bed the sand erosion is determined mainly by the ratio between the bed shear stress and the critical shear stress for mud erosion ($\frac{\tau_b}{\tau_c}$), and no longer by its own characteristics. Mud deposition and erosion are both dependent on the ratio between bed shear stress and the critical bed shear stress. Mud might exert a significant influence on estuary morphodynamics because it becomes the dominant factor which determines erosion once it exceeds a certain percentage.

2.5 Typical estuarine vegetation

Estuaries contain unique plants and a high animal diversity for they are one of the most productive ecosystems around the world. The estuary consists of different zones, which are determined by the tidal range. The channels and their neighbour areas are a marine habitat which is dominated by seagrasses. Areas more distal from the channels consist of mudflats. The intertidal area consists of salt marshes (or mangroves in tropical ecosystems) and the area which is rarely flooded is dominated by riparian vegetation (Figure 7). Dependent on the location in the estuary these zones can be either smaller, larger, or absent (Figure 2). Below we will describe the different types of vegetation in more detail in relation to their habitat in the estuary.

submerged areas

Estuarine channels and their neighbour areas are permanently submerged. If they are vegetated they are occupied by macrophyte communities which consist of brown, green and red macroalgae and submersed vascular plants. There is only a small amount of submersed vascular plants which thrive in seawater, so called seagrasses.

Zostera marina

The *Z. marina* species (Figure 8A) is the subtidal species that will be included in the model and is therefore discussed in more detail. *Z. marina* is an eelgrass species which is common in the northern hemisphere (Den Hartog, 1970). *Z. marina* occurs usually as a perennial species, but sometimes it has an annual or semi-annual life cycle (van Lent and Verschuure, 1994). The species is very dependent

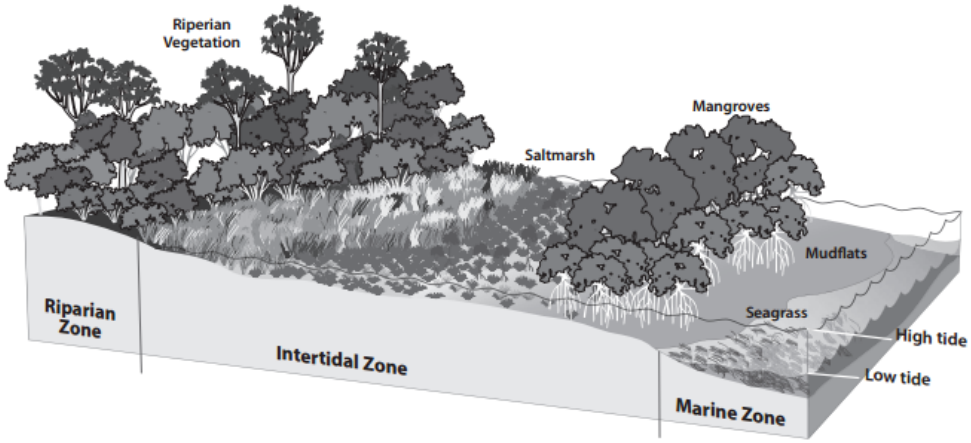

Zone	Habitat	Features
Marine	Seagrass/ mudflats	Covered by tides for most of the time. May be uncovered twice each day for short periods
Intertidal	Mangroves	Covered by tides twice each day and exposed for greater periods of time
	Saltmarsh	Covered by tides for shorter periods, less often
Riparian	Riparian vegetation	Never covered by tides, unless from an extreme weather event (floods)

Figure 7: Different vegetation types surrounding the estuary with respect to their tidal zone, here for a tropical environment (Waterwatch New South Wales, 2010)

on light conditions, it can occur up to depths of 40 meter, but usually they are not present below approximately 10 meters or the secchi depth (Sand-Jensen et al., 2005). The seagrass has adapted itself to marine conditions and desiccates quickly when emerged. Seagrass spreads both through rhizomes and seed dispersal and has an initial density of approximately 300 plants per square meter which increases to approximately 700 (Qin et al., 2016). Leaves grow to become approximately 6 mm wide and its length increases from approximately 5 cm to over 70 cm after several months (Qin et al., 2016). *Zostera* can survive flow velocities of 0.5 m/s (Wijgergangs and de Jong, 1999).

Mud flats

Mud flats and salt marshes develop in areas with relatively limited flow velocity. Flow velocity is linearly coupled to inundation height which means that shallow areas contain lower flow velocities (Bouma et al., 2005). This causes mudflats and salt marsh vegetation to develop in the shallow areas of the estuary, which often lie in the intertidal zone.

Mudflats contain little visible vegetation. Due to the harsh physical conditions on mudflats only a small amount of species thrives here. The macro vegetation consists mainly of green algae and eelgrass. The main biodiversity of mudflats comes in the form of invertebrate macrobenthos which are abundant and biologically very productive. Mud flat vegetation is, however, beyond the scope of this research and therefore no further information is provided.

Salt marshes

Shoreward from the mudflats the vegetation changes to salt marshes. Salt marshes are colonized by halophyte species, which are able to withstand the high salt content and the frequent changes in inundation. Salt marsh vegetation consists of grasses, herbs and shrubs. Largely abundant salt marsh species in Europe are the *Phragmites* and *Spartina* genera (Figure 8B,C).

To make realistic predictions of the effects of vegetation on estuary morphodynamics it is of importance to understand which factors determine their distribution. There are quite some factors which influence the distribution of halophytic species, but there is no easy way to distinguish them. Soil moisture saturation is often mentioned as an important control on vegetation distribution in salt

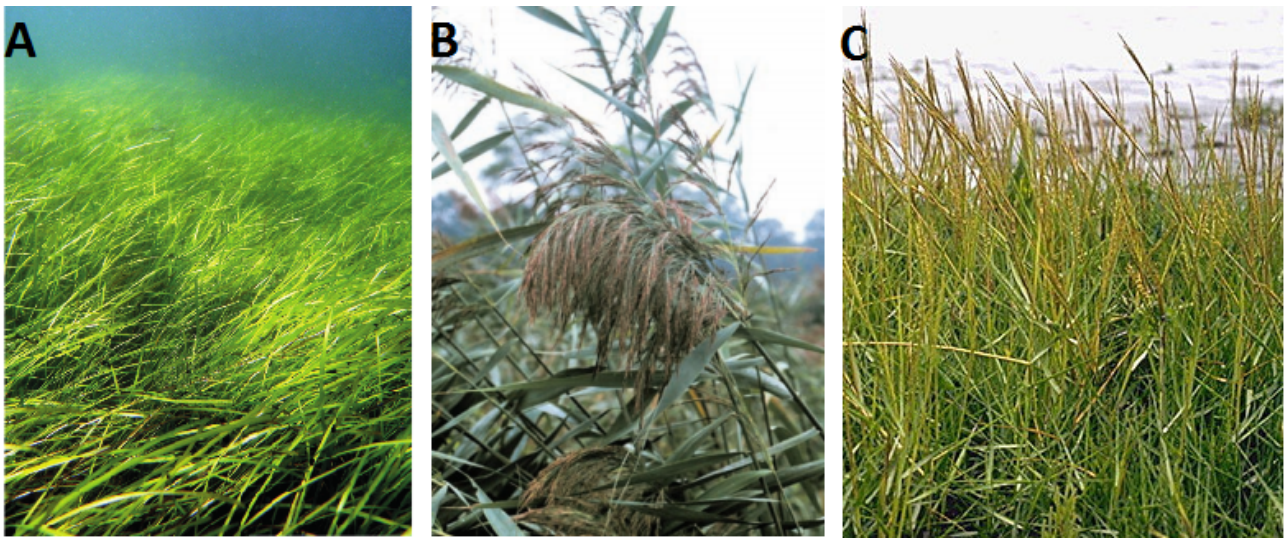

Figure 8: A: *Zostera marina (Olsen et al., 2016)*, B: Phragmites australis (Joseph McCauley, USFWS) and C: Spartina anglica (K. Ybema, ETI BioInformatics)

marshes, because a fully saturated soil disables plants from aerating (Li et al., 2008; Ursino et al., 2004). The total inundation time, due to the tidal fluctuation, influences the saturation, but it is also dependent on highly spatially variable soil properties. Similar relations hold for salinity, plants often have a clearly defined minimum and maximum salinity which they can survive, but salinity is a function of local groundwater movements, tidal inundation and evapotranspiration, which makes it a complicated variable as well.

The dependence of vegetation on both tidal conditions and local soil conditions has led to the conclusion that there is not always a logical succession towards a climax ecosystem (Silvestri et al., 2005). There appears to be a correlation between biomass and soil elevation (Figure 9), and also between soil elevation and vegetation species (Marani et al., 2004). The relation between species and soil elevation is, however, relative. When one goes up in elevation in two marsh areas the sequence in vegetation species tends to be similar, but their absolute elevation and inundation time are likely to be different (Figure 10).

Rand (2000) has shown that seed dispersion exerts a major control on the areas which can be colonized by a certain species while Bockelmann and Neuhaus (1999) have shown that the lower elevation boundary of a species is usually set by physical conditions (most likely salt content and oxygen availability and the plant its tolerance to these) while the upper elevation boundary is set by competition. This shows that vegetation zonation patterns are difficult to explain, especially without a high resolution soil knowledge. This creates difficulties in incorporating salt marsh vegetation in morphodynamic models which have to be overcome.

Spartina anglica

S. anglica (Figure 8C) will be discussed in more detail for this is the marsh species which will be included in the estuary model. *S. anglica* is a crossing between *Spartina maritima* and *Spartina alterniflora* (Nehring and Adsersen, 2006). *S. anglica*, or English cordgrass, is a hybrid, salt tolerant, grass species. The species became very successful and is now considered as a major invasive species which is known to cause rapid sedimentation. The species spreads through seeds and underground rhizomes, starting from small patches and eventually developing to larger meadows (Nehring and Adsersen, 2006). The plants obtain a height of 30-130 cm and its leaves obtain a length of approximately 40 cm (Nehring and Adsersen, 2006). A typical stem diameter is 6 mm and vegetation density can reach up to 13000 stems m^{-2} for seedlings and 800 stems m^{-2} for further developed vegetation (Graham and Manning, 2007). *S. anglica* occurs in both the low and high marsh zones, which makes it a very dominant species with a large geographical distribution. This is also represented in its range of tolerated salinity concentrations: 5-40 ppt. *S. alterniflora* (and probably also its hybrid successor

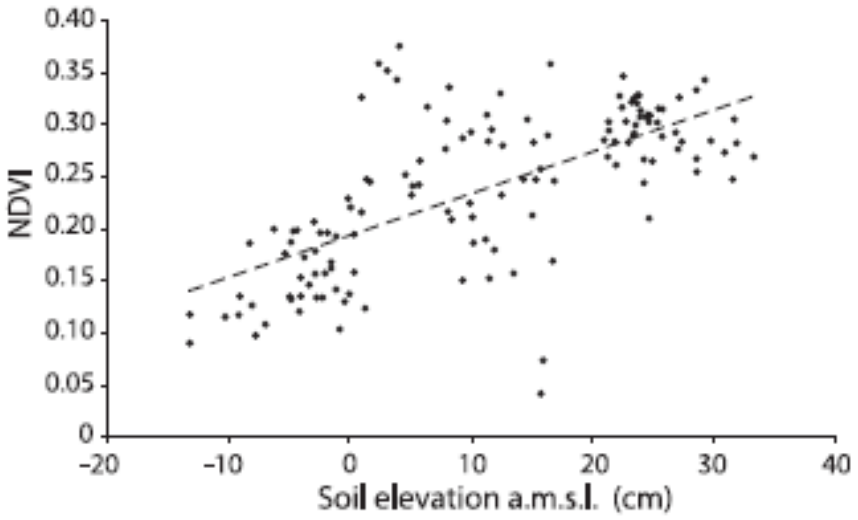

Figure 9: The relation between soil elevation and NDVI, which is an indicator of total biomass (Marani et al., 2004)

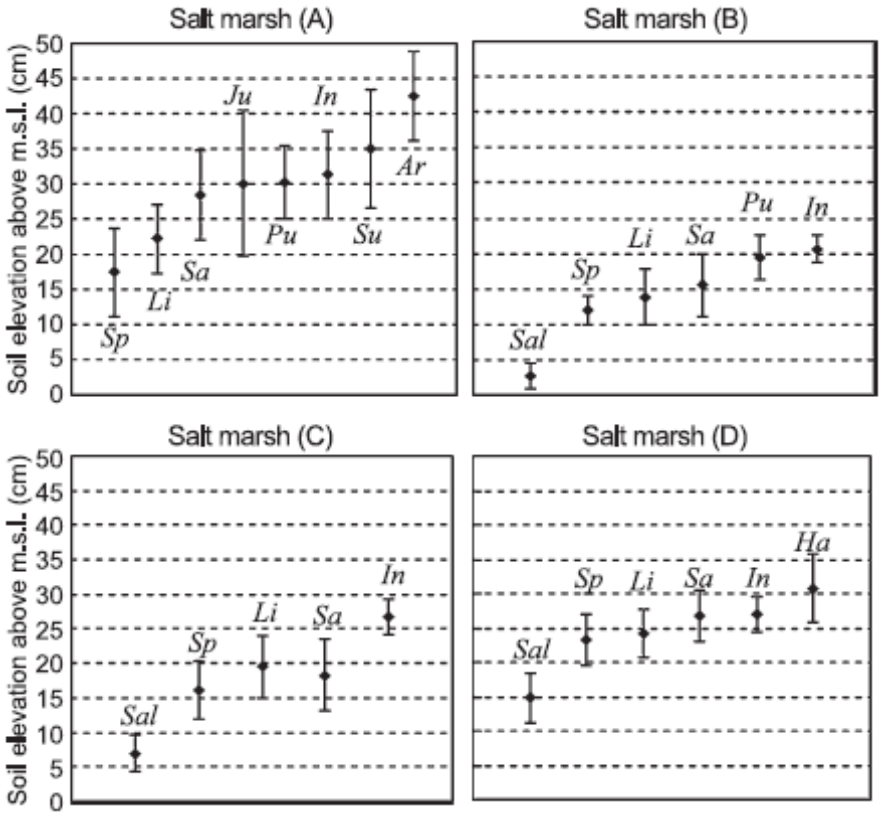

Figure 10: Occurence height of several marsh vegetation species in four different marshes in the Venice lagoon. As can be seen the species change in a similar manner with respect to elevation but not to absolute height (Marani et al., 2004).

S. anglica) can survive drought relatively well unless the soil salinity is (too) high (Figure 11).

Riparian vegetation

Riparian vegetation, which grows above high tide, is flooded only during spring tide conditions and has different characteristics than salt marsh vegetation. While intertidal vegetation usually has a grass-like morphology riparian vegetation tends to be dominated by shrubs and trees. Though riparian vegetation is hydrophilic it is unable to survive on salt marshes because it is in general not adapted to salt conditions. For riverine riparian vegetation holds that exposed riverine sediments pose difficult conditions for vegetation to establish itself. Due to a rapidly changing habitat and poor soil conditions only limited amounts of species manage to colonise these areas (Karrenberg et al., 2002). Several

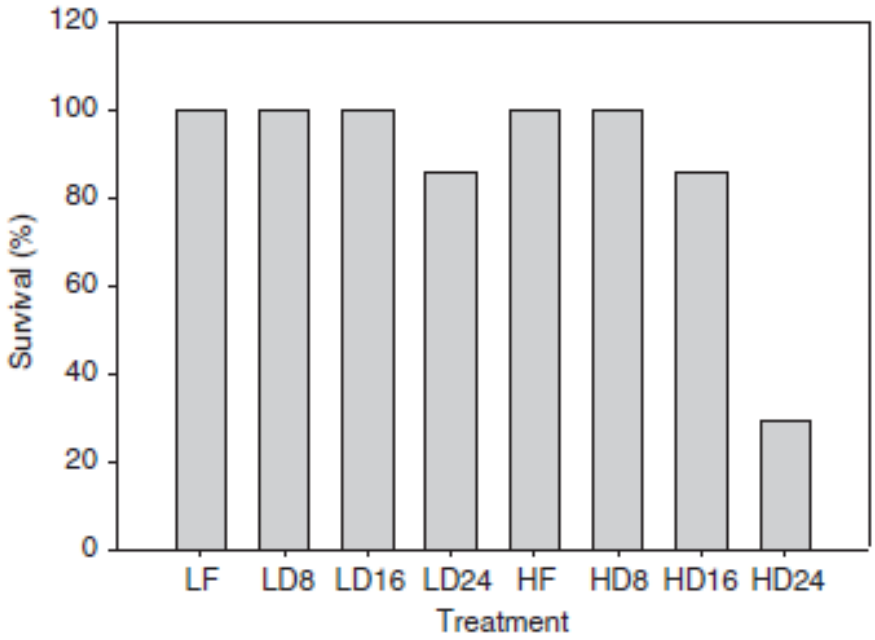

Figure 11: The survival of *S. alterniflora* after different periods of dessication for a low (L) and high (H) salt content of 3-5 and 35-38 ppt respectively. Experiments were carried out in a controlled environment (Brown and Pezeshki, 2007).

plant species, so called riparian vegetation, adapted so that they are able to withstand this environment (Karrenberg et al., 2002). Most likely this applies to estuarine riparian vegetation as well. For riverine riparian vegetation the most important controls on vegetation establishment are flow velocity, flooding and dessication duration, and scour and burial of seedlings (Oorschot et al., 2015).

2.6 Morphological effects of vegetation

Vegetation has significant impact on river morphodynamics and affects flow conditions, sediment movement and sedimentation (Bertoldi et al., 2009). There is not enough knowledge to predict river evolution due to vegetation yet, though its influence is better understood than for estuaries (Vaughan et al., 2009). The impact of vegetation on estuary morphodynamics has been studied little and is therefore largely unknown. This section will first discuss the effect of vegetation on hydrodynamics and then go into detail on the interaction between vegetation, hydrodynamics and morphodynamics.

Vegetation affects flow patterns because it increases the hydraulic resistance and lowers the flow velocity (Figure 12). The magnitude of the effects is determined by the vegetation its relative roughness, the flow velocity and the flow depth (with respect to the vegetation height) and whether the plants carry leaves (Järvelä, 2002). Increased hydraulic resistance may lead to increased sedimentation of both organic material and fine sediment (Zong and Nepf, 2011). The Chezy value, which is a measure for flow resistance, for vegetation can be calculated with the following equation (Baptist et al., 2007):

$$C = \frac{1}{\sqrt{\frac{1}{C_b^2} + \frac{C_d n h_v}{2g}}} + \frac{\sqrt{g}}{\kappa} ln \frac{h}{h_v} \tag{6}$$

In the equation above C is the Chezy value of the vegetation, C_b is the bed Chezy coefficient, or the Chezy coefficient for the unvegetated parts. C_d is the drag coefficient, n is the vegetation density (percentage of the area perpendicular to the flow direction), h_v is the vegetation height, g the gravitational acceleration, κ the von Karman constant and h is the water depth. Vegetation affects topography because it is able to influence the sedimentation rate. Vegetation acts as an ecosystem engineer by

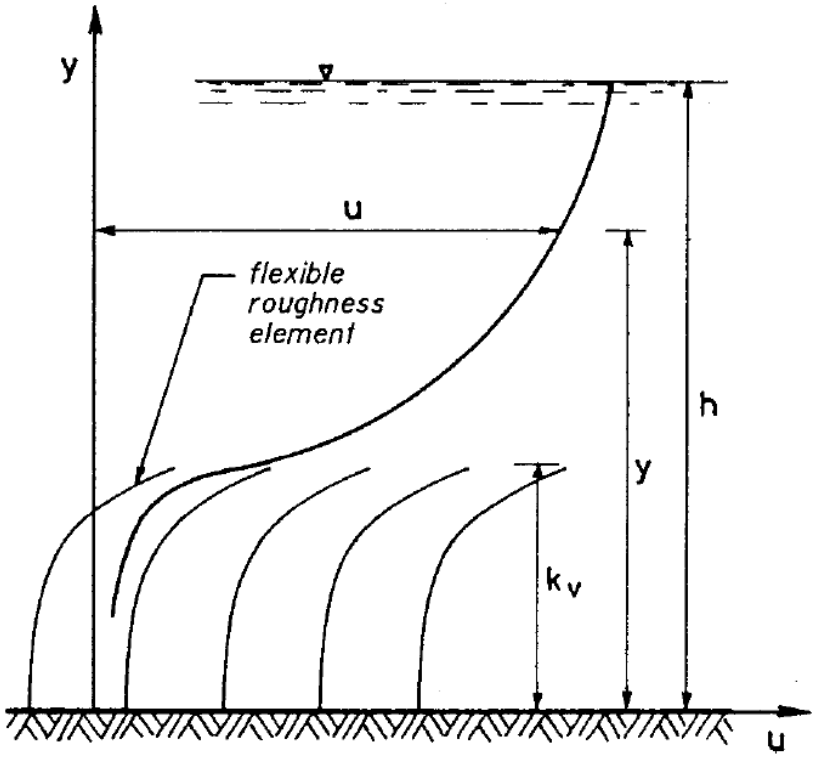

Figure 12: A typical flow velocity pattern through a flexible vegetation patch (Kouwen et al., 1969). As can be seen flow velocity decreases within the patch.

stabilizing the area where it grows, while it makes areas surrounding it more likely to erode (Corenblit et al., 2009).

It is not individual plants which affect flow, but individual plant characteristics and plant density as can be seen in equation 6, therefore the effect of vegetation on the flow can best be studied at patch scale first and later on system scale (Luhar and Nepf, 2013). On a patch scale, flow enters the vegetation patches at their upstream edge and leaves them at the downstream edge, the so called leading and trailing edge. Due to the resistance of the vegetation patch the water levels rise at the leading edge, after which they decrease within the vegetation patch and some distance behind the patch they return to their original values (Figure 13). The flow velocity decreases within the patch due to the increased resistance, and water is forced around the patch which results in increased flow velocities at the patch edges (Bouma et al., 2007b). This could result in increased erosion on the patch edges and thus limit the patch development (Temmerman et al., 2007).

On a system scale vegetation has shown to affect sinuosity in meandering rivers and even to stabilize them entirely (Schuurman et al., 2016). Vegetation is known to increase the sedimentation of fines which increases floodplain formation and thus affects bank strength (Wolanski et al., 2004). In estuaries, however, two different types of models have been used, models with overly simplified hydrodynamics and morphodynamics and models with simplified static vegetation. This has resulted in a relatively poorly understood interaction between morphodynamics and vegetation in estuaries though it is known that some marsh species, for example *S. anglica*, can cause significant sedimentation and thus vertical marsh accretion.

Morphology vegetation interaction

The difficulty of simulating vegetation is its complex interaction with morphodynamics, and its variability in time. Figure 14 has divided the vegetational development and its physical effects on an estuary in six distinct parts (Oorschot et al., 2015). The lower three boxes are the purely physical processes which all do affect or are affected by the vegetational development. Before vegetation is established (colonization) the flow conditions and bed level must have the right dimensions. Once

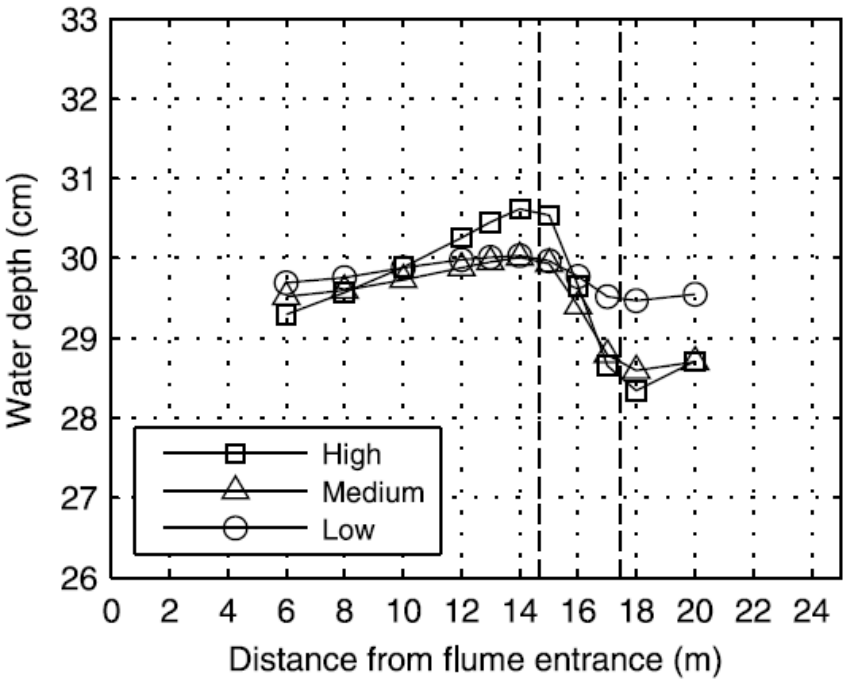

Figure 13: The effect of a vegetation patch on the water depth. The vegetation patch is located between the dashed lines from 14.5 to 17.5 m. Water depth increases at the patch its trailing edge, decreases inside the patch and then goes back to its original height some distance behind the patch (Siniscalchi et al., 2012)

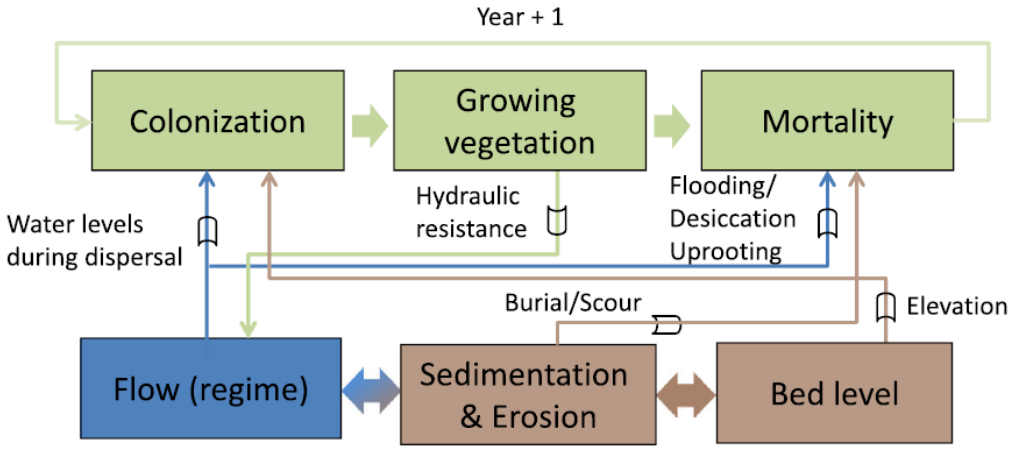

Figure 14: A schematic overview of the interaction between the biotic and abiotic components of an estuarine system (Oorschot et al., 2015).

vegetation grows and develops it increases hydraulic resistance within the vegetation patches. This increased hydraulic resistance leads to additional sedimentation and thus an increasing bed level (Gurnell et al., 2012). Also the root development of plants adds to the cohesion which further decreases erosion. Changes in bed level might trigger new plant species to start colonizing an area which is also an important part of the vegetation morphology interactions. Whether vegetation survives or dies is determined in the mortality part of the overview. As can be seen the flow can cause mortality due to uprooting, but also when the area is inundated to long (flooding) or to short (dessication). Sedimentation and erosion can either bury or scour the plant respectively if they become to large (Oorschot et al., 2015). For submerged vegetation the light availability at the estuary bottom is also a condition for mortality (Van Katwijk et al., 2000). The combination of these processes determines whether the plant will survive another year and continue to grow or that new colonization will have to occur.

As the riparian zone, shoals, mudflats and the marsh zone around an estuary are subject to signifi-

cant ecological stress, the mortality rate of species is high. Burial, flooding, dessication and changing hydrodynamical conditions put large amounts of pressure on species and are able to significantly decrease the vegetation density regularly.

In rivers the occasional mortality of vegetation has shown to be essential to maintain dynamic meandering (Oorschot et al., 2015). Dense vegetation covers cause flows to concentrate in a deep, relatively static, narrow channel while dynamic vegetation causes more actively meandering channels and unvegetated rivers tend to become relatively straight (Oorschot et al., 2015; Dijk et al., 2013a; Nicholas, 2013; Temmerman et al., 2007). Temmerman et al. (2007) have shown that the narrowing and flow concentration due to vegetation also applies to tidal environments.

2.7 Gaps in knowledge

The morphological development of estuaries has been studied relatively little because they could not be modelled analogue until recently. The complex interaction of tides, river currents, morphodynamics, and vegetation makes it difficult to fully understand estuaries. It is quite well known that mud effects bank strength, but it has barely been studied on estuary scale. The influence of vegetation on hydromorphodynamics has been studied extensively, but mainly on patch scale and in a riverine setting, and the effects of vegetation on an estuary spatial scale and engineering time scale which take into account the development of the vegetation have not been studied yet. So there are two major gaps in the present knowledge:

- The effects of mud and vegetation on hydromorphodynamics have been studied mainly on a small/local scale and its effects on a system scale are unknown.
- The two-directional interaction between vegetation and hydromorphodynamics is usually studied one way, which means that the effect of hydromorphodynamics on vegetation development is often ignored and this limits our knowledge of what drives vegetation zonation.

2.8 Hypotheses

2.8.1 Effects of mud on hydromorphodynamics

Mud will likely settle in the areas where flow velocity is small or where water depth is little, because else it does not deposit. This means that it will deposit predominantly around the TMZ and in the intertidal areas. Mud acts cohesively and can add significantly to bank strength in rivers (Dijk et al., 2013b). This increase in bank strength results in narrower, deeper channels in rivers. Mud also shifts braiding systems to meandering ones in rivers (Dijk et al., 2013b), because of which we assume a decrease in braiding index when the mud concentration increases. We assume that mud accumulates close enough to estuarine channels to affect these which leads to the first hypothesis:

1. Mud deposition leads to a decreased braiding index in the estuary but with channels which are deeper.

2.8.2 Patterns and effects of *Spartina anglica*

Vegetation exerts a significant effect on shallow water flow velocities. Flow velocity through vegetation is usually an order of magnitude lower than the flow velocity on bare mudflats with the same water depth (Figure 15)(Bouma et al., 2005). Salt marshes might significantly decreases the mean ebb and flood flow velocities because they can occupy a fairly large part of the estuary width. Because of this *Spartina* can significantly enhance the deposition of cohesive fines (Wolanski et al., 2004).

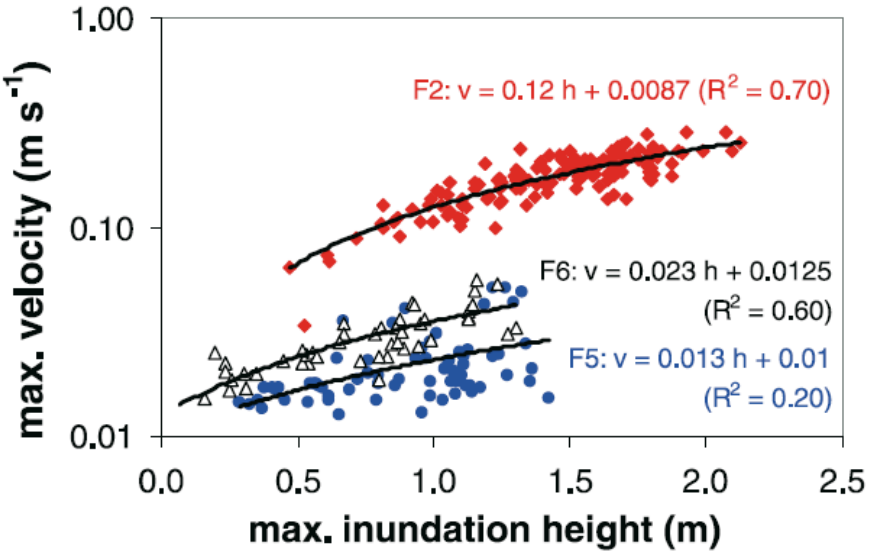

Figure 15: The relationship between waterdepth and flow velocity for a mud flat (F2) and vegetated patch (F5) (Bouma et al., 2005)

The combination of enhanced mud sedimentation and mass conservation (and thus limited amounts of mud in the system) will probably change mud deposition patterns in the estuary.

Because *Spartina* grows in the intertidal areas it probably predominantly increases sediment accumulation on shoals and at the estuary edges. *Spartina* is, however, also known to increase the flow velocity at its patch edges which can drive additional erosion (Figure 16). This additional erosion at the patch edges of *Spartina* will probably limit the lateral development of the intertidal area. Friedrichs (2010) states that channels become more ebb dominant when the tidal amplitude is small with respect to channel depth and the intertidal storage volume is large compared to the channel storage volume. Because *Spartina* drives sedimentation in the intertidal area the intertidal storage volume decreases and its ratio to the channel storage volume decreases as well.

Pringle (1993); Temmerman et al. (2007) assume that *Spartina* is able to deepen estuary channels because they confine these. The process described by Bouma et al. (2007b) shows erosion at the patch edges but this seems like a fairly local effect, which will probably have no influence on estuary channels. Based on Pringle (1993); Temmerman et al. (2007), however, we hypothesize that channels will deepen under influence of *Spartina*. This leads to the following hypotheses:

2. The mud deposition pattern will change and follow the vegetation distribution pattern, which leads to enhanced mud deposition in areas where vegetation grows and probably reduced mud deposition in areas where it does not.
3. *Spartina anglica* drives accretion on shoals and the estuary edges but does not laterally extend the intertidal area.
4. The tidal amplitude, mean ebb and mean flood flow velocities will decrease due to the added flow resistance by *Spartina*.
5. The estuary will become more flood dominated (or less ebb dominated) because *Spartina* drives accretion in the intertidal area which leads to a decreased intertidal storage volume relative to the channels' storage volume.
6. *Spartina anglica* deepens estuary channels because it confines these.

2.8.3 Patterns and effects of *Zostera marina*

Zostera will likely develop on the submerged parts of shoals and other submerged areas more distal from the (main) estuary channel(s) where flow velocity is low and light availability is high. *Zostera*

might drive an increase of shoal and intertidal area because it increases sedimentation in the adjacent subtidal areas. This would, however, exert a negative feedback on *Zostera* its own development as *Zostera* does not survive in intertidal areas. This is a process which is described in detail by Gurnell et al. (2012) (Figure 17). Dependent on how close to the channels *Zostera* survives it might limit the movement of channels and cause them to incise and limit the morphodynamics of the estuary. This leads to our final hypotheses:

7. *Zostera marina* drives the formation of more and larger shoals and an increase in intertidal area.
8. *Zostera marina* drives deepening of estuarine channels.

Figure 16: Typical patches of Spartina in the Gironde estuary which show a strong difference in elevation at its edge, both due to increased sedimentation in the patch and increased erosion on its borders (http://canope.ac-besancon.fr/).

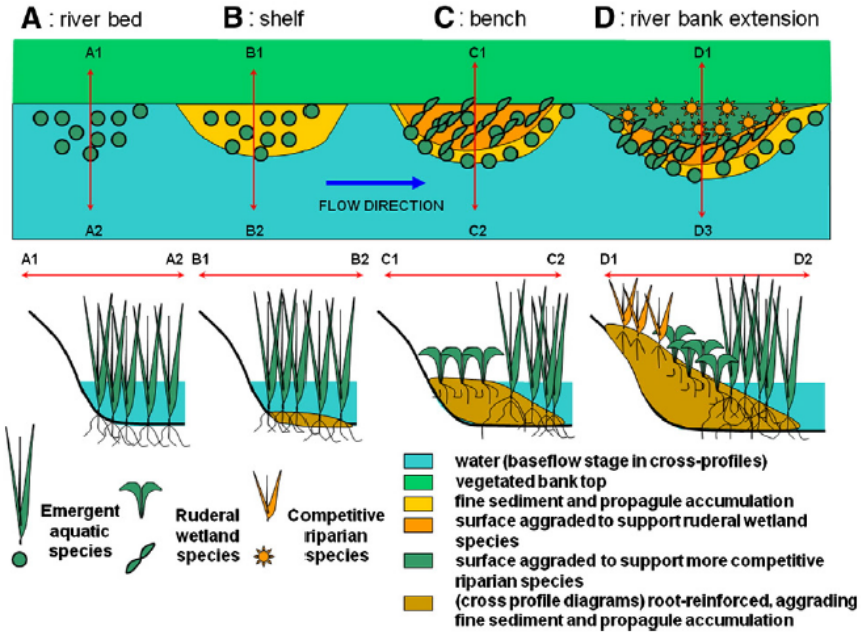

Figure 17: A stand of consecutively aquatic, wetland and riparian species which drive sedimentation and turn a river bed through a shelf and bench towards an extension of the river bank (Gurnell et al., 2012). Though this is an example for a river, similar evolutions might hold for tidal environments with marsh species turning low intertidal areas into high intertidal areas.

3 Methods

Realistic estuarine morphodynamics have been reproduced somewhat in the lab but not yet in computer models. Therefore the choice was made for a combination of modelling and validation with field maps. Recent advances in modelling meandering rivers with realistic vegetation dynamics have been made (Oorschot et al., 2015). This creates the possibility to expand an existing schematic estuary model including sand and mud with dynamic vegetation. A digital model is the best way to quickly assess effects of vegetation on long timescales. It gives control over the conditions in a way that is not possible for real estuaries. Several downsides of this approach are, however, simplification of the natural processes, errors due to the choice of numerical parameters and sensitivity to input parameters. As the interest of the study are channel and estuary dimensions and dynamics from a process based point of view it works best to use a schematic estuary, because we do not want to compare it with the development of an actual estuary yet. We would have liked to start with a fully trumpet shaped estuary but to reduce computation time we started with a somewhat realistic initial bathymetry (Figure 18).

The methods section is subdivided in five parts, first the hydrodynamic and morphological model will be described, then the vegetation model which is implemented in the hydrodynamic and morphological model, third the different scenario's, fourth the data analysis, and last the comparison with field data.

3.1 Hydrodynamic and morphological modelling

A simplified estuary is modelled which consists of a straight coast, converging, trumpet shaped estuary and a straight river at the upstream boundary (Braat and Kleinhans, 2016). The total dimension of the area is 15 by 30 km, consisting of 10 km sea and 20 km estuary and river. The initial estuary mouth is 3.2 km wide and the upstream boundary of the river is 300 m wide (Figure 18A). This estuary is modelled for 1000 years with 0.2 kg/m^3 mud input from the river to obtain an initial bathymetry (Figure 18B). By starting with a realistic initial bathymetry computation time can be reduced. This is a clearly tide dominated estuary, which was created without wave action. A Cartesian co-ordinate system is used with 290 grid points in the M-direction and 162 in the N-direction. A 2-D depth averaged model is used, with a multi-layer bed composition to account for mud cohesiveness effects.

Boundary conditions

The modelled estuary has a discharge from the river and a tide at the seaward boundary. Waves are not included for these would have increased the running time of the model to much. The river consists of 4 grid cells with a constant discharge. The total river discharge is $100 m^3/s$, similar to the discharge through the Western Scheldt. An equilibrium sand concentration boundary is used for the river. A tidal wave propagates along the coast with an 1.5 m amplitude and 12 hour period, similar to the M2 tide with an amplitude typical for the Dutch coast. It is defined through two harmonic boundaries at the north and south part of the sea with a three degrees phase difference.

Calculations

The model uses two main hydrodynamic equations, the first being the conservation of mass equation:

$$\frac{\partial h}{\partial t} + \frac{\partial hu}{\partial x} + \frac{\partial hv}{\partial y} = 0 \tag{7}$$

In this equation h is the waterdepth, t is time, u is the flow velocity in the x-direction and v is the flow velocity in the y-direction. Equation 7 basically states that any change in water depth follows from a gradient in q_x in the x-direction or a gradient in q_y in the y-direction, for a 2-D model. Momentum is calculated through momentum conservation as well:

$$\frac{\partial u}{\partial t} + u\frac{\partial u}{\partial x} + v\frac{\partial u}{\partial y} + g\frac{\partial z_w}{\partial x} + \frac{gu\sqrt{u^2+v^2}}{C^2 h} - V\left(\frac{\partial^2 u}{\partial x^2} + \frac{\partial^2 u}{\partial y^2}\right) + F_x = 0 \tag{8}$$

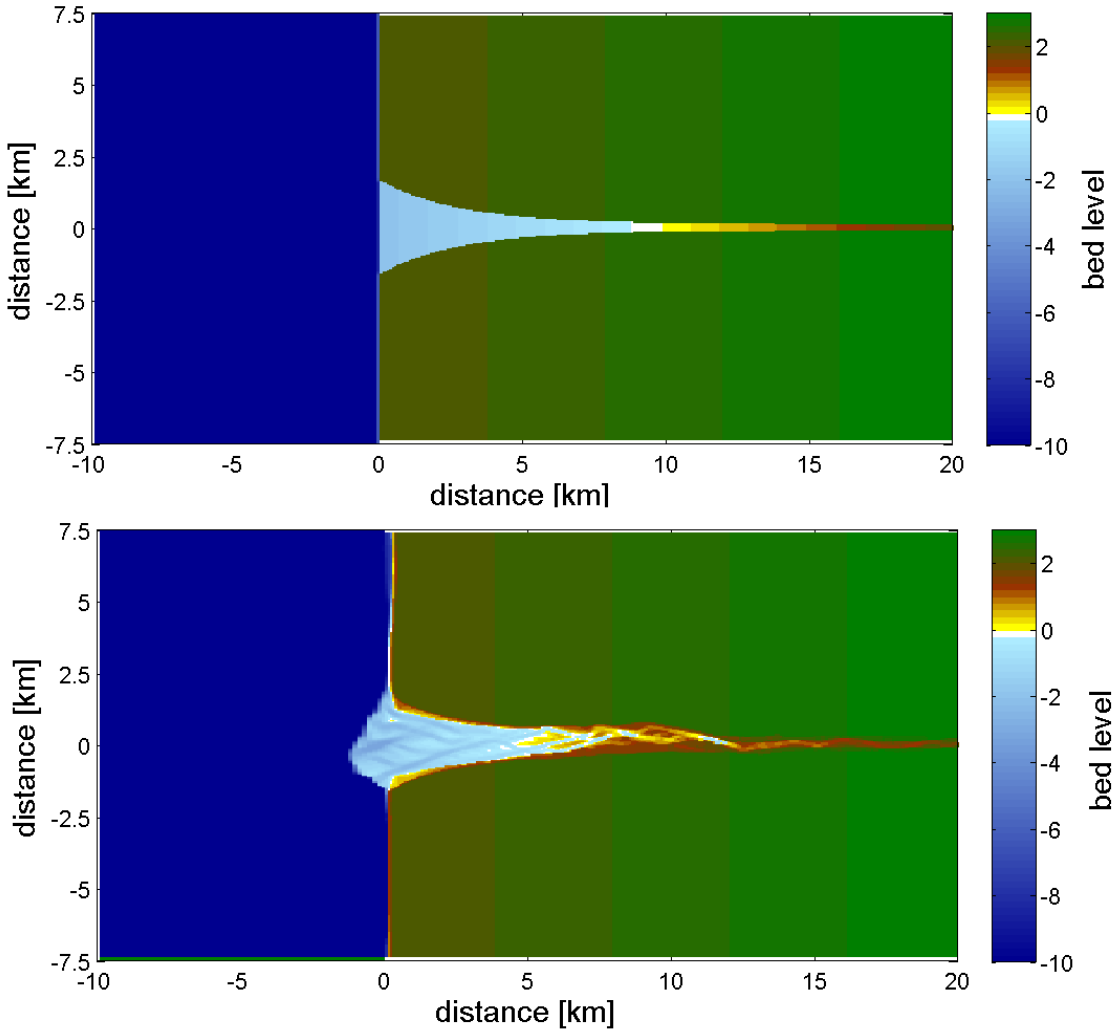

Figure 18: A) The initially trumpet shaped estuary which was modelled for 1000 years to obtain the initial bathymetry for our simulations. B) The initial bathymetry used for the simulations in this research.

$$\frac{\partial v}{\partial t} + u\frac{\partial v}{\partial x} + v\frac{\partial v}{\partial y} + g\frac{\partial z_w}{\partial y} + \frac{gv\sqrt{u^2+v^2}}{C^2 h} - V\left(\frac{\partial^2 v}{\partial x^2} + \frac{\partial^2 v}{\partial y^2}\right) + F_y = 0 \tag{9}$$

In which z_w is the water surface height, C is the Chezy roughness, which will in our model be substituted by the vegetation model, V is the horizontal eddy viscosity and $F_{x,y}$ is the stream line curvature driven acceleration term (Schuurman et al., 2013). These two equations describe the velocity variations in the x-y plane in one grid cell over time under influence of advection, eddy diffusivity, friction, changing water depth and stream line curvature.

Sediment transport is calculated using different formulas for the different sediment constituents. Sand transport in case of a non-cohesive bed is calculated with the Engelund-Hansen sediment transport predictor:

$$S = S_b + S_{s,eq} = \frac{0.005\alpha q^5}{\sqrt{g}C^3 \frac{\rho_s - \rho_w}{\rho_w} D_{50}} \tag{10}$$

This equation calculates the total sediment transport, but it does not distinguish between bedload (S_b) and suspended load ($S_{s,eq}$). In the function α is a calibration coefficient, q the one dimensional discharge, ρ_s the sediment density, ρ_w the water density and D_{50} the median grainsize. The mud fraction of the model is calculated by using the Partheniades-Krone equations:

$$E_m = M_m\left(\frac{\tau_{cw}}{\tau_{cr,e}} - 1\right) \qquad \tau_{cw} > \tau_{cr,e} \tag{11}$$

Parameter	Value	Unit	Reference or motivation
Timespan model run	50	year	Minimum time for significant morphological changes
Hydrodynamic timestep	0.2	min	Based on grid cell size
Morphological scale factor	30	-	Required to avoid large scale burial and scour of seedlings
Timestep bed-level change	6	min	
Timestep vegetation	21600	min	Captures most important biological processes
Grid size (width x length)	15x30	km	Some sea area and the estuary
Cell size estuary (width x length)	50x80	m	
Cell size sea (width x length)	125x230	m	
Chezy value bare substrate	50	$m^{\frac{1}{2}}/s$	Default Delft3D value
D50 (sand)	$3*10^{-4}$	m	Medium sand
Sediment transport predictor	Engelund-Hansen	-	(Schuurman et al., 2013)
Tidal amplitude	1.5	m	Realistic value for the Dutch coast
Tidal period	12	h	Roughly M2 tide
River discharge	100	m^3/s	Discharge through Western Scheldt

Table 1: Some of the important Morphodynamic parameters. For a full list of all settings see Appendix B

$$D_m = w_s c_b \left(1 - \frac{\tau_{cw}}{\tau_{cr,d}}\right) \tag{12}$$

In the equations above E_m is the mud erosion, M_m is an erosion parameter, τ_{cw} is the maximum bed shear stress due to currents and waves, $\tau_{cr,e}$ is the critical erosion shear stress. D_m is the mud deposition flux, w_s is the mud settling velocity and c_b the average sediment concentration in the near bottom layer.

Spiral flow is of crucial importance in a depth-averaged simulation to create pointbars in river bends and is therefore included in the model. The bedload transport direction ϕ_τ is given by the following equation:

$$tan(\phi_\tau) = \frac{v - \alpha_I \frac{u}{U} I_s}{u - \alpha_I \frac{v}{U} I_s} \tag{13}$$

In this equation U is the depth averaged flow velocity, I_s is the spiral flow intensity and α_I is given by the following equation:

$$\alpha_I = \frac{2}{\kappa^2}\left(1 - \frac{1}{2}\frac{\sqrt{g}}{\kappa C}\right) \tag{14}$$

Last bed slope effects are included in the model to simulate a deviation in sediment transport direction from the shearstress direction due to grains moving downslope. The sediment transport in the x and y direction under influence of the bed slope effect is given by:

$$q_x = q_s\left(cos(\phi_t) - \frac{1}{f(\theta)}\frac{\partial z_b}{\partial x}\right) \tag{15}$$

$$q_y = q_s\left(sin(\phi_t) - \frac{1}{f(\theta)}\frac{\partial z_b}{\partial y}\right) \tag{16}$$

$f(\theta)$ is given by the following equation:

$$f(\theta) = \alpha\theta^\beta \tag{17}$$

In this equation theta is the shields parameter and α and β are calibration parameters.

Bed composition

The bed composition is of major importance in this research as the mud content determines whether the bed behaves cohesive or not. To model this a sand-mud bed module is used which splits the bottom in 50 Eulerian layers and 1 Langrangian toplayer. The advantage of the Langrangian toplayer is that it has a constant thickness and moves up or down with the sedimentation or erosion. The advantage of this method is that the grid cells have a constant height, but it creates artificial diffusion between

the layers due to its vertical movement (and can thus reduce mud content in a single layer). Eulerian layers are able to aggrade and erode through changing the thickness of the toplayer while keeping the other cells fixed in size and location. The combined approach results in a realistic massflux in the bottom and thus a realistic bed composition while reducing the effect of sedimentation or erosion on the time scale of the system as is the case with a fully Eulerian bottom.

Natural input parameters

Two sediment types are included in the model, a sand fraction and a mud fraction. The sand fraction has a 2650 kg/m^3 density and a dry bed density of 1600 kg/m^3. A median grainsize D_{50} of $0.3 * 10^{-3}$m is specified with a piecewise loguniform spreading which results in a D_{10} of $0.225 * 10^{-3}m$ and a D_{90} of $0.45 * 10^{-3}m$, this is a typical medium sand fraction. The mud fraction has the same dry bed density and specific density as the sand fraction, but some different characteristics were specified to simulate its erosion and settling processes. The settling velocity in fresh and salt water is set to $2.5 * 10^{-4}$ m/s, the critical sedimentation shear stress is $1*10^3$ N/m^2 and the critical erosion shear stress is $2 * 10^{-1}$ N/m^2. The critical mud content above which the bed behaves cohesive was set to 40%, this is approximately 8% clay if the mud contains 20% clay content. The water density was set to 1000 kg/m^3 and the gravitational acceleration to 9.81 m/s^2.

Numerical input parameters

It is important to chose numerical parameters in such manner that they fit both the hydrodynamic and morphological model as well as the vegetation component. For the morphodynamic modelling a morphodynamic acceleration factor is applied. This factor increases the sediment transport by a factor to reduce simulation time. For estuaries values up to approximately 500 provide realistic results, which enables simulations of more than 1000 years. The vegetation model, however, measures burial and scour of vegetation through comparing the bed level before and after a certain time. If the morphology is accelerated by a factor 500 this results in large erosion and/or deposition within an ecological timestep and thus massive vegetation mortality. An acceleration factor of 30 is used, because test simulations with higher values resulted in large scale burial and scour. A timestep of 0.2 minutes was found to give adequate results because it is small enough to capture the required detail in water movements as indicated by the courant number. A year of 360 days was simulated because this fits an integer amount of morphological accelerated 12 hour tidal waves. To be precise, 24, 12 hour tidal periods with a 30 times morphological acceleration. This is required to avoid jumps in the water level on the year boundaries. Finally two important parameters are the flood dry boundary and the dry cell erosion factor. For the flood dry boundary a value of 8 cm water depth is taken. A flood dry boundary is required because Delft3D has problems with making cells fall dry completely. This is a fairly large uncertainty in the model when it comes to modelling intertidal area and estuary width because a different threshold can change the area which is considered dry significantly. When it comes to erosion of dry cells, this is done by taking 50% of the erosion of neighbour cells. This results in sloping areas instead of cliff formation, which might affect the area suitable for different vegetation types.

3.2 Vegetation model

Vegetation was modelled in a Matlab model which interacts with the Delft3D model. The Delft3D model calculates hydro- and morphodynamics and its water level, bed elevation and flow velocity were used as input for the matlab vegetation model. The Matlab model calculates vegetation development and exports this to the Delft3D model where the new flow resistance is calculated, which replaces the Delft3D Chezy value.

Two different habitats were modelled, salt marshes and submerged areas, both with one characteristic species. The included marsh species is *S. anglica* because this is a dominant species in north-western Europe (Corenblit et al., 2009). The subtidal species used is *Z. marina* because this is a typical eel grass which used to be abundant and has typical characteristics for a broader range

of subtidal plants. An ecological timestep is created to account for the main ecological processes on a system scale. The time involved is approximately two weeks. After each timestep each cell in Delft3D got updated with new vegetation characteristics and vegetation location information. Each vegetation type is described by (Table 2):

- initial shoot length
- initial root length
- maximum age
- (initial) stem diameter
- growth curves
- seed dispersal timing
- life stages
- critical light penetration

The life stages contain varying values for the plants resistance to flow velocity, dessication, and flooding, but also variables for the number of stems per square meter, and the drag coefficient (Table 3). This enables the model to include evolution in the plants their shape and resistance with age.

Initial marsh vegetation colonizes the areas between low and high water, during the month(s) of seed dispersal. Seeds transported by the flow end up on cells which are flooded, but will not establish in cells which are permanently inundated. Initial subtidal vegetation establishes itself below the high tide level as seeds end up anywhere below the high tide, but the ones in the intertidal area die off quickly. The model assumes an infinite seed supply, which means that all cells which are between high and low water for marsh species and below high water for subtidal species, during the months of seed dispersal, will obtain the plant cover which was defined as initial cover. If a cell is already partially covered by (other) vegetation it is filled up with seedlings till a larger fraction of the cell is covered. This means that multiple vegetation types can be present in one cell (and compete for space).

Vegetation mortality is calculated on a yearly basis based on the subsequent days the vegetation was either dry or flooded, maximum flow velocities experienced, scour and burial. Mortality through burial and scour was determined by comparing the shoot length with the sedimentation or the root length with the erosion respectively. If erosion exceeds the root length, or sedimentation exceeds the shoot length the plant dies. Erosion and deposition are determined through comparing bedlevel change between two subsequent ecological timesteps. The relation between dessication, flooding and flow velocity and mortality is not as straightforward. If a fixed value for mortality due to flow velocity would be included this would cause all vegetation to suddenly die if the flow accelerates to this threshold. Instead a threshold value with a dose-effect relation is included for dessication, flooding and flow velocity (Figure 19) (Oorschot et al., 2015). The number of plants removed from each cell is determined by multiplying the mortality as calculated with the dose-effect relation with the initial plant fraction. The new fraction of the plant in the cell is then determined by subtracting these plants from the total number of plants in the cell at that moment. By multiplying with the initial fraction instead of the current fraction it is avoided that low unnatural plant covers remain if mortality remains just below 100%. If vegetation reaches its maximum age as defined it will die naturally. Table 2 and 3 give the characteristics of both vegetation types.

Light mortality is calculated with a similar dose effect relation as dessication, flooding and flow velocity, but light penetration is not standard calculated by Delft3D. Instead a function for light penetration based on suspended sediment concentration was used (Figure 20). The following equation gives a measure for visibility in the water (van Zuidam et al., 2014):

$$Sd = -0.183 + 2.969/\sqrt{C_s} \tag{18}$$

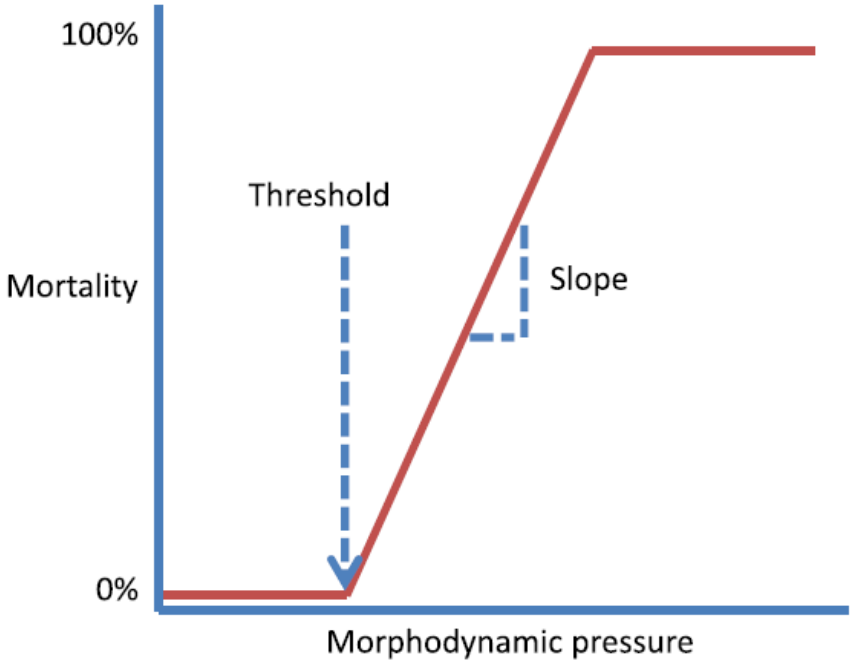

Figure 19: The dose-effect relation between morphodynamic pressure and mortality (but applies to hydrodynamic pressure as well). The plants can survive a certain amount of morphodynamic pressure, up to the threshold. After the threshold an increasingly large part of the vegetation dies due to the unfavourable conditions. A steep slope indicates a sudden death once the threshold is exceeded while a gentle one indicates a slow increase in mortality (Oorschot et al., 2015).

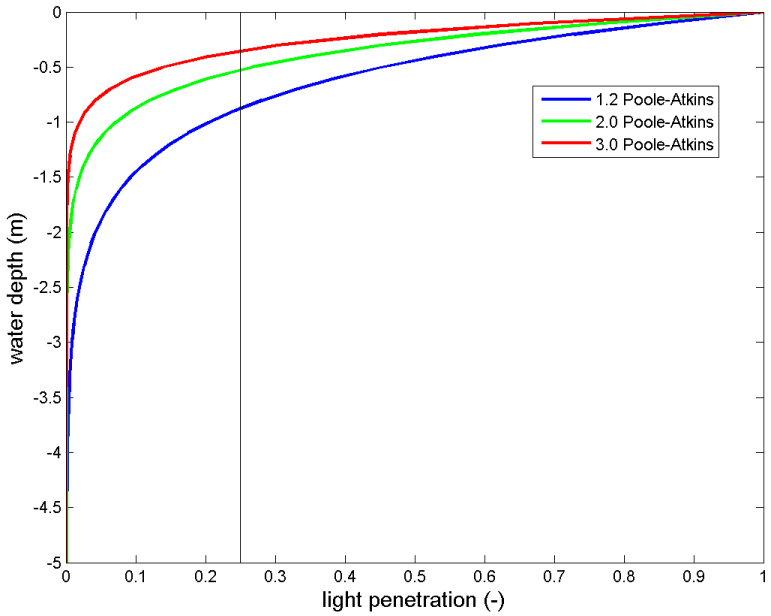

Figure 20: Light availability for a 10 mg/l sediment concentration for different Poole-Atkins values. The black line at 0.25 light penetration gives the critical value used for *Zostera*.

Parameter	Unit	Vegetation type 1	Vegetation type 2	Reference or motivation
Vegetation type	-	*Spartina anglica*	*Zostera marina*	Common European subtidal and marsh species
Maximum age	yr	20	50	
Initial root length	m	0.02	0.01	Deng et al. (2009), Qin et al. (2016)
Initial shoot length	m	0.07	0.05	Deng et al. (2009), Qin et al. (2016)
Initial stem diameter	m	0.001	0.001	
Logarithmic growth factor root	-	0.19	0.1	Deng et al. (2009), Qin et al. (2016)
Logarithmic grow factor shoot	-	1	0.88	Nehring and Adsersen (2006)
Logarithmic growth factor stem diameter	-	0.005	0.007	
Timing of seed dispersal	Month	April	April	Nehring and Adsersen (2006)

Table 2: Parametrization of general characteristics of *Spartina anglica* and *Zostera marina* in the model

Parameter		*Spartina anglica*			*Zostera marina*			
	Unit	Ls 1	Ls2	Ls3	Ls1	Ls2	Ls 3	Reference or motivation
Numbers of years in life stage	yr	1	10	9	1	29	20	...
Number of stems	$stems/m^2$	13.000	1500	600	300	700	700	Nehring and Adsersen (2006), Qin et al. (2016)
Area fraction (0-1)	-	0.05	0.5	0.8	0.05	0.5	0.8	
Drag coefficient	-	1	1	1	1	1	1	...
Desiccation threshold	days	360	360	360	10	10	10	No desiccation assumed for *S. anglica*, guess for *Z. marina*
Desiccation slope	-	1	1	1	0.75	0.75	0.75	No dessication for *S. anglica*, fast dessication for *Z. marina*
Flooding threshold	days	20	40	40	360	360	360	No flooding for *Z. marina*, guess for *S. anglica*
Flooding slope	-	0.75	0.75	0.75	1	1	1	No flooding for *Z. marina*, fast flooding for *S. anglica*
Flow velocity threshold	m/s	0.5	1	1	0.25	0.5	0.5	Wijgergans and de Jong (1999)
Flow velocity slope	-	0.75	0.75	0.75	0.75	0.75	0.75	guess
Critical light penetration	-	360	360	360	0.25	0.25	0.25	Deltares HABITAT
Light penetration slope	-	1	1	1	0.5	0.5	0.5	guess

Table 3: Parametrization of life stage specific characteristics of *Spartina anglica* and *Zostera marina* in the model

In this equation Sd is a water sight variable and C_s is the suspended sediment concentration. It is an empirical relationship calibrated for the Markermeer. The Sd value is used to calculate the extinction coefficient with the following equation:

$$K = c/Sd \tag{19}$$

In this equation K is the light extinction coefficient and c the Poole-Atkins constant (value between 1.2 and 3.0 (Figure 20) (Bakema, 1988). The light extinction is then given by:

$$I_d = I_0 * e^{-Kd} \tag{20}$$

In this equation I_d is the light intensity at depth d, I_0 is the light intensity at the surface and d is the water depth. In this research a constant light intensity at the water surface is assumed which reduces equation 20 to:

$$P_l = e^{-Kd} \tag{21}$$

P_l is the relative light penetration, the fraction of the surface light which reaches the water bottom. Then a dose effect relationship between the number of days that a minimum light penetration value is not reached and mortality is applied.

3.3 Modelled scenarios

Several scenario's have been run to test the effect of mud and vegetation on estuary morphodynamics. The simulations without vegetation have been performed solely through Delft3D without matlab to reduce the simulation time. This has, however, resulted in a different output frequency. Simulations without vegetation have data every 3 hours and simulations with vegetation every hour. This implies that analyses at a fixed moment in time can be compared (think of bed level distributions, estuary width, braiding index etc.) but analyses which are dependent on the temporal data resolution cannot be compared as easily (think of maximum tidal velocity and intertidal area) because extreme values might not be captured in the larger 3 hour data interval while they are captured in the 1 hour interval. To compensate for this problem the default simulation without mud and vegetation has been run through the combined Delft3D and matlab model as well to allow for comparison. The simulations with a given mud concentration but no vegetation can, however, not be directly compared to simulations with vegetation when it comes to analyses dependent on temporal data resolution.

A default run without mud and without vegetation was created (Table 4 #1). This default simulation has been used to test several variations. First two different mud concentrations are added to the simulation, subsequently 20 mg/l and 50 mg/l. After the investigation of mud, *Spartina* was added. The analysis of *Spartina* consists of three parts, the effect of *Spartina* with respect to increasing mud concentrations, a small sensitivity analysis with respect to *Spartina*'s modelled characteristics and the influence of the initial bathymetry. The effect of the initial bathymetry was investigated because we hypothesized that *Spartina* colonizes intertidal areas but does not increase its own living area and thus the initial presence of intertidal area might have significant influence on the effects of *Spartina*.

Zostera has been modelled in different combinations of suspended sediment concentration, maximum height, Poole-Atkins constants and colonization patterns. This has been less structured because we are still looking for relevant default conditions (Table 4). Finally one successful run with both *Spartina* and *Zostera* was performed (Table 4 #26).

3.4 Data analysis: methods and choices

Data were analysed over time and over space. In this way both changes in different parts of the estuary and changes over the entire estuary can be found. The data were analysed both qualitatively/visually, and quantitatively/mathematically. The analyses can be split into three parts, vegetation zonation and sediment accumulation patterns, morphodynamics, and hydrodynamics, which of course do interact.

#	sediment input	Vegetation type(s)	PA constant	Colonization	Special characteristic
1	-	-	-	-	default scenario, performed with 1 and 3 hour temporal resolution
2	0.02 kg/m^3 mud	-	-	-	-
3	0.05 kg/m^3 mud	-	-	-	-
4	0.02 kg/m^3 sand	-	-	-	0.02 kg/m^3 sand additional to the equilibrium boundary
***Spartina*:**					
5	-	*S. anglica*	-	entire area	-
6	0.02 kg/m^3 mud	*S. anglica*	-	entire area	-
7	0.05 kg/m^3 mud	*S. anglica*	-	entire area	-
Sensitivity:					
8	-	*S. anglica*	-	entire area	less resistant seedlings (flooding threshold 10 days, flow velocity threshold 0.25m/s)
9	-	*S. anglica*	-	entire area	late seedling dispersal (October)
10	-	*S. anglica*	-	entire area	high initial area fraction of vegetation (0.4 instead of 0.05)
***Spartina* reproducibility:**					
11	-	-	-	-	different initial bathymetry , performed with 1 and 3 hour temporal resolution
12	0.02 kg/m^3 mud	-	-	-	different initial bathymetry
13	0.05 kg/m^3 mud	-	-	-	different initial bathymetry
14	-	*S. anglica*	-	entire area	different initial bathymetry
15	0.02 kg/m^3 mud	*S. anglica*	-	entire area	different initial bathymetry
***Zostera*:**					
16	-	*Z. marina*	-	entire area	-
17	0.02 kg/m^3 mud	*Z. marina*	-	entire area	-
18	0.05 kg/m^3 mud	*Z. marina*	-	entire area	-
19	-	*Z. marina*	-	entire area	continuous bending assumed (logarithmic growth factor shoot:0.26)
20	0.02 kg/m^3 mud	*Z. marina*	-	entire area	continuous bending assumed (logarithmic growth factor shoot:0.26)
21	0.05 kg/m^3 mud	*Z. marina*	-	entire area	continuous bending assumed (logarithmic growth factor shoot:0.26)
22	0.02 kg/m^3 mud	*Z. marina*	1.2	entire area	continuous bending assumed (logarithmic growth factor shoot:0.26)
23	0.02 kg/m^3 mud	*Z. marina*	2.5	entire area	continuous bending assumed (logarithmic growth factor shoot:0.26)
24	0.05 kg/m^3 mud	*Z. marina*	1.2	entire area	continuous bending assumed (logarithmic growth factor shoot:0.26)
25	0.02 kg/m^3 mud	*Z. marina*	1.2	random 10%	continuous bending assumed (logarithmic growth factor shoot:0.26)
***Zostera* & *Spartina*:**					
26	0.02 kg/m^3 mud	*Z. marina*, *S. anglica*	1.2	random 10%	continuous bending assumed (logarithmic growth factor shoot:0.26)

Table 4: Different scenario's which have been run to test the influence of mud and vegetation

In the analyses the cells covered by the sea (more than 50% of the wet area) were excluded. The sea is necessary to model realistic tidal water movements, but is not within the scope of interest in this research. Due to its large area the sea also exerts a strong influence on analyses of the wet area, which is another reason to leave it out. For the data analysis the 24th timestep of each year is used. Finally all results which involve the estuary bathymetry have been detrended with the valley gradient before analysis.

When it comes to morphodynamics important analyses are the total braiding index and the change in braiding index over the estuary. This is determined by comparing the bed elevation with the mean water level and counting its intersections (Schuurman et al., 2013). The braiding index calculated this way determines the number of channels, regardless of them being active or not.

The estuary width is determined as the active area during high tide, with the active area defined as all cells with at least 8 cm water. This means that if there are shoals or bars which are exposed during high tide, these are subtracted from the estuary width but this does probably never happen. The intertidal area was determined by comparing the maximum width averaged active area (area with wet cells) with the minimum width averaged active area during the tidal cycle. In this manner the intertidal area is measured correctly also for progressive tides because the maximum and minimum width might occur at different moments in time for the different cross sections. The 5th percentile, median and 95th percentile bed level are calculated for the active area at high tide. This gives an indication of the depth of the main channel (5th percentile) and higher intertidal area (95th percentile). Bed level distribution plots have been made for the initial and final situations to compare the bathymetric development of the estuary. This shows which area with respect to the tidal regime is subject to erosion or deposition.

The ebb and flood velocities are measured as the width averaged minimum and maximum over the tidal cycle respectively. Next to this, the maximum and minimum ebb and flood velocities over the width are also measured. We trace the development of the ebb and flood velocity in the channels and the width averaged ebb and flood velocity. For the tidal amplitude the maximum and minimum water level over a tidal cycle in each estuarine cross section are determined and subtracted. Neither a straight line from the sea to the river boundary nor a width averaged value was used because these might include intertidal areas in their calculation which lowers the determined tidal amplitude.

Bar diagrams which show the relative mud cover with respect to vegetation cover, divided in 0.05% intervals, are created. This shows whether vegetation enhances mud deposition. A cross corre-

lation is made between the scenario with *Spartina* and 20 mg/l mud and the simulation with 20 mg/l mud without *Spartina*. This is done to test whether the locations which are subject to significant erosion or deposition which coincides with *Spartina* presence also experience this erosion or deposition without *Spartina*. As a final remark, most plots have been treated with a 3 cells moving average filter to smooth outliers.

3.5 Comparison between model and field data

Complete maps of (submerged) estuarine vegetation are fairly rare which makes it difficult to qualitatively validate the model. As time series are even more rare it is difficult to make a decent assessment of how well the model represents nature. To get a first indication of the validity of the model, however, the available maps for estuarine vegetation distribution are compared with the final outcome of the model based on visible patterns. Vegetation distribution will be assessed by its zonation, and visual cover fraction. This gives a first indication of the validity of the model.

4 Results

Adding mud and vegetation to simulations has significant influence on the morphodynamic development of estuaries within 50 years. Figure 21 shows the bathymetries, vegetation covers and mud cover of several scenario's after 50 years. As can be seen the addition of *Spartina*, *Zostera* or a combination of the two gives different final bathymetries. The addition of mud without vegetation results in mudflats fringing the estuary. When vegetation is present, however, this mud distribution pattern changes and follows the vegetation zonation. This is especially the case for the simulations with *Spartina*. *Zostera* seems to have a fairly limited effect on the mud distribution in the estuary (Figure 21). When *Zostera*, however, is simulated together with *Spartina* it appears to affect the mud distribution, but probably through changing the bathymetry and not so much through enhancing mud deposition. When looking at figure 21 it is important to notice that for the simulations with *Zostera* and *Zostera* and *Spartina* not only mud was added to the simulation but the colonization module of *Zostera* was changed as well. *Zostera* no longer colonizes all submerged cells in the simulations with 20 mg/l mud, but a random 10% to avoid the overflowing which was visible in the simulations without mud.

Addition of mud to the simulations also strongly affects the vegetation patterns. *Spartina* concentration in the estuary increase when mud is added. This is because it drives sedimentation in the lower intertidal zone where the physical conditions are harsh for *Spartina*. Through this sedimentation a situation is reached where *Spartina* survives more easily which results in higher concentrations. *Zostera* on the other hand starts to disappear if mud is added to the simulations because it is sensitive to light availability, and light availability decreases if the suspended sediment concentration increases. A very important observation is therefore that not only the mud accumulation pattern changes significantly under influence of vegetation but also the vegetation patterns are changed when mud is available. This points to a two-directional interaction between mud and vegetation.

In the following parts of this section the results of the model simulations are presented. First the effects of mud are described, followed by *Spartina*, *Zostera*, and finally a combination of these. For *Spartina* a sensitivity and reproducibility analysis is included.

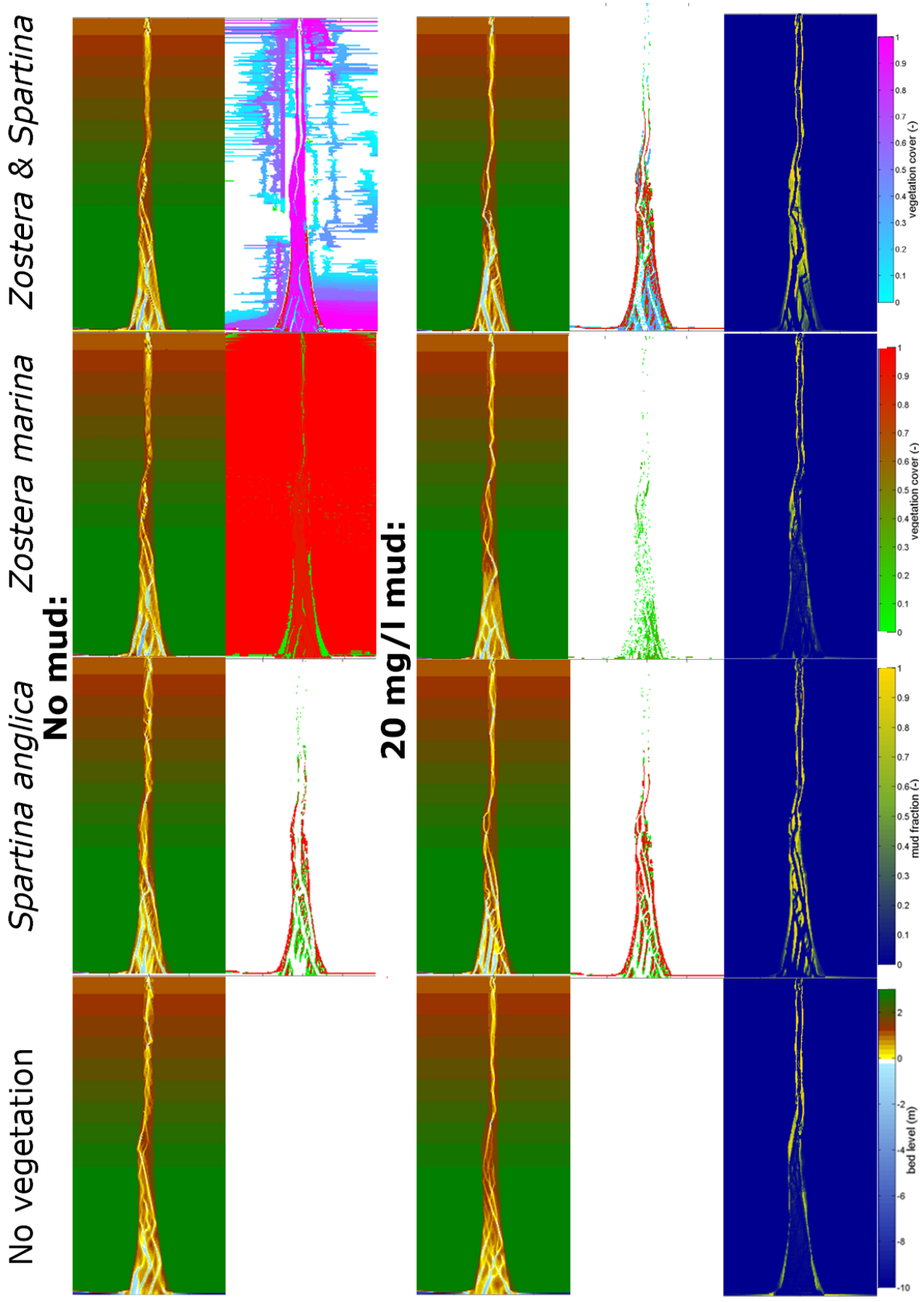

Figure 21: Bathymetry, vegetation cover and mud cover after 50 years of simulation for several scenario's. The simulations with *Zostera* and *Zostera* and *Spartina* without mud were stopped after approximately 30 years and the simulation with *Zostera* with 20 mg/l mud after 32 years because of overflowing.

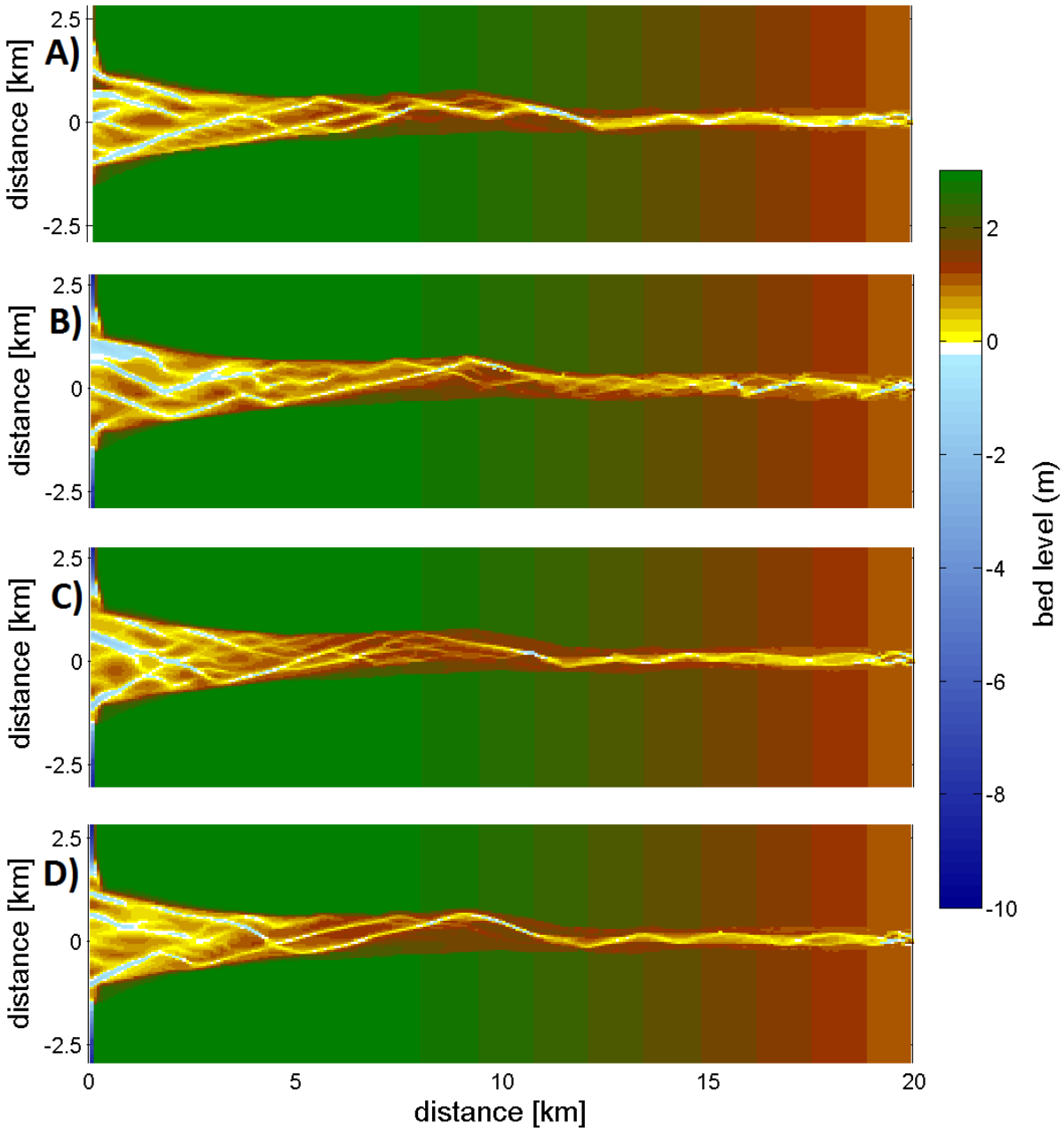

Figure 22: A) the initial bathymetry, and the bathymetry after 50 years for B) no mud, C) 20 mg/l mud at the river, and D) 50 mg/l mud at the river

4.1 Effects of mud on hydromorphodynamics

The inclusion of mud in the simulations results in significant changes in the bathymetry after 50 years. Figure 22 shows (A) the initial bathymetry and the bathymetry after 50 years for (B) the simulation without mud, (C) with 20 mg/l mud and (D) with 50 mg/l mud from the river. There are two pronounced trends when mud is added to the simulations.

First of all there is a significant decrease in morphodynamic activity in the river reach. This can be explained by the accumulation of cohesive mud on the edges of the river. A continuous mudcover has developed at the edges of the river which laterally confines it (Figure 23). This mud cover continuous along the edges of the estuary up to the estuary mouth. The mudflats at the edges of the estuary can reach cover fractions of up to 100%. These fractions are usually higher for the simulation with 50 mg/l mud. Not only the mud cover in individual cells is higher for simulations with more mud, but the lateral extent of the mud accumulations is larger as well (Figure 23).

The second trend is a decrease in the number of parallel channels (braiding index) in the estuary. This is most clear in the simulation with 50 mg/l mud around 9 km. A large mudflat has developed here which has forced the system to a single channel (Figure 23). This process of canalization and reduction of the braiding index occurs in areas where the critical mud fraction of 40% in the toplayer is exceeded (Figure 22, 23).

The outer zone of the estuary shows not as much canalization as the inner zone (for a 50 mg/l mud content), and there are no canalization effects for the simulation with 20 mg/l mud. Apparently

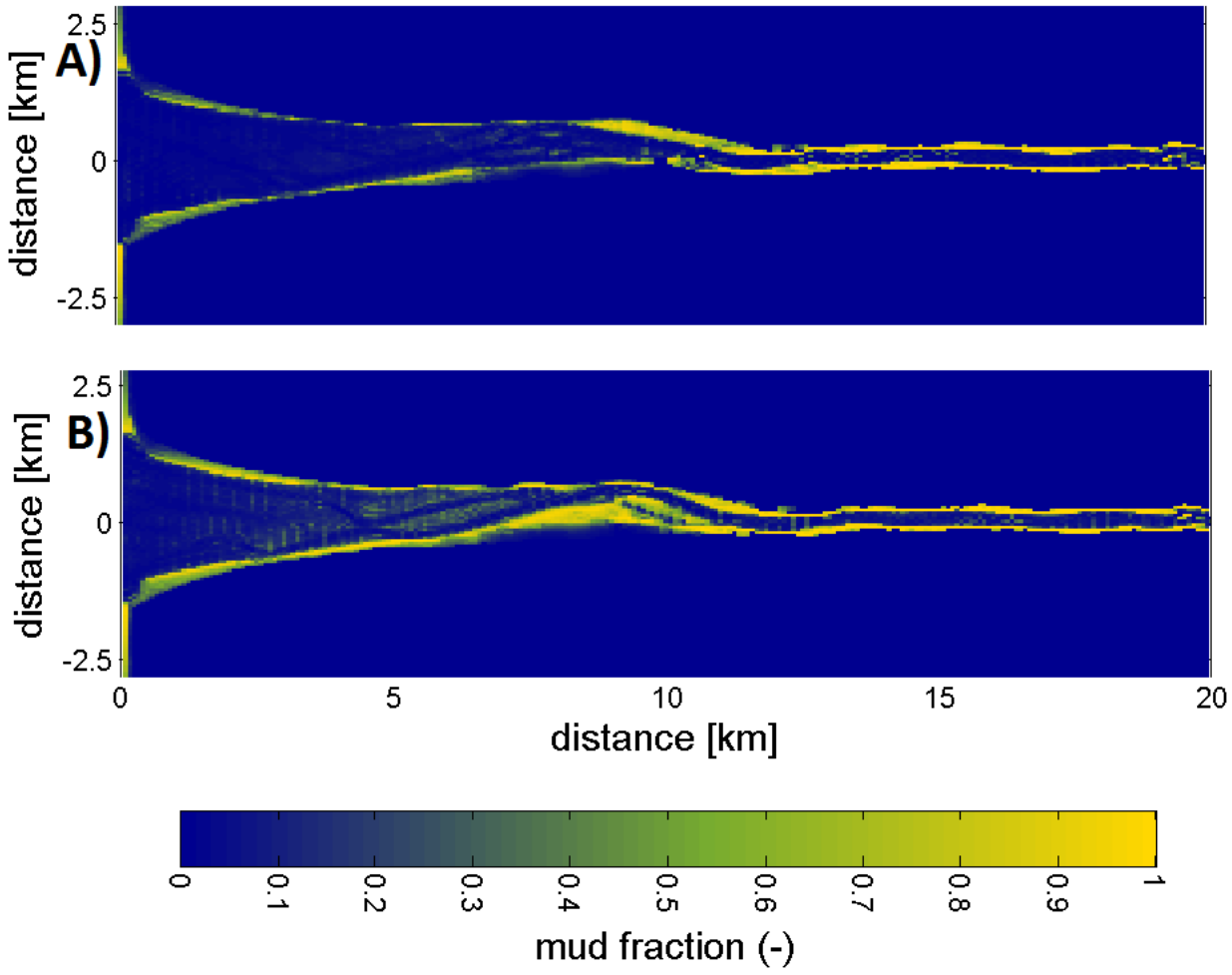

Figure 23: The final mud cover in the top layer after 50 years for A) 20 mg/l mud at the river, and B) 50 mg/l mud at the river

mud accumulates more easily on the intertidal areas at the edges of the estuary than on the tidal bars. Because of this, bars accumulate some mud when the concentration is 50 mg/l and do barely accumulate mud when the concentration is 20 mg/l. This can be explained by the higher settling flux of mud when concentrations increase (eq. 5). Because mud does not accumulate as much on tidal bars, it is less able to influence the channels in the outer zone of the estuary.

4.1.1 Morphodynamics

The presence of mud stabilizes the highest intertidal areas, but does not increase these. There is no clear influence of mud on the channel depth though mud drives a decrease in braiding index for the

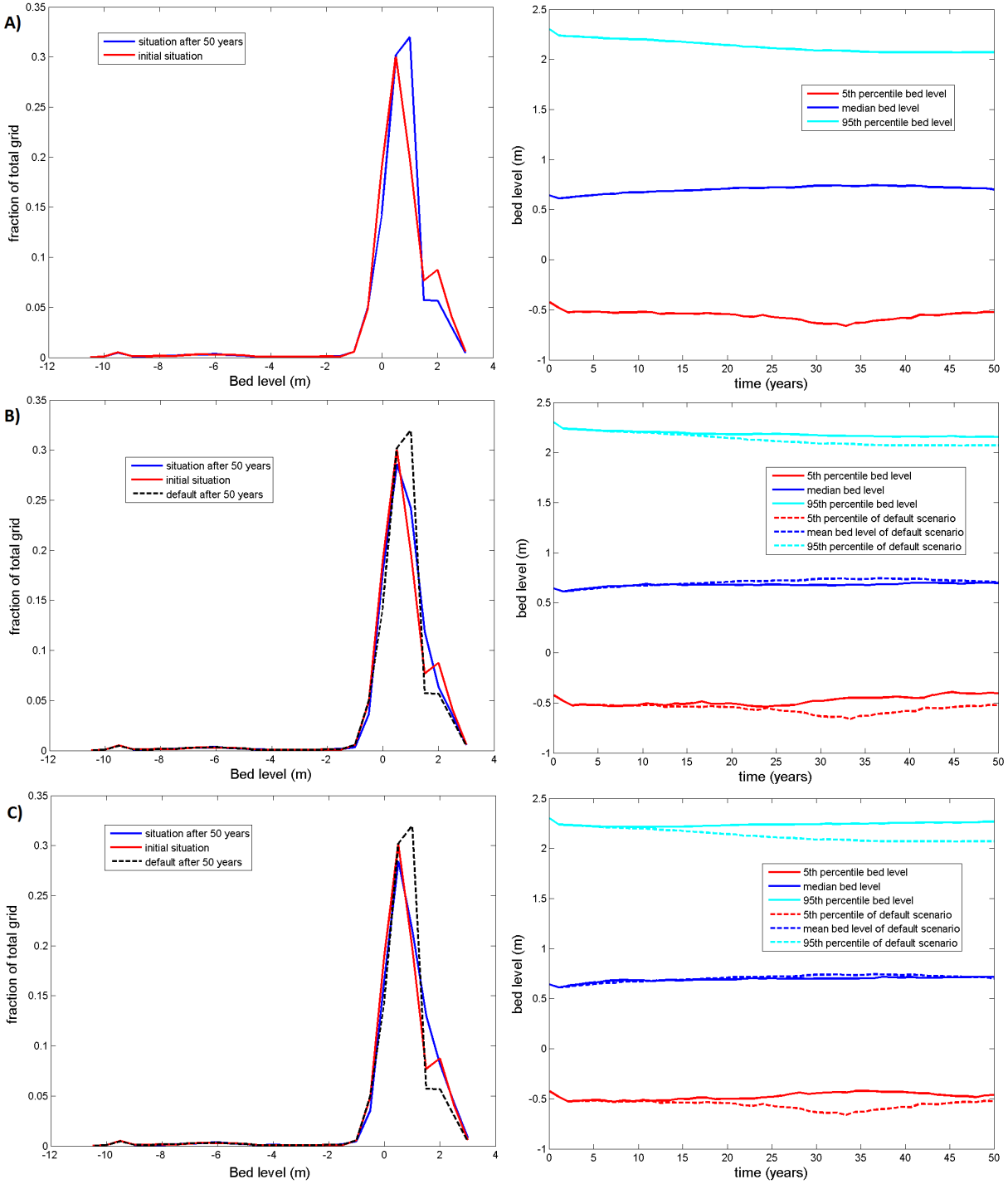

Figure 24: The bed level changes for scenario's with A) no mud, B) 20 mg/l mud and C) 50 mg/l mud

50 mg/l mud simulation.

The default simulation shows a decrease in its 95th percentile bed levels, a pattern which is also visible in the bed level distribution plot (Figure 24A). The bed level distribution plot shows that the decrease in the 95th percentile bed level comes mainly from a decrease in the approximately +2 m area, which is compensated by an increase in the +1 m area. Therefore a part of the upper intertidal area erodes which becomes part of the mean intertidal area. The channel depth (as indicated by the 5th percentile) does not change. When consecutively 20 and 50 mg/l mud are added to the simulation the decrease in 95th percentile bedlevel becomes less (20 mg/l simulation) until it disappears (50 mg/l simulation). The channel depth seems to decrease in the simulation with 20 mg/l mud, but this pattern is absent in the simulation with 50 mg/l mud.

The width of the estuary is only very limitedly changed during the 50 years default simulation (Figure 25). The main change appears from 12-20 km, which is the river. Here the width has significantly increased, in some areas up to a factor two. In the simulation with 20 mg/l mud this widening of the river has almost disappeared. This happens because the mud accumulates at the river edges, confines it, and keeps its width fairly constant (Figure 22). The confinement of the river is visible in the simulation with 50 mg/l mud as well. The simulation with 50 mg/l mud, however, also shows a significant decrease in the estuary width around 10 km (Figure 25). This is the area where the large mudflat developed which partly extends to the supratidal zone.

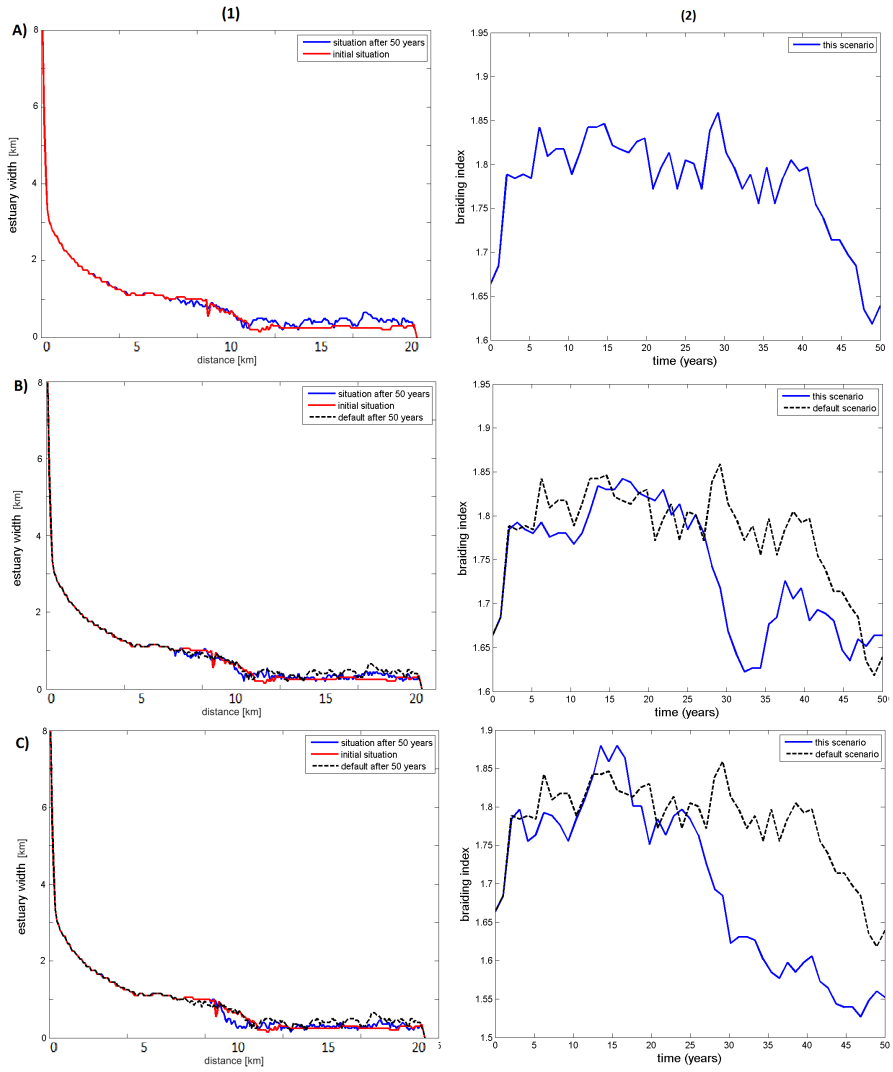

Figure 25: 1) Width along the estuary 2) the change in braiding index over the years. A) is the scenario without mud, B) with 20 mg/l mud and C) with 50 mg/l mud

The default scenario shows a slight increase in its braiding index during most of the simulation, but after 50 years the braiding index is almost back to its original value (Figure 25A). When 20 mg/l mud is added to the simulation the braiding index develops differently over the years, especially around 30 years, where it suddenly drops with respect to the default simulation. After 50 years the value for the simulation with and without mud is, however, nearly the same (Figure 25B). The simulation with 50 mg/l mud shows a decrease in its braiding index with respect to the default simulation which might be significant (Figure 25C). After approximately 30 years it starts to decrease quickly, but the difference with the default simulation after 50 years is not too large. This is interesting because visual interpretation of the bathymetry maps (Figure 22) shows a more clear reduction in braiding index.

4.1.2 Hydrodynamics

The tidal amplitude and tidal flow velocity in the estuary decrease for increasing mud concentrations, especially in the central and inner zone. The extent of the intertidal area seems to be unaffected by the presence and concentration of mud.

The tidal amplitude in the default simulation shows some small changes along the estuary but there are no large changes (Figure 26A). The only clear change is a slight increase in the tidal amplitude in the central/inner part of the estuary around 10 km. When 20 mg/l mud is added to the simulations this pattern inverses and the tidal amplitude starts to decrease from 7 to 12 km, both with respect to the default simulation and with respect to the initial situation. The decrease in tidal amplitude becomes even slightly larger for the simulation with 50 mg/l mud.

Both the width averaged and maximum tidal flow velocity increase in the default simulation (Figure 26A). The width averaged ebb velocities in the river decrease, because the river widens itself here (Figure 25). The flood and ebb velocity increase mainly in the central part of the estuary (50-120 hm) and are barely affected in the outer zone. The large peaks in the maximum ebb velocity are caused by conveyance of the flow in small channels when the water level is low. When mud is added to the simulation the flow velocities no longer increase, instead they start to decrease except for a peak which develops exactly at 50 hm. As the concentration increases from 20 mg/l to 50 mg/l the flow velocities decrease further with respect to the default simulation. This holds for both the peak and width averaged flow velocities.

The development of the total intertidal area shows a very strong decrease at the beginning (Figure 26). This is caused by the initial water level in the model, which has to flush once and is therefore not realistic. The default scenario shows a slight increase in intertidal area over the modelled 50 years. The addition of mud results in a slight decrease in the total intertidal area with respect to the default simulation for both the simulation with 20 mg/l and 50 mg/l mud (Figure 26). The decrease in intertidal area after 50 years is, however, so small that it is not significant.

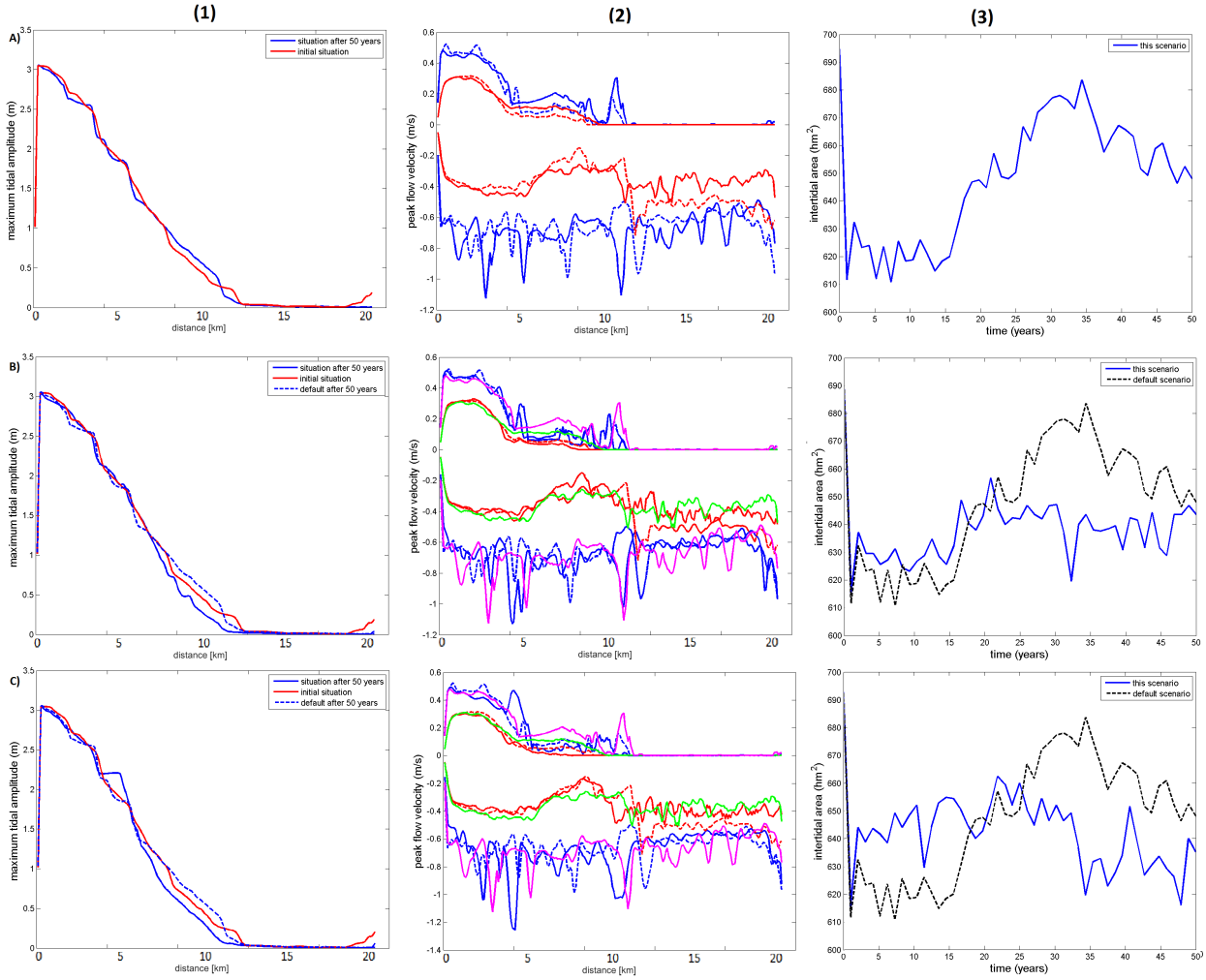

Figure 26: 1) tidal amplitude, 2) maximum flow velocity and 3) total intertidal area for scenario's A) without mud, B) with 20 mg/l mud and C) with 50 mg/l mud. In the flow velocity plots (2) the blue lines give the maximum ebb and flood velocity and the red lines give the width averaged ebb and flood velocity. The dashed lines give the initial situation and the green and magenta lines give the default width averaged and default maximum flow velocities respectively.

4.2 Patterns and effects of *Spartina anglica*

Spartina colonizes the intertidal edges of the estuary and the tidal bars (Figure 27). The edges of the estuary have a small band of low density *Spartina*, followed by a broader band of high density *Spartina*. This low density band shows where the physical stress becomes too high for *Spartina* to survive. The tidal bars are mostly occupied by low concentrations of *Spartina*, but with a small higher concentration area in the middle of the bar (Figure 27).

Simulations with mud and *Spartina* show two distinct changes compared to simulations without mud or without *Spartina*. First of all the mud accumulation pattern changes and follows the vegetation distribution (Figure 28B). Simulations without *Spartina* show mud accumulations on the edges of the estuary, while simulations with *Spartina* have large mud accumulations on the tidal bars as well. Secondly the *Spartina* cover became significantly higher in large parts of the estuary when mud was added to the simulation (Figure 28A).

This section will start with analyses of the effect of *Spartina* on sediment accumulation, followed by its effect on morphodynamics and hydrodynamics and finally a sensitivity and reproducibility analysis will be presented.

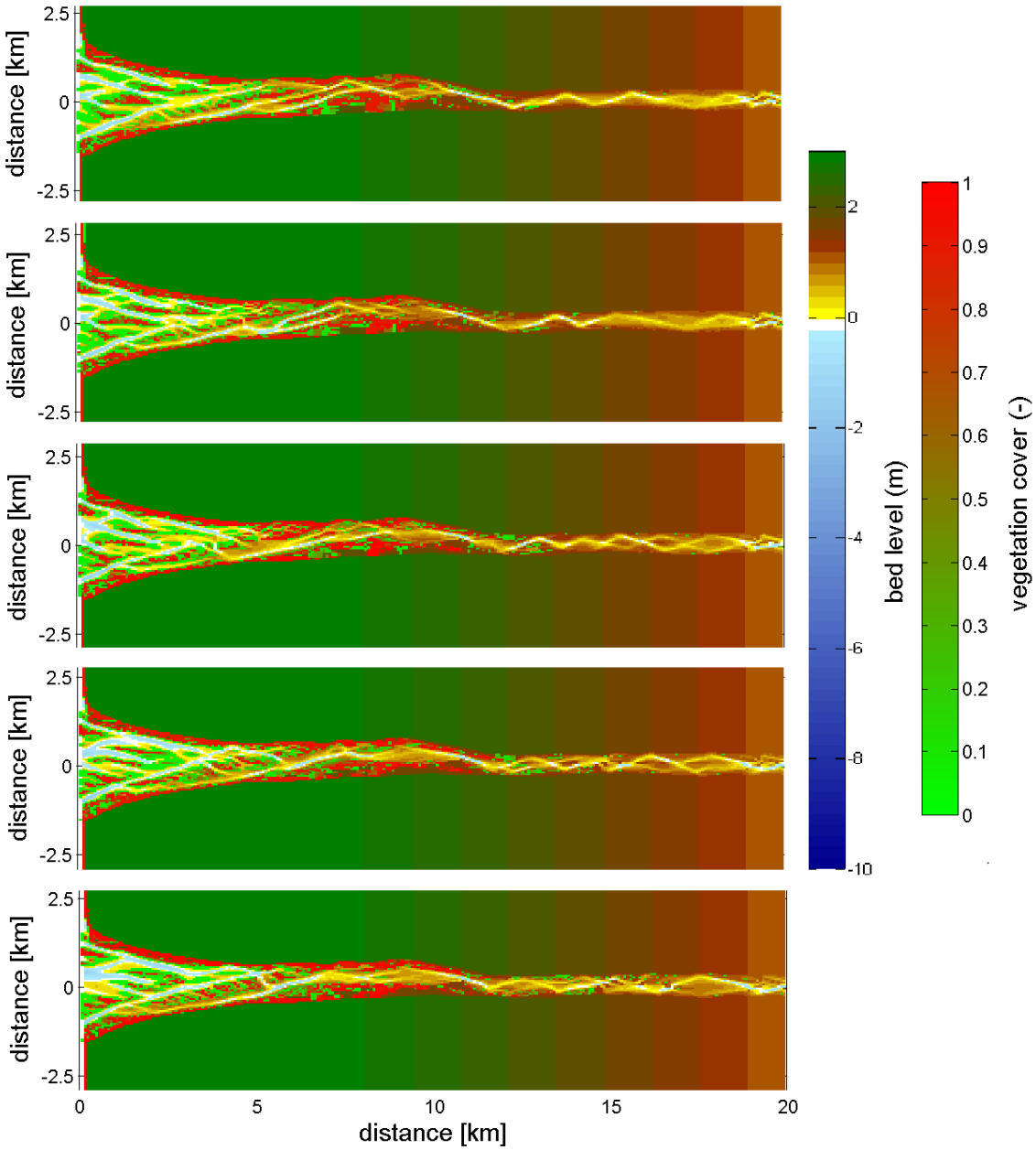

Figure 27: *Spartina anglica* development over the years for the simulation without mud (#5). The number gives the amount of years which have passed. Areas without green/red color have zero vegetation cover.

4.2.1 Vegetation and sediment accumulation

Spartina increases sedimentation in areas where it grows and increases erosion in areas where it does not. A similar relation holds for the mud cover in the toplayer, once *Spartina* colonizes an area more than 1 year the mud cover in the toplayer is significantly higher. *Spartina* drives accumulation in the lower intertidal area which becomes part of the middle to upper intertidal area. These trends are enhanced by the presence of increasing mud concentrations.

The simulation with *Spartina* but without mud shows a clear correlation between the presence of *Spartina* and the erosion or deposition in the cell (Figure 29). Cells without any vegetation cover after 50 years have on average more than 20 cm erosion, while cells with *Spartina* have, on average, sediment accumulation.

The simulations with mud show the same relation between erosion/deposition and the *Spartina* cover (Figure 29). The absolute accumulation is, however, significantly larger.

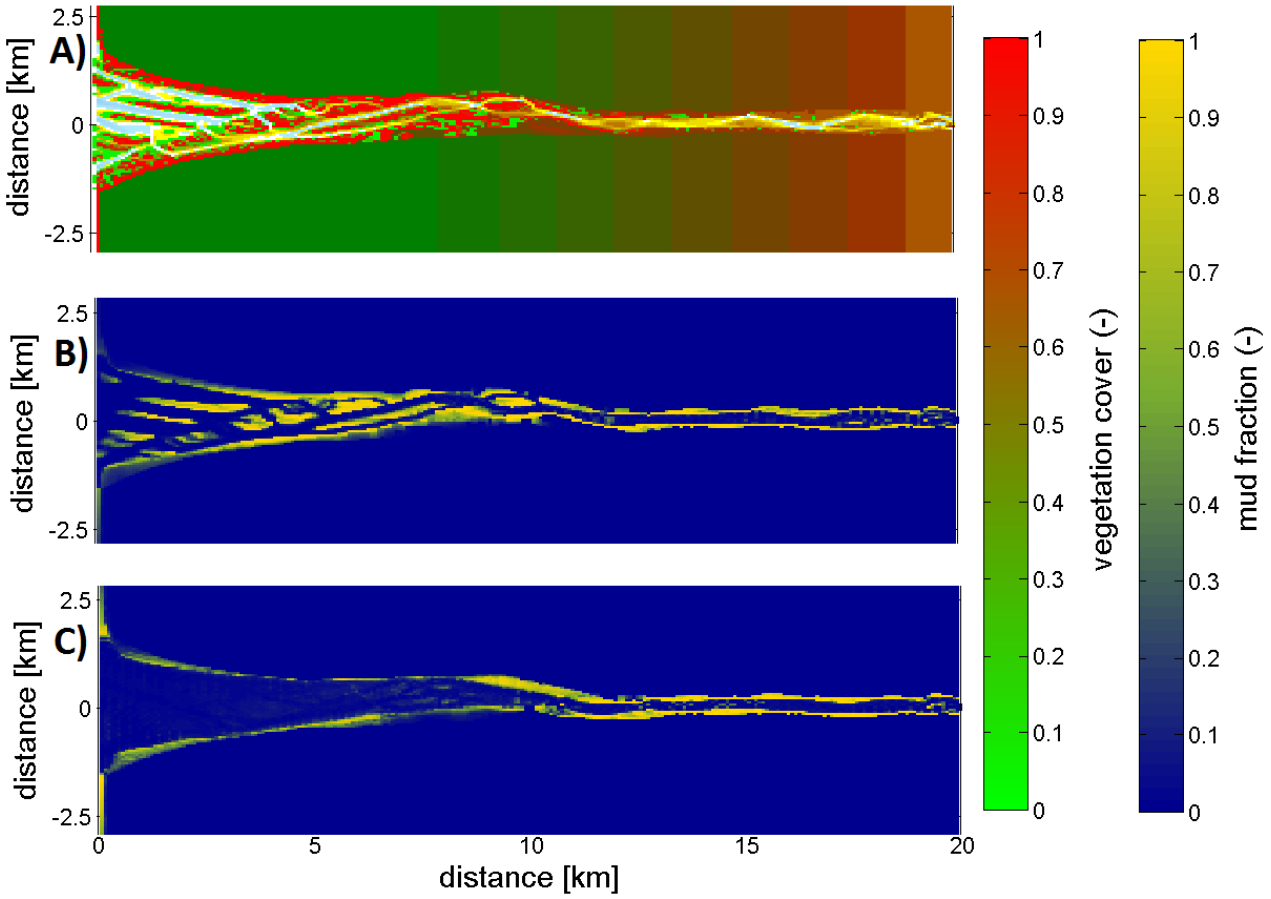

Figure 28: A) the vegetation cover after 50 years of simulation with *Spartina* and 20 mg/l mud, B) the mud distribution map after 50 years of simulation with *Spartina* and 20 mg/l mud and C) the mud cover map after 50 years of simulation with 20 mg/l mud without *Spartina*

A relation similar to the one described above is found between the mud cover in the toplayer and the presence of *Spartina* (Figure 29). The simulation with 20 mg/l mud shows a strong increase in the mean mud cover in the toplayer once the vegetation cover exceeds 10%. The same relation is visible in the simulation with 50 mg/l mud, except that the average mud covers are significantly higher here.

The simulation with *Spartina* without mud shows a change in its bed level distribution which is similar to what happens in the default simulation. There is a slight decrease in the +2 m area, which is partly compensated by an increase in the +1 m area (Figure 29). The simulation with *Spartina*, however, also has a slight increase in the deeper areas. When mud is added to the simulations the pattern changes significantly. Just as in the simulations with mud but without *Spartina* the highest intertidal areas (>2 m) are stabilized when mud is added. The increase in the deeper areas which was found in the simulation with only *Spartina* has become slightly larger in the simulation with mud. The simulations with mud and *Spartina*, however, show a very strong increase in the +1-2 m area, which is compensated by a strong decrease in the +0-1 m area (Figure 29). The shift from 0-1 m towards 1-2 m coincides with the rapid increase in vegetation cover which indicates that this might be the cause. This shows that *Spartina* drives sedimentation and increases the area in the 1-2 m reach.

To compare the simulation with 20 mg/l mud and *Spartina* with the situation with 20 mg/l mud but without *Spartina* a cross correlation has been made (Figure 30). The cells which were occupied by *Spartina* at the end of the simulation, regardless of their cover, have been investigated in the simulation without *Spartina*. Through determining the mean erosion and deposition in areas which would potentially grow *Spartina* we could see whether the accumulation here is driven by the presence of *Spartina* or does occur solely morphodynamically as well. As can be seen the run without *Spartina* had erosion in the areas where *Spartina* does not grow and deposition in the areas where it does grow,

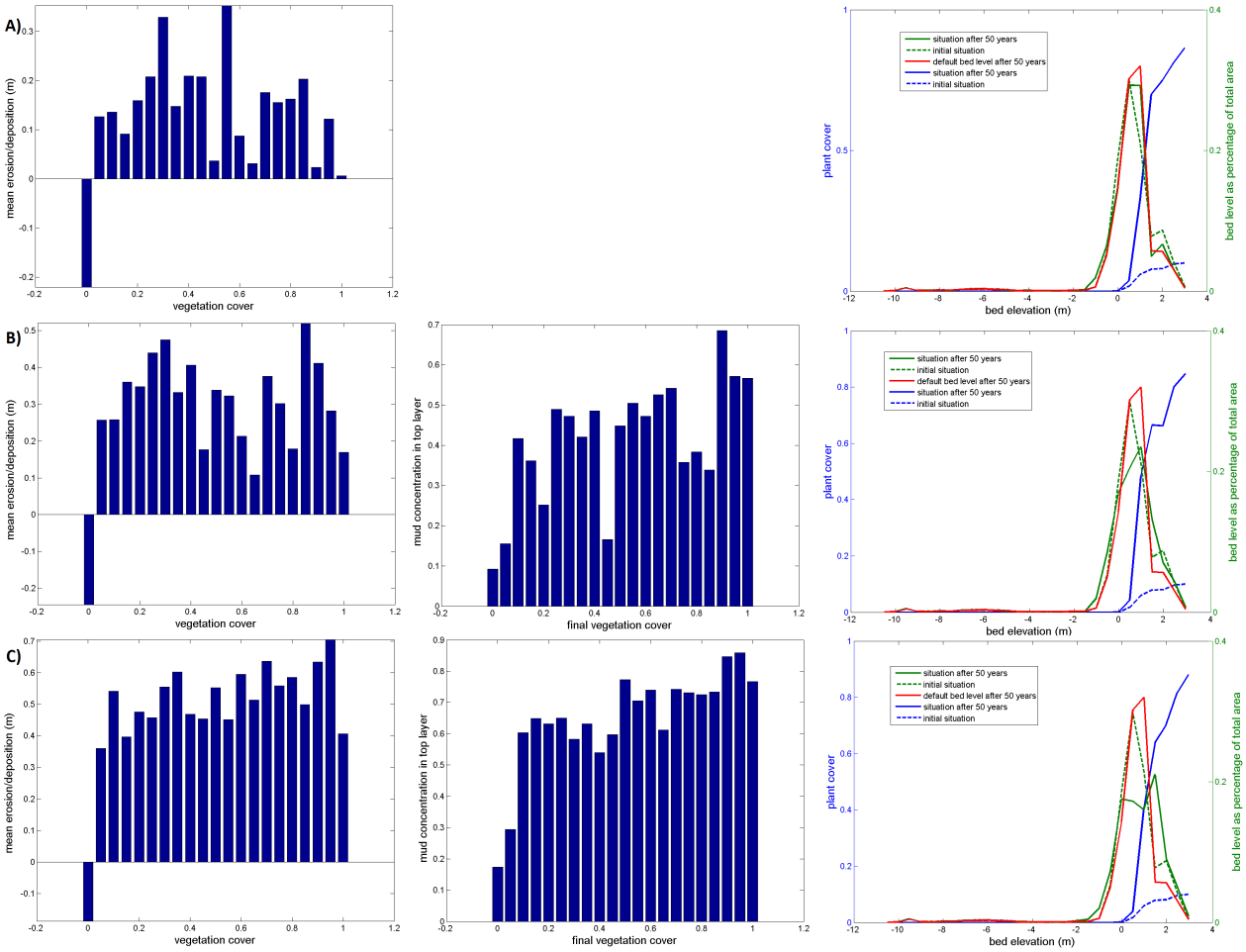

Figure 29: Erosion and deposition patterns under influence of *Spartina anglica*. Row A) is the simulation without mud, B) with 20 mg/l mud and C) with 50 mg/l mud

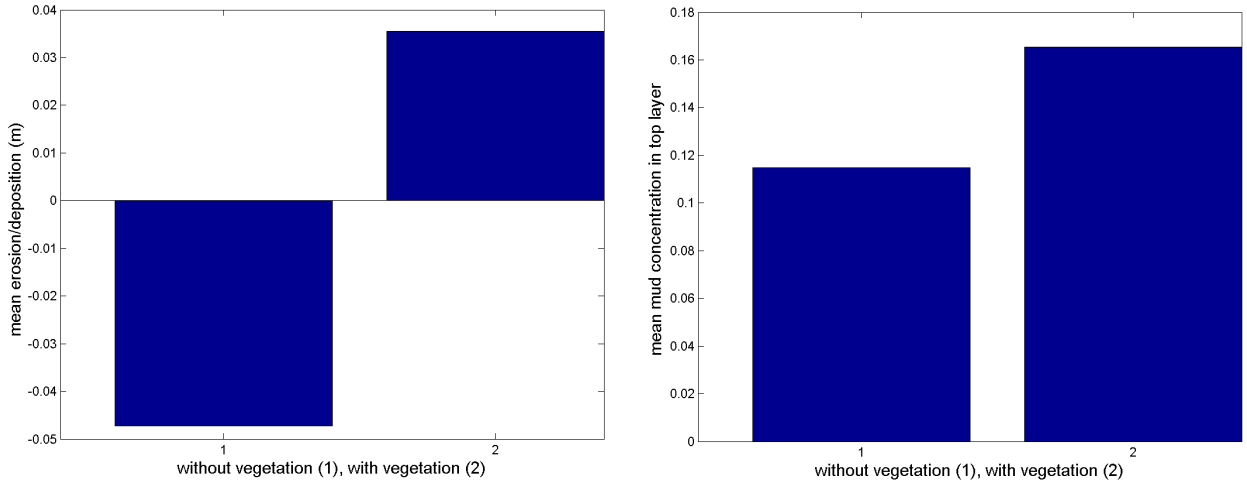

Figure 30: The erosion and deposition (left) and the mean mud concentration in the top layer (right) in the run without *Spartina* with 20 mg/l mud. 1 are locations where *Spartina* would not occur after 50 years and 2 are locations where *Spartina* would occur after 50 years.

so the pattern in erosion and deposition is similar for both simulations. The mean accumulation, however, is much smaller without *Spartina*, and so is the erosion. The same pattern holds for mud deposition. The mud concentration in the toplayer is relatively high in areas where *Spartina* can grow, also if *Spartina* is not actually modelled. The concentrations are, however, much larger for the simulation with *Spartina*, which shows that *Spartina* enhances the mud accumulation. A critical remark is, however, that the bathymetry has developed differently so some of the areas might no longer be suitable for *Spartina* growth in the simulation without *Spartina*.

4.2.2 Morphodynamics

Spartina drives an increase in braiding index, deepens channels and stabilizes the intertidal area. Inclusion of mud does not affect the braiding index while it enhances *Spartina*'s effect on channel depth and the intertidal area.

Addition of *Spartina* to the default simulation shows a clear increase in braiding index (Figure 31A). When mud is added to the simulations the development of the braiding index over the years is almost the same as for the simulation without mud (Figure 31). This is remarkable because addition of mud did significantly affect the development of the braiding index in the simulations without *Spartina*.

Adding *Spartina* to the default simulation has a clear influence on the bed level distribution. First of all the 5th percentile bed level, which is an indication of the channel depth, becomes deeper than in the default simulation (Figure 31A). The 95th percentile, on the other hand, shows a slight increase compared to the default simulation. These two patterns are enhanced when mud is added to the simulations in increasing concentrations. The simulation with 20 mg/l mud shows a stronger increase in the 95th percentile bed level and a stronger decrease in the 5th percentile bed level (Figure 31B). This effect is even stronger when 50 mg/l mud is added to the simulations. This is an interesting result because mud did not affect channel depth in simulations without *Spartina*.

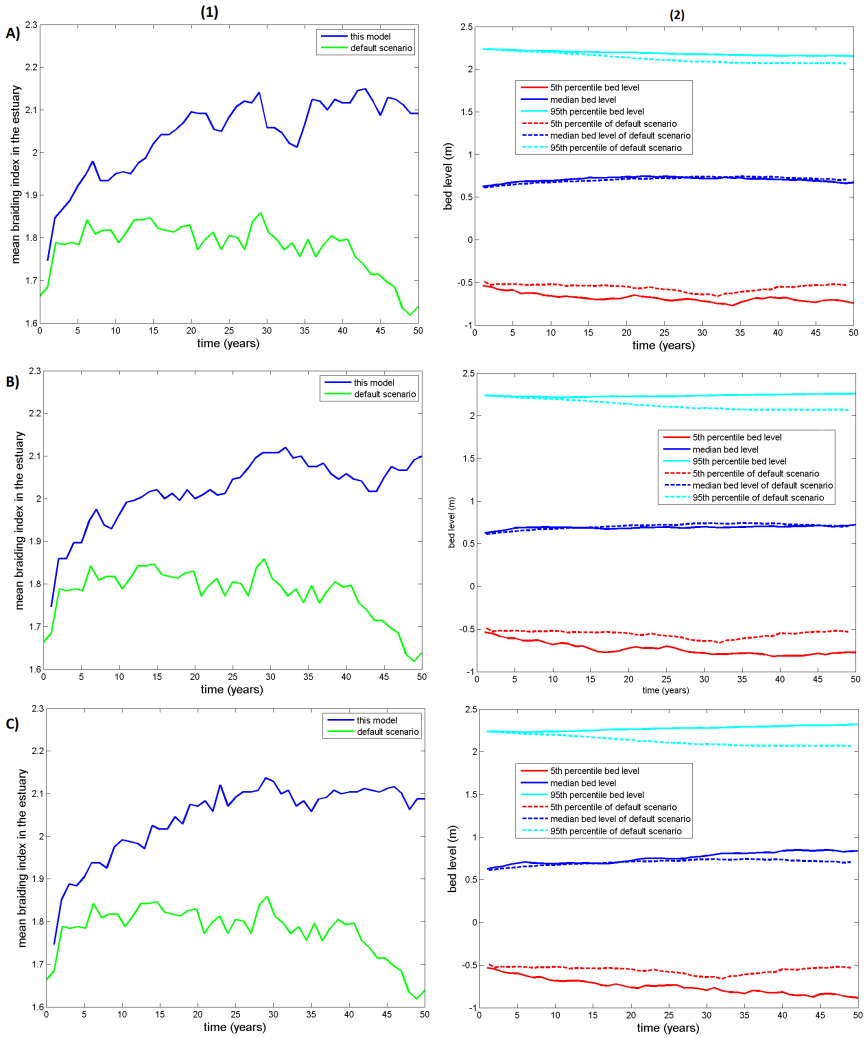

Figure 31: 1) The change in braiding index over the years, 2) the percentile bed level development of the estuary. A) is the simulation without mud, B) with 20 mg/l mud and C) with 50 mg/l. All runs were performed with *Spartina*.

4.2.3 Hydrodynamics

Spartina drives an increase in tidal amplitude. It increases the peak ebb and flood velocities (in the channels), but simultaneously decreases the width averaged flood and ebb velocity. *Spartina* also causes a decrease in the intertidal area with respect to the default scenario. The trends in tidal amplitude and tidal flow velocities are enhanced when mud is added to the simulations while the development of the intertidal area appears to be unaffected by mud.

Spartina slightly increases the tidal amplitude in the estuary both with respect to the initial and the default situation (Figure 32A). When mud is added to the simulations in increasing concentrations the increase in tidal amplitude becomes significantly larger especially in the outer zone of the estuary (Figure 32B,C).

The effect of *Spartina* on flow velocity differs for the width averaged and the peak flow velocities. The width averaged flow velocities decrease slightly, especially with respect to the default simulation. The peak flow velocities, on the other hand, increase significantly both compared to the default and initial situation (Figure 32A). The increase in peak flow velocity is more clear for the flood flow than for the ebb flow but it is present in both. Addition of mud to the simulation enhances both trends, the width averaged flow velocities decrease further and the peak flow velocities increase further. The simulation with 50 mg/l mud also shows a shift in the area where the peak flow velocities increase most, the velocities increase more in the outer area and less in the central and inner area (Figure 32C).

The intertidal area without *Spartina* increases during the simulation, but when *Spartina* is added

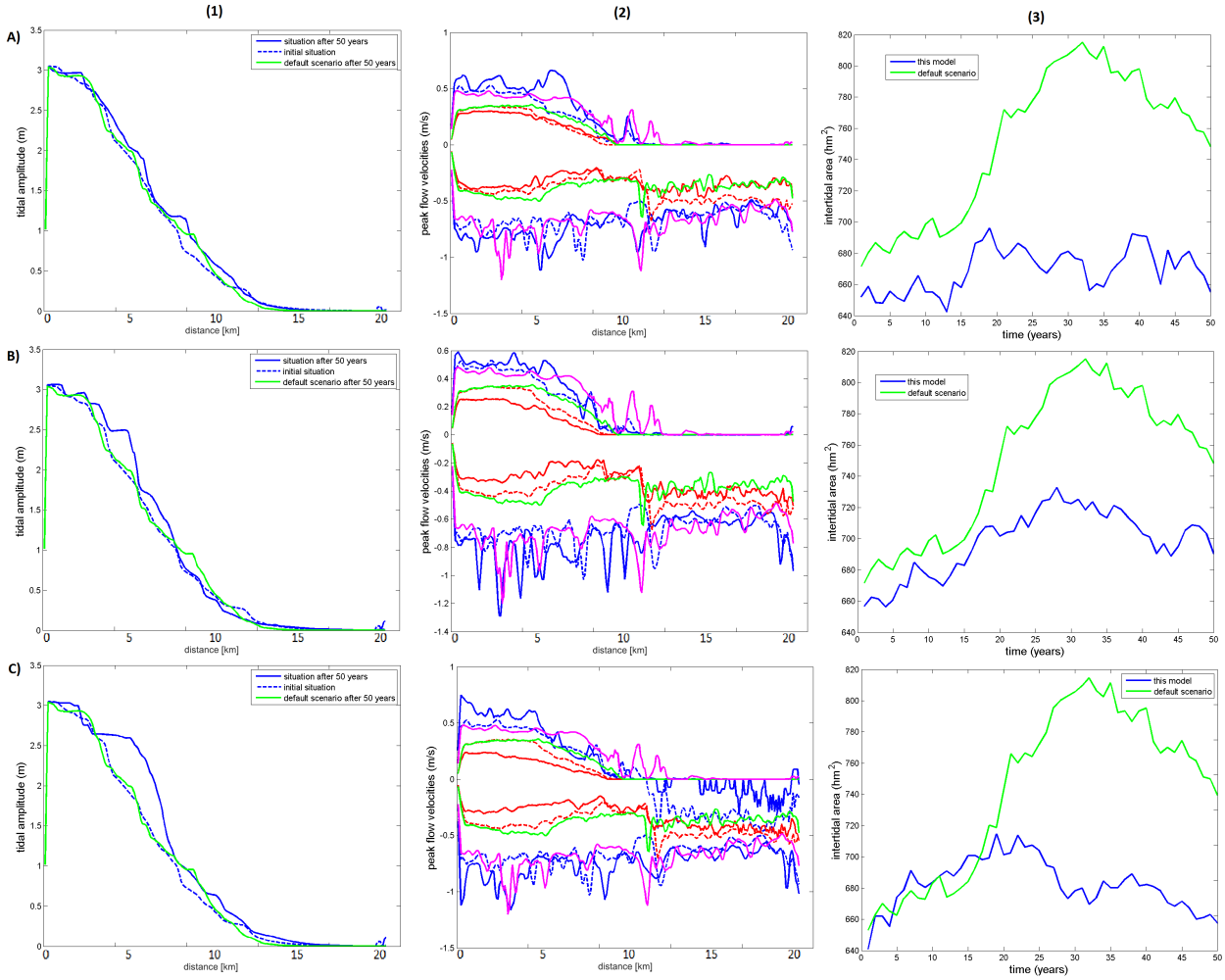

Figure 32: The tidal amplitude (1), maximum width averaged flow velocity (2) and total intertidal area (3) for scenario's without mud (A), with 20mg/l mud (B) and with 50 mg/l mud (C). All scenario's contain *Spartina*. The green line is the result after 50 years without mud and *Spartina* which is plotted against the scenario's for comparison. The dashed lines are the initial situation. 2) The blue lines give the maximum ebb and flood velocity and the red lines give the width averaged ebb and flood velocity. The dashed lines give the initial situation and the green and magenta lines give the default width averaged and default maximum flow velocities respectively.

this trend disappears. In the simulation with *Spartina* the intertidal area does not increase and thus there is disappearance of the intertidal area with respect to the default simulation (Figure 32A). The inclusion of mud in the simulations has no significant influence on the development of the intertidal area (Figure 32B,C).

4.2.4 Sensitivity and reproducibility

The simulation of *Spartina* has been analysed for several vegetation characteristics and on a different initial bathymetry. Such an analysis has not been performed for mud because it uses an extensively tested Delft3D module. Neither has it been performed for *Zostera* because we are still looking for relevant default settings (section 4.3). First the small sensitivity analysis with respect to *Spartina* development will be presented. Afterwards a comparison is made with a simulation on a different initial bathymetry for some of the clearest trends in the default simulation with *Spartina*. This is done because we hypothesized that *Spartina* does not create new intertidal area and thus its effect might be dependent on the initially present intertidal area.

Spartina is not very sensitive to the input parameters in the model. Figure 33 shows the *Spartina* distribution on the bathymetry map after 50 years for simulations without mud. As can be seen the

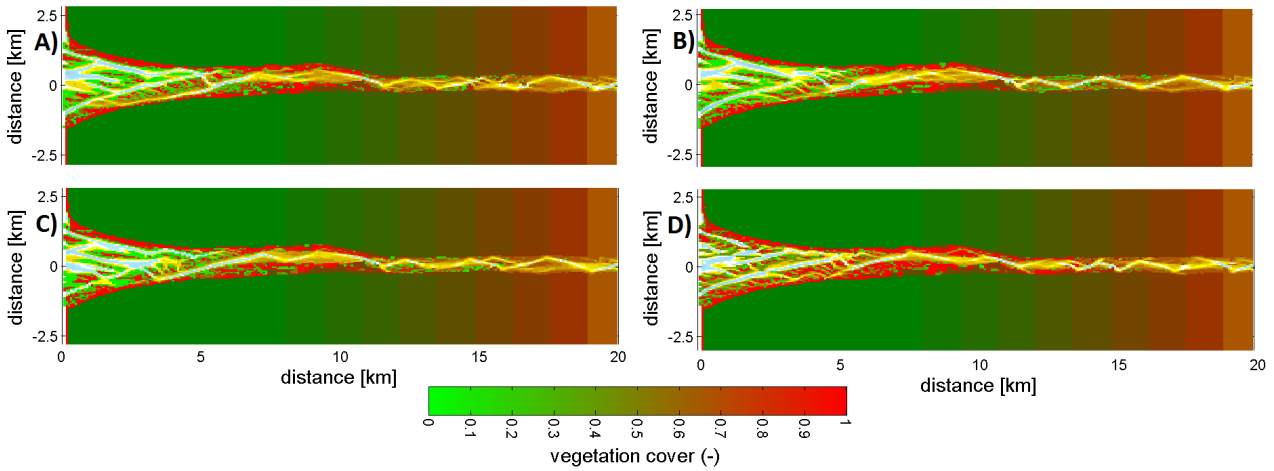

Figure 33: A) default run with *Spartina*, B) run with late *Spartina* dispersal, C) run with sensitive seedlings, D) default run with a high colonization density. All runs were performed without mud.

final patterns are very similar. The simulation with late *Spartina* dispersal was included because mortality based on dessication and flooding is applied once a year and dependent on the time between colonization and mortality different patterns could have emerged (Figure 33B). The final distribution is, however, very similar to that in the default simulation (Figure 33A). The simulation with sensitive seedlings has a nearly identical final distribution as our default run as well, which indicates limited dynamics in the *Spartina* population (Figure 33C). The simulation with the higher colonization density has a more significant effect, as it caused several of the tidal bars to grow together (Figure 33D).

The effect of the initial bathymetry is tested through simulations with a different initial bathymetry (Figure 34A). This initial bathymetry is deeper and significantly wider in the central zone of the estuary. The simulation with 20 mg/l mud but no *Spartina* shows a similar mud distribution pattern as the runs with the default bathymetry. Mud accumulates on the edges of the estuary and the lateral extent decreases in seaward direction. The main difference is the larger mud accumulation in the river reach due to the initially more braiding character of the river.

The *Spartina* distribution pattern is similar for the new bathymetry as well (Figure 34E). The vegetation grows on the edges of the estuary in the intertidal area and on the bars. The mud accumulation pattern does still follow the vegetation distribution, which shows that the *Spartina* colonization and survival mechanisms produce similar distribution patterns for different bathymetries (Figure 34F).

The effect of *Spartina* on the characteristics of the estuary is, not always the same in the new bathymetry. However, the relation between vegetation cover and erosion/deposition and the relation between vegetation cover and mud cover in the toplayer does show the same pattern for the two different initial bathymetries (Figure 35A,B,C,D).

The effect of *Spartina* on the development of the intertidal area is different in the new initial bathymetry. *Spartina* decreases the extent of the intertidal area in the default bathymetry. In the simulation with the different initial bathymetry, however, *Spartina* prevents the decrease in intertidal area which would happen without it (Figure 35E,F). When the different initial bathymetry is modelled without mud and *Spartina* the intertidal area starts to decrease rapidly (Figure 35F). When *Spartina* and mud are added to the simulation the decrease in intertidal area is still present, but its magnitude is significantly smaller. This therefore shows us that *Spartina* does not create new intertidal area, but it can prevent the erosion of the present intertidal area.

The development of the 5th and 95th percentile bed level under influence of mud and vegetation is different in the new bathymetry. In the default bathymetry the 5th percentile bed level decreases significantly under influence of *Spartina* and mud. The simulation with the different bathymetry, on the other hand, shows that *Spartina* and mud have no influence on the 5th percentile bed level at all. The 95th percentile bed level increases significantly in our default simulation when mud and *Spartina*

are added (Figure 35G). The new bathymetry shows an increase in the 95th percentile bed level as well, but this is not nearly as distinct as in the default bathymetry (Figure 35H).

The braiding index shows a different development in the new bathymetry as well. The simulation with the default bathymetry shows a clear increase in braiding index when *Spartina* and mud are added to the simulation. The simulation with the new bathymetry, on the other hand, shows that *Spartina* and mud have limited influence on the development of the braiding index.

The general distribution pattern of *Spartina* is the same when a different initial bathymetry is modelled and it still drives accretion of sediment and mud. Some effects are, however, changed because *Spartina* has a smaller lateral extend into the estuary or occupies a different part of the estuary.

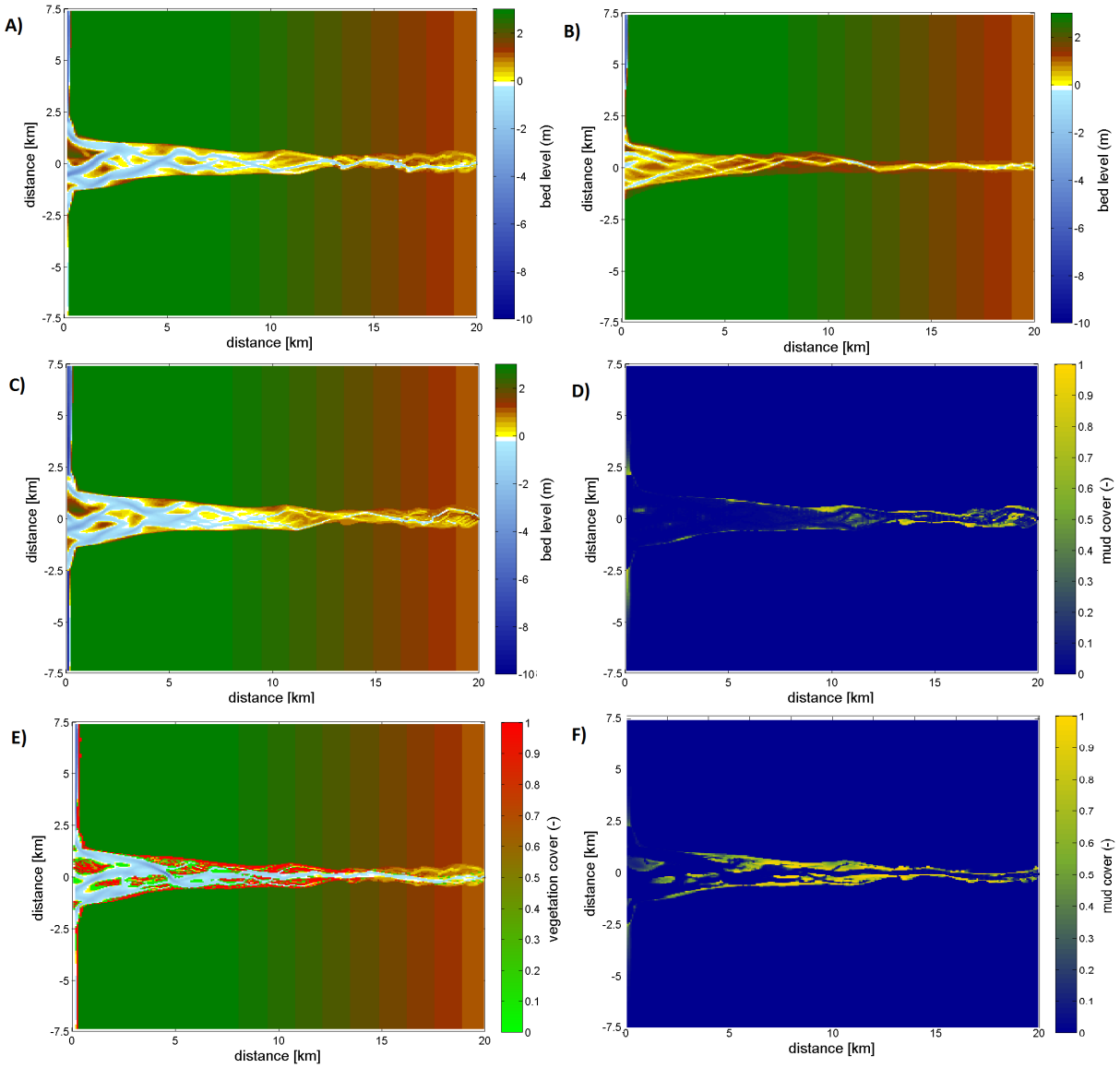

Figure 34: A) The new initial bathymetry, B) The default initial bathymetry, C) The final bathymetry for the simulation without *Spartina*, D) The mud cover distribution for the simulation without *Spartina*, E) The final vegetation cover for the simulation with *Spartina* and F) The mud cover distribution for the simulation with *Spartina*. Both simulations took place with 20 mg/l mud.

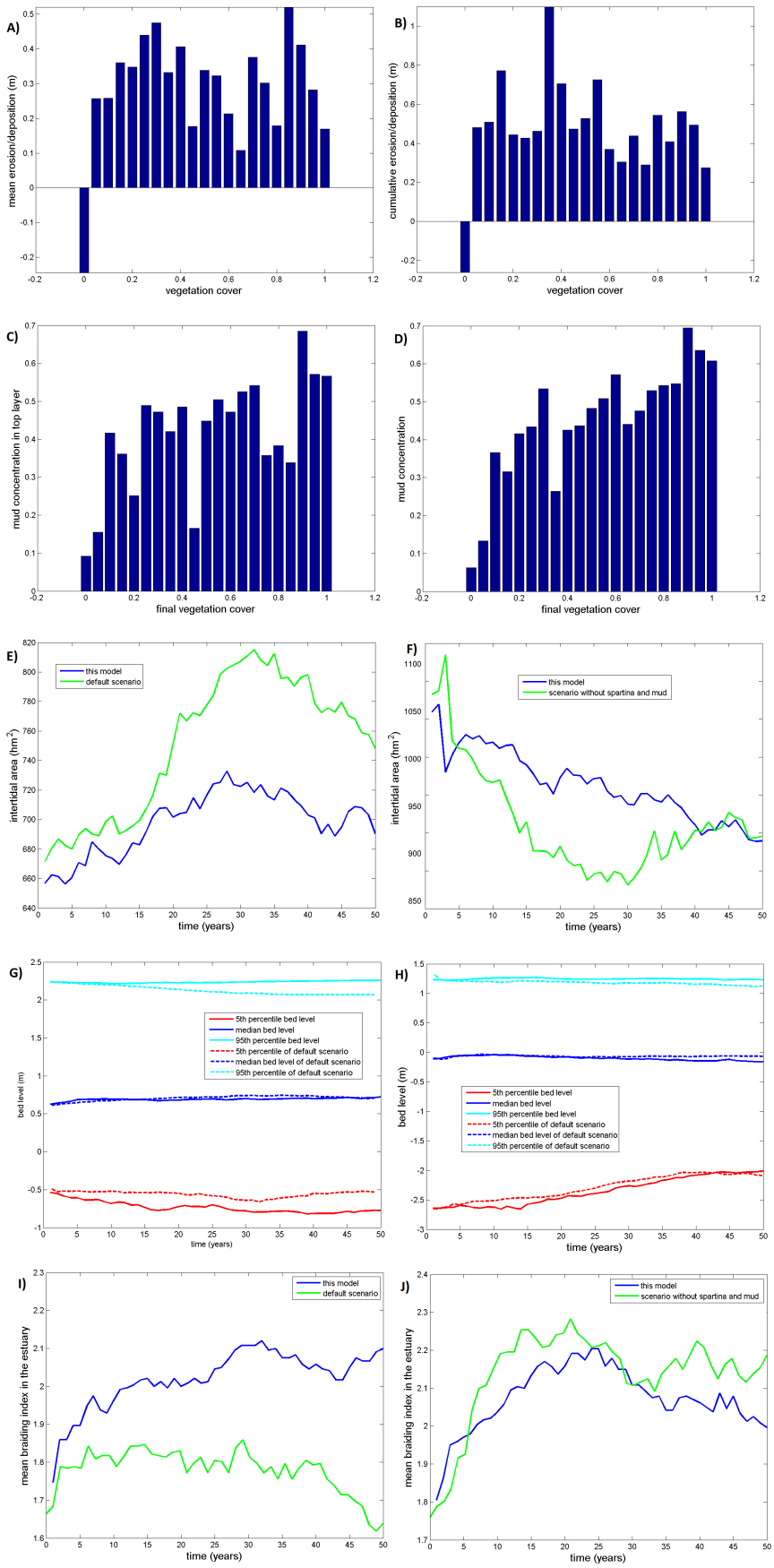

Figure 35: Comparison of some of the clearest trends for our default initial bathymetry (left) with the different initial bathymetry (right). Both simulations were performed with 20 mg/l mud and *Spartina*

4.3 Patterns and effects of *Zostera marina*

Zostera marina caused a lot of problems with its simulation, therefore issues encountered will be presented first and afterwards some preliminary results.

Zostera grows fast till a significant height. In nature *Zostera* bends under influence of currents which reduces its maximum height, but in the simulations this effect was absent. In our shallow estuary *Zostera*, therefore, exerts a strong influence on the water height in the river through the backwater effect. The increased water height due to *Zostera*'s resistance causes the river to overflow its banks and turn the area into some sort of swamp (Figure 36). Decreasing the maximum height to simulate continuous bending of *Zostera* helps to reduce this effect slightly but does not solve the problem. All simulations without mud resulted in an overflow of the river banks within 10 years after the start of the simulation and resulted in patterns similar to figure 36.

Inclusion of mud in the estuary helped to stabilize the model in two ways. The banks of the river are strengthened which helps to confine the river, and the areal cover of *Zostera* is decreased through mortality. Depending on the Poole-Atkins constant something interesting happens with the suspended sediment under influence of *Zostera*. If the suspended sediment concentration does not reduce the light penetration enough for *Zostera* to die, the suspended sediment does not manage to pass the most upstream *Zostera* species (Figure 37C). This results in large mud accumulations in this area, but also in an aggressive development of *Zostera* in the outer zone of the estuary (Figure 37A). As can be seen all areas except for the intertidal area and some of the channels developed a full *Zostera* cover. The scenario with a Poole-Atkins constant of 1.2 turned into a swamp after approximately 20 years (Figure 37).

A higher Poole-Atkins constant can reverse the development of *Zostera* in the estuary. Figure 38 shows a pattern which starts similar to that in figure 37, but turns out the opposite due to its higher Poole-Atkins constant. The first 15 years suspended sediment concentration barely passes the first *Zostera* settlements which results in high visibility in the outer zone of the estuary and large dense *Zostera* meadows (Figure 38A). Between 15 and 20 years, however, the suspended sediment concentration suddenly increases in the outer zone of the estuary which results in a strong decrease in visibility in the water and mortality of *Zostera* (Figure 38). This continues in the next 5 years, after which only a couple of dense *Zostera* patches remain and the rest of the area is brought back to the defined colonization density (Figure 38). The blocking of suspended sediment comes from the very rapid colonization of the area by *Zostera*, which then drives rapid sedimentation. In an attempt to solve this a random 10% of the area was colonized instead of the entire area.

The most realistic results were probably obtained with the simulation where a random 10 percent

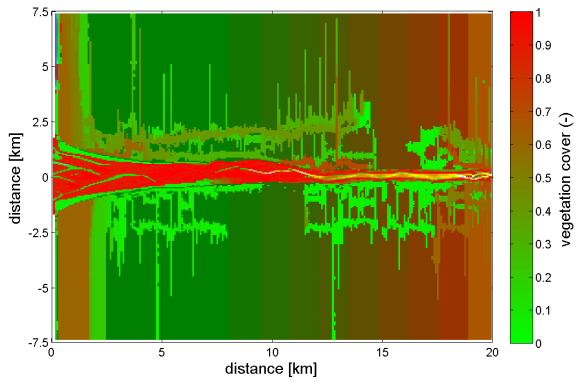

Figure 36: The vegetation cover of *Z. marina* in the estuary after 15 years, a common result when mud was excluded from the model

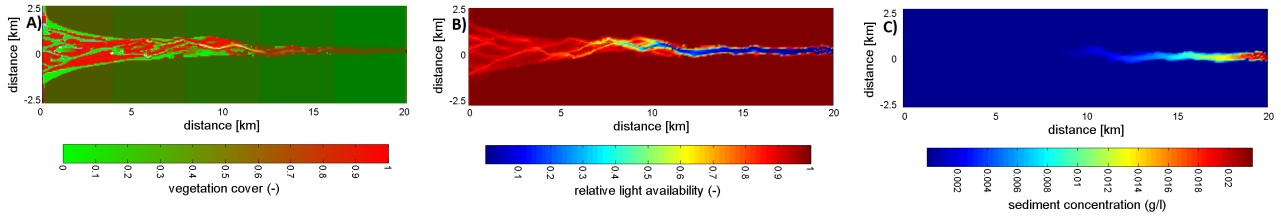

Figure 37: A) the vegetation cover of *Z. marina* after 15 years with mortality due to light deficiency. B) the light penetration in the estuary and C) the suspended sediment concentration. A Poole-Atkins constant of 1.2 is used in this simulation.

of the submerged area was colonized instead of the entire area and where the mud concentration was 20 mg/l (Figure 39). Unfortunately this run still overflowed after 33 years due to one troublesome pixel which created a dense vegetation patch at the river boundary. The displayed figures are therefore up to 32 years (Figure 39). This, however, shows that a different colonization module might be able to solve the problems with our simulations.

Two trends have been visualised because these are required to answer the hypotheses, the development of the intertidal area and the development of the bed level distribution (figure 39). These results must be interpreted while taking into account the large uncertainty of the *Zostera* distribution and are therefore more an indication of patterns which might occur than a reliable prediction of the eco-engineering effects of *Zostera*. There are mainly two clear trends, a significant decrease of the intertidal area and a deepening of the channels (as expressed by the 5th percentile bed level). The increase in channel depth is significantly larger than what we have seen in any other simulation (Figure 39). The reason for the decrease in intertidal area is probably the decreased tidal amplitude in the central zone of the estuary (Figure 39E). This is most likely driven by the development of the mudflat around 10 km which was also a reason for a significant decrease in tidal amplitude in the simulations without *Zostera* (Figure 39F, 26B). The intertidal area decreases significantly in simulations without *Zostera* with 20 mg/l mud around 30 years as well (Figure 26B). The development in the intertidal area might therefore not be attributable to the presence of *Zostera*.

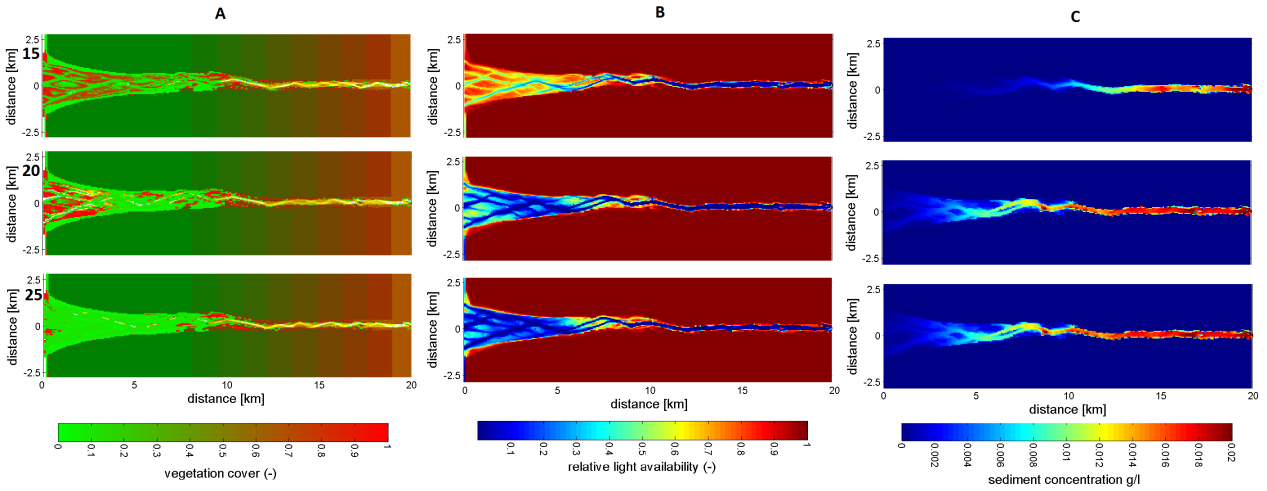

Figure 38: The development of a *Zostera* dominated estuary under influence of suspended sediment concentration for a poole-atkins constant of 2.5. A) shows the development of the vegetation, B) the development of the light penetration and C) the suspended sediment concentration. The simulation was performed with 20 mg/l mud.

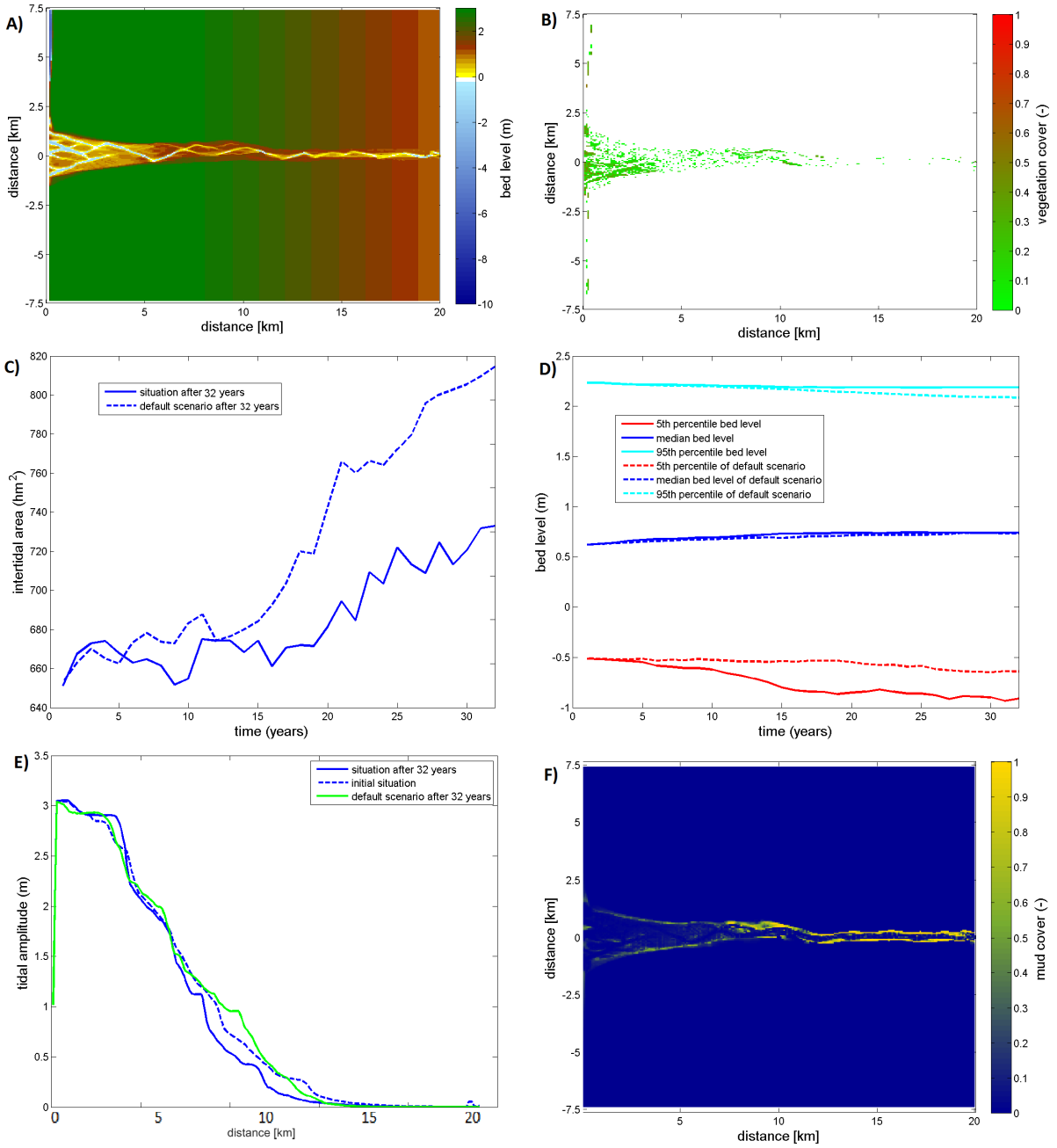

Figure 39: A) The final bathymetry after 32 years for the run with *Zostera* and 20 mg/l mud (#25), B) the corresponding vegetation cover, C) the development of the total intertidal area, D) the development of the bed level, E) the tidal amplitude and F) the mud distribution

4.4 The development of *Spartina* and *Zostera*

The development of *Spartina* and *Zostera* happens mainly next to eachother (Figure 40). There is no clear change from *Zostera* which turns into *Spartina* due to bed level sedimentation. It is interesting though that *Zostera* predominantly survives directly next to higher *Spartina* concentrations. This shows both the preference of *Zostera* for the shallow subtidal areas, but also probably some sort of symbiosis where the two might enhance living conditions for eachother. There are cells which contain both *Spartina* and *Zostera*, but these all have the colonization density of at least one of the two species. This is because *Spartina* cannot survive the minimum required inundation time for *Zostera* to survive, and vice versa.

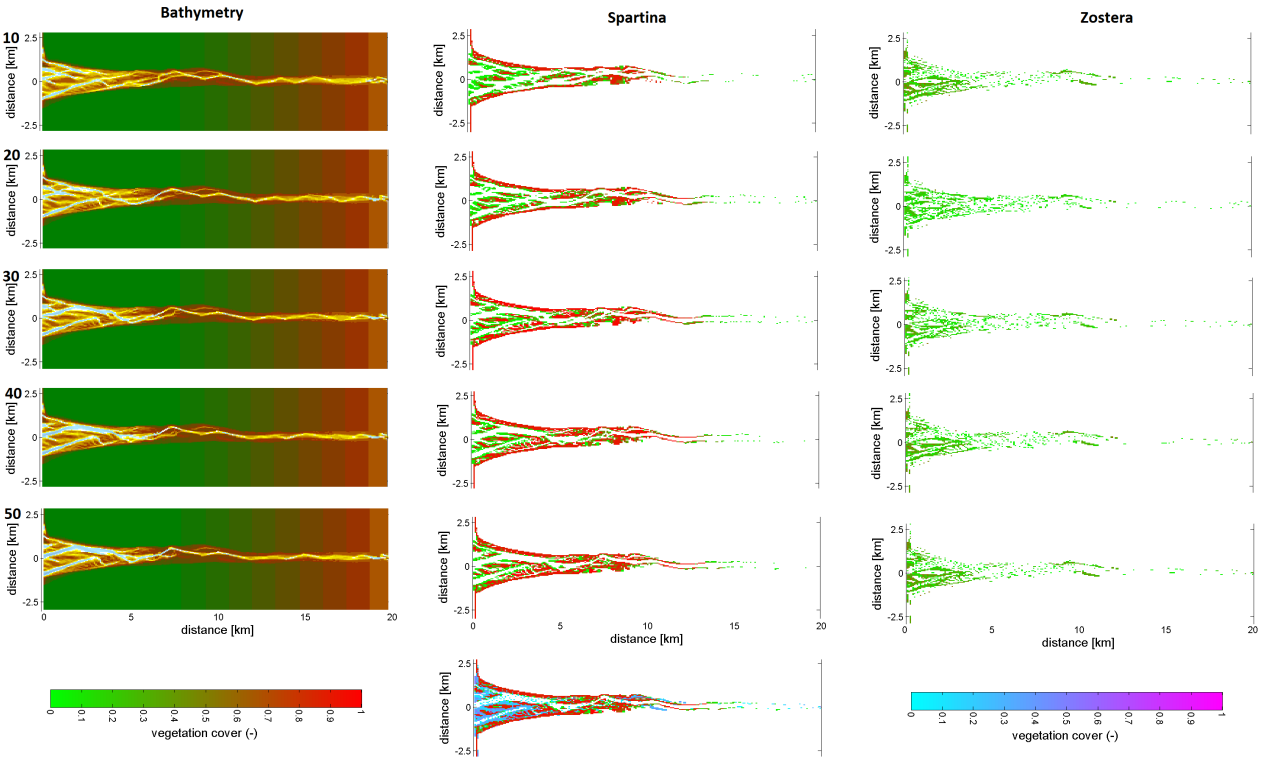

Figure 40: The development of the bathymetry, *Spartina* cover and *Zostera* cover in a simulation with 20 mg/l mud and both vegetation types (Run #26). The numbers give the years within the simulation. The lowest plot gives the *Zostera* map on top of the *Spartina* map, with *Zostera* using a different colorbar from the default representations.

5 Discussion

5.1 Model development

The Delft3D estuary model was combined with the dynamic vegetation model. The dynamic vegetation model was adjusted to incorporate cohesive sediment dynamics through making the vegetation model compatible with the latest Delft3D version. A new colonization method was developed which plants species in the subtidal zone, regardless of the location's conditions. This enables the model to incorporate subtidal and intertidal vegetation, which is of major importance in estuaries. The flooding and dessication modules where adjusted to determine the amount of days that species were exposed or flooded for more than 25% or 75% of the tidal cycle respectively instead of counting days with flooding or dessication, regardless of the time. The main physical control on *Zostera marina* spreading is light availability, which was added to the model as an empirical function of the suspended sediment concentration and water depth. Light attenuation has a double dose effect relation, plants die when they do not get enough light for too long, and plants die faster when the amount of light is decreased further (Moore et al., 1997). This model, however, uses only a time-mortality dose effect relation once a certain threshold of light attenuation is exceeded. A lot of possibilities are created to model different estuarine species, but there are several limitations left to overcome.

5.1.1 Limitations

An important limitation to the model is the colonization function. Based on the colonization method by Oorschot et al. (2015) the vegetation was allowed to colonize all cells to a predefined cover. The effect of estuarine vegetation on hydrodynamics is, however, more significant than that of riparian vegetation in rivers. This is because submerged estuarine vegetation exerts friction on the flow continuously and intertidal vegetation exerts friction at least part of every day.

Vegetation is known to improve its own living conditions and this is visible in the runs with *Zostera* which rapidly colonizes to dense meadows. *Zostera* causes significant accumulation of suspended sediment due to its rapid colonization. This accumulation reduces the suspended sediment concentration which increases light penetration in the water and in this manner prevents other *Zostera* vegetation from dying. Wijgergangs and de Jong (1999) have thoroughly described the development of *Zostera* in the Wadden sea where large fields used to be abundant, but which have never regrown after the wasting disease events in 1930. It has proven to be very difficult to plant new *Zostera* species in the Wadden sea once the population has disappeared and it no longer enhances its own living conditions. Simulations with less aggressive (and thus probably more realistic) colonization avoid overflowing of the river and provide fairly realistic zonation patterns in the long run as they occupy shallow tranquil areas (Wijgergangs and de Jong, 1999), but a more realistic colonization module is important nonetheless.

A second important limitation of the model comes from the flexible nature of seagrasses. It is well known that seagrass bends under influence of currents, but there is no decent mathematical description of the induced flow resistance which takes this bending into account yet (Ganthy et al., 2015). In our model an approach was made by using a reduced maximum height, which therefore assumes the seagrass is always bending. This gives probably better results than using the maximum height because the influence of the Chezy value on shear stress is largest when flow velocity is largest:

$$\tau = \frac{\rho g U^2}{C^2} \tag{22}$$

In this equation τ is the bottom shear stress, ρ the water density, U the flow velocity and C the Chezy value. The influence of the vegetation during times of slack water is, however, underestimated in this way. Probably improvements can be made by applying the equation of Luhar and Nepf (2011) which

takes bending into account though it requires a lot of knowledge of the grasses:

$$\frac{l_e}{l} = 1 - \frac{(1 - 0.9Ca^{-1/3})}{1 + Ca^{-3/2}(8 + B^{3/2})} \tag{23}$$

In this equation l_e is the effective length, l is the actual length of the seagrass, B is the ratio of the restoring force due to buoyancy and the restoring force due to stiffness, Ca indicates the hydrodynamic drag with respect to the stiffness induced restoring force, the so called Cauchy number. But even this equation does not take sheltering effects of seagrass on the sediment bed into account which shows that there are still problems to overcome before we can realistically model seagrasses.

A third important limitation is the discrepancy between the vegetation growth and vegetation mortality timescale. Vegetation grows every ecological timestep (approximately two weeks) but dies only once a year under influence of flooding, dessication and light attenuation. This means that vegetation which would die two timesteps after its colonization due to flooding, dessication or light attenuation will continue to affect the hydromorphodynamics until the end of the year before it is removed from the simulation. Vegetation enhances mud deposition and thus reduces light attenuation. Mortality due to light attenuation is therefore much lower now than it would be if vegetation would disappear faster after its mortality.

The model has a couple important limitations which will have to be overcome. It is, however, the first model with hydromorphodynamics, cohesive sediment, intertidal and subtidal vegetation ever and therefore it also creates a lot of possibilities.

5.2 The effect of mud, *Spartina anglica*, and *Zostera marina*

There is a strong correlation between the occurrence of *Spartina anglica* and mud (Table 5). The mud deposition pattern follows the *Spartina* distribution, which could be expected based on Wolanski et al. (2004) who described the large influence of vegetation on sedimentation and mud accumulation. In our simulations the mud cover in the toplayer increased significantly once the final vegetation cover exceeded 5%. This 5% cover is the colonization density and might indicate the transition of seedlings to vegetation which has been present for multiple years. The inclusion of mud has shown to enhance a lot of morphological patterns which occur under the influence of *Spartina* even if the pattern under the influence of mud without *Spartina* is the opposite. This could be compared to a reduction in the required morphological timescale as is also described by Van Ledden et al. (2004). On the other hand it might be because the flow, which is retarded by the vegetation, is retarded further due to enhanced sedimentation and thus a reduction of the water depth. It is not clear what the critical property of mud is, its cohesiveness, its transport in suspension instead of as bedload or the fact that there is just more sediment available in our simulations with mud. Accretion in salt marshes comes usually for 90% from suspended sediments unless flow velocities are particularly high, which might indicate that its transport in suspension is the critical property (Mudd et al., 2010). Mud and *Spartina* do naturally occur in the same areas, but the sedimentation under influence of *Spartina* is an order of magnitude larger. Most of the effects of *Spartina* are strengthened by the presence of mud and even the concentration of *Spartina* in the estuary increases as is visible in the main results (Table 5). This increased *Spartina* concentrations occurs because the enhanced sedimentation lifts *Spartina* from the lower to the higher intertidal zone where the physical stress is less.

The hypothesis that the mud deposition pattern will follow the vegetation distribution is confirmed.

5.2.1 Mud

Mud has shown to form mudflats on the intertidal edges of the estuary and to stabilize these. Cohesive sediment leads to meandering in rivers and also shifts the system to one deeper channel instead of multiple shallow ones (Dijk et al., 2013b). Mud decreases the number of channels (braiding index) in

Effect of:	Run #	Result
Mud	3	• Stabilization of upper intertidal area • Mudflats fringing estuary • Reduced braiding index
Spartina	5	• Accretion in upper intertidal area • Channel deepening • Reducing intertidal area if naturally stable • Stabilizing intertidal area if naturally eroding • Decreases width averaged flow velocities • Increases peak flow velocities
Spartina & mud	6, 12	• Mud enhances *Spartina*'s morphodynamic effects • Mud accumulation pattern follows vegetation distribution • *Spartina* concentration increases
Zostera	16	• Not successful, but not modelled with random 10% colonization
Zostera & mud	25	• *Zostera* mortality due to light attenuation • Channel deepening

Table 5: Main effects of adding vegetation and mud to the estuary

deltas as well (Edmonds and Slingerland, 2010). These researches show that mud reduces the braiding index of rivers and deltas. This pattern is also visible in our simulations, though it is not very clear. The underlying mechanism is, however, deposition of mud on the floodplains close to the channels. This is a major difference between rivers and deltas and estuaries because estuary channels are, in the outer zone, not bordered by floodplains. The shift towards a single channel, and thus a decrease in braiding index, is most clear in the central zone of the estuary, where the influence of cohesive fines is the largest (Dalrymple et al., 1992). Van den Berg et al. (2007) indicated that the system switches to a single channel in the central zone of the estuary because the flood velocity decreases to much to scour channels, this pattern is also visible in our simulations (Figure 26). Once the system its width decreases, floodplain like areas can develop which laterally limit the channel movement and reduce braiding index (Figure 23). The simulation with 50 mg/l mud has shown to deposit some mud on the bars in the outer zone, which are positioned close enough to the estuarine channels that they further limit their dynamics (Figure 22 run #3). This shows that mud can decrease the braiding index but its effects are smaller than in delta or river systems because it deposits to far from the channels in the outer zone. The presence of mud, however, helps to force the system to a single channel in the central zone of the estuary, additional to the decrease in flood velocity (Van den Berg et al., 2007). The hypothesis that mud concentration decreases braiding index in estuaries seems to be correct, though its effects are limited compared to its effect in rivers and deltas. The hypothesis, however, that mud would drive a deepening of channels appears to be wrong when mud is the only variable.

Channel width and depth are dependent on bank strength through either cohesive fines or vegetation and an increasing bank strength results in deeper smaller channels (Hey and Thorne, 1986; Leopold and Maddock Jr, 1953; Parker, 1979). In our simulations the changes in bathymetry development under influence of mud all appear in the higher intertidal areas on the edges of the estuary. In riverine setting mud accumulates in the higher areas (floodplains) as well, but these are located adjacent to the channels. Our channels are not as much affected by it because they are located more distal from the mud accumulations. It might depend on the channel depth indicator used as well. The 5th percentile mainly gives the development of the outer zone channels, so probably a different indicator would show (slightly) different results. Braat et al. (2016) have shown that channel depth in estuaries is not influenced by mud concentration on a millennial timescale though the estuary width is decreased and mud does accumulate next to the channels. Their estuary, however, obtained a totally different bathymetry with a more delta-like planform. It is interesting to investigate whether estuaries

always develop this planform, because this probably strongly decreases the tidal prism which might cause shallower channels.

The hypothesis that mud decreases the braiding index in the estuary has been found to be correct while the channel depth appears to be unaffected by the presence of mud.

5.2.2 *Spartina anglica*

In our simulations *Spartina anglica* colonizes the intertidal area at the edges of the estuary as it does in nature (Ibáñez et al., 2012; Hammond et al., 2002). The dynamics in its development are, however, relatively minor in our simulations which was especially visible in the sensitivity analysis. This means that *Spartina* probably colonizes the estuary more aggressively than it would in nature. Extreme hydrodynamic events have to be included on top of basic hydrodynamic conditions because these exert a strong influence on ecosystem development (Gaines and Denny, 1993).

Spartina has shown to increase sedimentation and mud accumulation in the simulations. The process of increased sedimentation rates is confirmed by Lee and Partridge (1983); Thompson (1991) who also pointed to increased mud deposition. Widdows et al. (2008) state that *Spartina anglica* actually increases erosion because it increases turbulence, turbulent kinetic energy and bed shear stress. Their study, however, focussed strongly on the influence of waves and storms, so probably this holds for areas where wave action is of major importance. These effects are not incorporated in our representation of *Spartina*, and neither did we model waves because of which our model shows accretion under influence of *Spartina*, as do most studies.

Spartina grows on the edges of the estuary, tidal bars and shoals and turns these intertidal areas into salt marshes. It causes sedimentation in the upper intertidal areas as indicated by the 95th percentile and bed level distribution. This matches the development of *Spartina* as described by Pringle (1993). Our models show mud and sediment accumulation on the tidal bars under influence of *Spartina* as well, which could be a possible explanation for the emergence of tidal bars. This pattern is described for river banks by Gurnell et al. (2012). There is little literature on *Spartina* occupying tidal bars when they are still submerged for a significant part of the tidal cycle. *Spartina* can survive up to 9 hours of consecutive flooding (Nehring and Adsersen, 2006), but probably it only colonizes areas which are flooded up to 3 hours as is indicated by Rijkswaterstaat (Bouma et al., 2007a). This makes it difficult to tell whether the pattern is fully realistic though it is interesting to further investigate as *Spartina* is known to occupy tidal bars in a later stage where it can facilitate mud accumulation.

The effect of *Spartina* on the development of the intertidal area depends on the sole morphological development of the estuary. Our default bathymetry has an increasing intertidal area, where *Spartina* results in a relative decrease of the intertidal area. *Spartina* does increase sedimentation within its patches but enhances erosion adjacent to it (Bouma et al., 2007b). This drives erosion of the intertidal area and therefore the increase in intertidal area which is visible without *Spartina* is absent in the simulations with *Spartina* (Run #1&5). A different pattern emerges in the second tested bathymetry. This bathymetry has a decreasing intertidal area without *Spartina* (Run #11) and here *Spartina* actually stabilizes the intertidal area for a large part of the simulation which keeps the intertidal area relatively large (Run #15). This matches with Wolanski et al. (2004) who have shown that *Spartina* stabilizes intertidal areas. In nature *Spartina* might also drive a decrease in intertidal area due to intertidal area loss to the supratidal zone. In our simulations, however, this did not happen, but this might be because Delft3D has problems with turning cells dry.

The hypothesis that *Spartina* drives accretion on shoals and the estuary edges but does not create new intertidal area is correct. It can, however, stabilize the present intertidal area extent in case it is eroding, or erode the intertidal area if the system tends to increase its intertidal areas.

Spartina increases the roughness in the intertidal areas and thus decreases flow velocities. This decreased flow velocities in the intertidal area are partly due to the sole presence of *Spartina*, but

also partly because it enhances sediment deposition and shallower areas have lower flow velocities. The maximum flow velocities, however, increase for both the ebb and the flood flow. Lawrence et al. (2004) describe an increased flow velocity in channels adjacent to vegetation because the retarded flow in the vegetation is compensated by increased flow velocities in neighbour areas. A different explanation, however, might be that the convergence in the estuary has increased because of sedimentation in the intertidal areas. This would also explain the increased tidal range in the estuary.

Sedimentation in the intertidal area decreases the intertidal area its storage volume with respect to the channel storage volume (V_s/V_c decreases). A decreased storage volume in the intertidal area can result in a more flood dominant system (Friedrichs, 2010). However, the channels in the estuary increase in depth as well, which decreases the average channel depth to tidal amplitude ratio ($a/ < h >$). The relative increase of the average channel depth ($< h >$) with respect to the tidal amplitude (a) favours a more ebb dominated system and therefore these two effects might counteract eachother.

The hypothesis that tidal amplitude and flow velocity decrease under influence of *Spartina* is partly correct. The tidal flow velocity decreases in the marsh area as well as the width averaged flow velocity. However, the peak flow velocity increases because a relatively larger part of the tidal prism is conveyed through the permanently submerged area. The tidal amplitude increases, which is the opposite of what we expected. This might be because the flow is more converged and transported through narrower cross sections for most of the time and this effect is probably stronger than the increased friction due to the vegetation. The hypothesis that the system will become more flood dominant was not found to be true, the magnitude of the ebb and flood flow were changed equally.

When it comes to channel development it depends on the initial bathymetry what the effect of *Spartina* is. D'Alpaos et al. (2006) have shown that *Spartina* either drives channel deepening or channel infilling in tidal marsh channels. *Spartina* increases the flow velocity beyond the marsh edges, which can result in additional scour of the channels and thus in channel deepening. Marsh development, on the other hand, can decrease the tidal prism in the estuary which leads to decreased flow velocities and therefore results in channel infill (D'Alpaos et al., 2006). Our simulations show a deepening of the channels for the default bathymetry (Run #6), but this pattern no longer holds for our simulations with the different bathymetry (Run #12). Simulations with our wider initial bathymetry show that *Spartina* has zero influence on estuary channels. Probably this is because the 5th percentile is an indication of channel depth in the outer zone, where channels are located distal from the *Spartina* growth locations in the simulations with a different bathymetry. This might show that the pattern described by D'Alpaos et al. (2006) only holds for situations similar to tidal marshes where the channels are directly bordered by *Spartina*.

The hypothesis that *Spartina* deepens estuary channels is partly true. *Spartina* has shown to be able to deepen channels. However, it depends on the initial bathymetry, and thus the location of *Spartina* with respect to the estuary channels whether *Spartina* causes channels to deepen. It is uncertain whether the main reason for the channel deepening comes from the lateral confinement of the channels or the increased flow velocity beyond the marsh edges.

5.2.3 *Zostera marina*

The simulation of *Zostera* does an attempt at reproducing the natural condition enhancing effects of *Zostera*. Simulations show a strong decrease in suspended sediment concentration under influence of *Zostera*, a pattern which is also shown in flume experiments (Ganthy et al., 2015). The magnitude of this decreased suspended sediment concentration is, for the runs with aggressive colonization, larger than realistic (Figure 37, Run #22). Our simulations also show that the ecosystem has difficulties with recovering once the vegetation disappears and the condition enhancing effects disappear, a pattern described by Wijgergangs and de Jong (1999). These two observations indicate that, to sustain dynamic vegetation development, average estuary conditions might not suffice. As is the case with *Spartina*, population dynamics depend on variability in conditions and extremes (Gaines and Denny, 1993).

It might be important to temporally vary suspended sediment concentrations and tidal conditions to produce dynamic *Zostera* development.

Zostera seems to drive a deepening of the estuary channels. The effect of *Zostera* on channel depth has never been researched, which makes it hard to compare our results to reality. It might, however, work through a similar mechanism as described for *Spartina* where vegetation redistributes peak flow velocities which could drive channel deepening as *Zostera* tends to grow next to channels. Gacia et al. (1999) have shown that the seagrass *Posidonia oceanica* significantly reduces erosion in its meadows and increases sedimentation. *Zostera* grows predominantly in shallow tranquil areas (Wijgergangs and de Jong, 1999). The presence of *Zostera* in shallow tranquil areas is also present in our simulations, the increased sedimentation which could extend the intertidal area, however, is not. The decreased intertidal area is probably a result of the presence of mud and not of the presence of *Zostera* itself. Mud has shown to result in a decreased tidal amplitude in the simulations without *Zostera* and might therefore reduce the intertidal area. The expected increase in intertidal area due to increased sedimentation, however, is absent as well. This might be because *Zostera* does not significantly increase deposition in our simulations, probably because its covers remain fairly low.

The hypothesis that *Zostera* drives the formation of more and larger shoals and increases the intertidal area appears to be wrong. *Zostera* grows on the shallow subtidal areas but it does not increase deposition enough to elevate itself into the intertidal area. The hypothesis that *Zostera* drives deepening of estuarine channels is correct, probably due to increased flow velocities adjacent to *Zostera* fields or channel confinement.

5.2.4 *Spartina* and *Zostera*

The combined effect of *Spartina* and *Zostera* has not been investigated because the simulation of *Zostera* took to long to work out. However, there appears to be some interaction between the two, though they do not show succession patterns of *Zostera* into *Spartina* as is described by Gurnell et al. (2012). *Spartina* and *Zostera* occur predominantly next to eachother, which indicates that they might help eachother to survive, probably because *Spartina* increases the visibility in the water when it sedimentates the suspended sediment during high water conditions.

5.3 Comparison between model and field data

5.3.1 Mud

In the Western Scheldt mud accumulates on the edges of the estuary and on the higher tidal bars (Figure 41). However, there is no continuous mud cover on the estuary edges, except for several patches. There are mud accumulations on some of the larger tidal bars as well, these are predominantly bars which are submerged a relatively short part of the tidal cycle. Our models show mud accumulation on the edges of the estuary as well, but the cover is more continuous, comparable to the Gironde estuary in France (Figure 43). Our simulations have shown to have little mud accumulation on tidal bars without *Spartina*, but significant accumulations when *Spartina* is present. A similar pattern is found when the *Spartina* occurrence map of van Schaik AWJ and van der Pluijm AM (1988) is laid on top of the ecotope map from the Nationaal Georegister (Figure 41). Mud accumulates predominantly on the bars with *Spartina* though there are also bars with some mudcover but no *Spartina*. Figure 42 shows that the relative extent of the mud accumulation is larger in the upstream than the downstream reach of the Western Scheldt. This matches with our simulations which show a decrease in the relative extent of mud accumulations from the upstream to downstream reach. Our simulations with 50 mg/l mud show large mud accumulations around 10 km in the estuary, this is relatively close to the tidal limit (tidal amplitude becomes zero after 12 km and the flood velocity goes to zero here as well). This shows that the maximum mud accumulation occurs around the TMZ and that deposition patterns match the classical overview by Dalrymple et al. (1992).

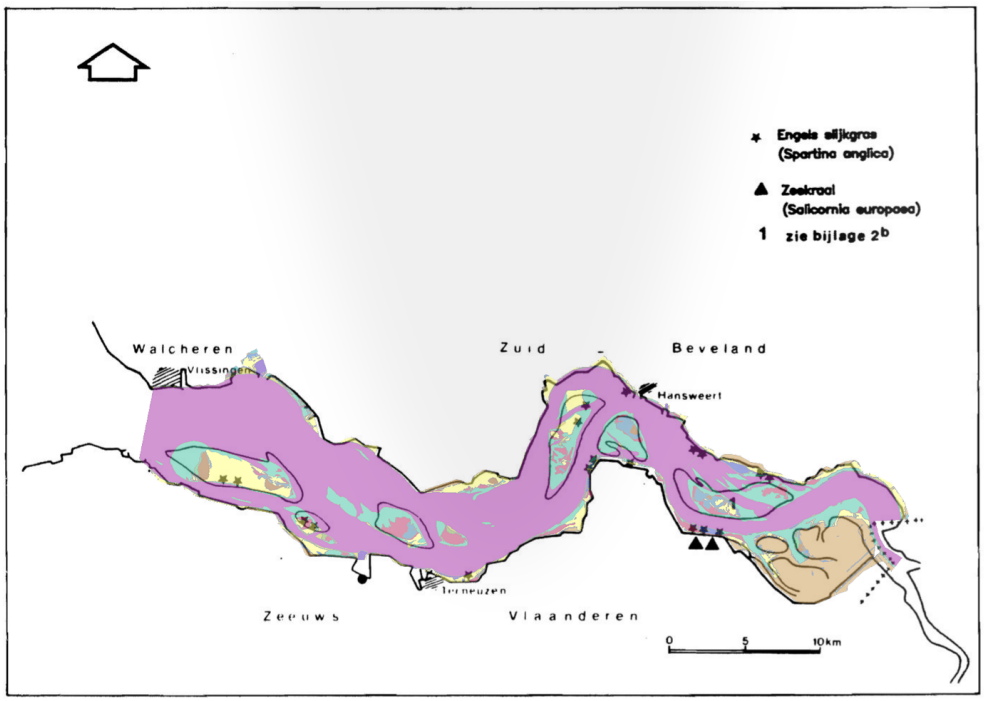

Figure 41: Area of the Western Scheldt for which ecotope maps are available (Nationaal Georegister). Yellow areas are rich in mud and stars mark *Spartina anglica* habitats (van Schaik AWJ and van der Pluijm AM, 1988).

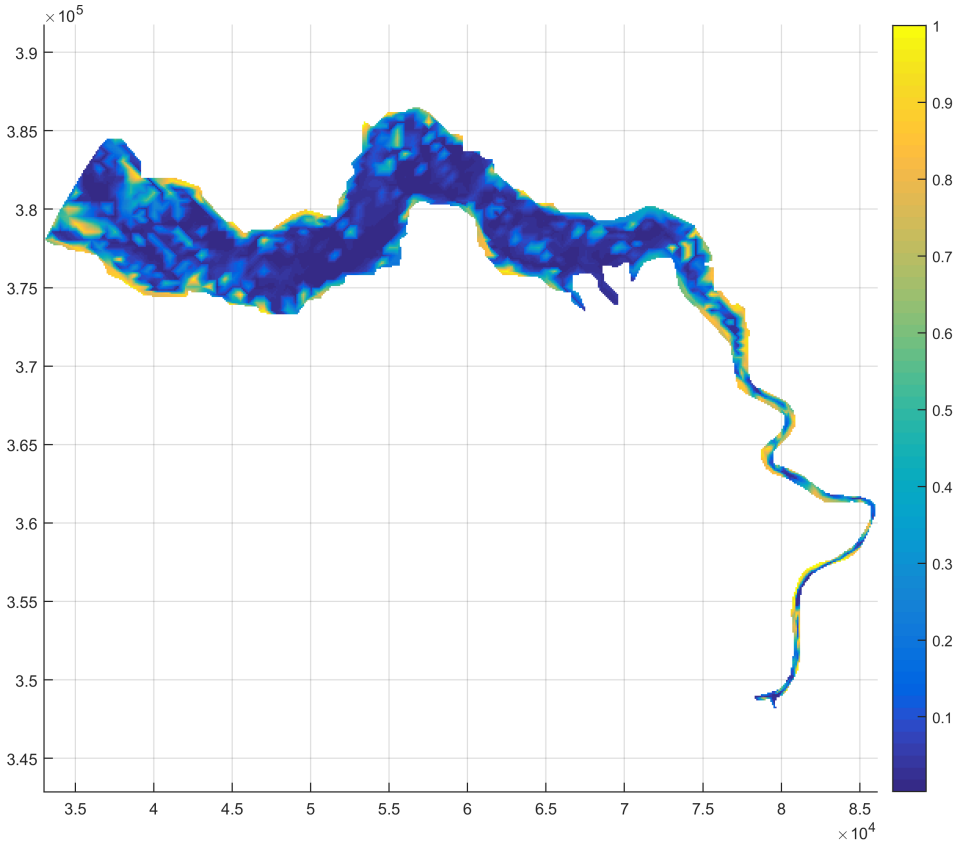

Figure 42: The mud distribution over a larger part of the Western Scheldt. As can be seen the relative extent of mud at the estuary edges decreases in the downstream reach (MClaren ??).

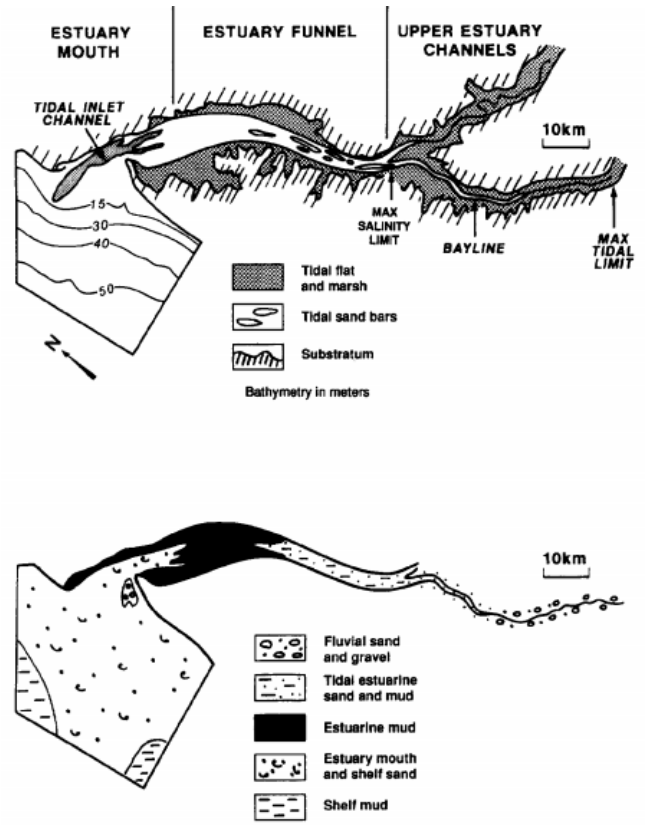

Figure 43: The mud distribution in the Gironde estuary, france (Allen and Posamentier, 1993)

5.3.2 Vegetation patterns

Vegetation is often mapped on a small scale, especially when it comes to submerged vegetation. An attempt has been made to find some estuary maps of *Spartina* species and seagrass species. These are not solely *S. anglica* and *Z. marina*, but should give an indication of their areal extent. Figure 44 shows *Spartina* occurence for 6 different estuaries. As can be seen *Spartina* can cover large areas, growing from the edge of the estuary, expanding towards the main channel (Figure 44D,E,F). Figure 44C shows that *Spartina* also occupies bars/islands, but this image makes it hard to determine the spatial extent on these. Figure 44B shows that *Spartina* can occupy larger areas very fast, similar to what we find in our simulations. On the other hand figure 44B,D,E also shows that *Spartina* expansion tends to focus on areas surrounding current patches, a pattern which our model does not reproduce because radial growth of patches and seed dispersal patterns are lacking. A final remark is that the *Spartina* concentration in our simulations keeps increasing with increasing elevation. This is because the upper boundary of *Spartina* is set by competition which is not present in our simulations (Bockelmann and Neuhaus, 1999). It is, however, common that biomass increases with height and therefore this should not affect the simulations to much (Marani et al., 2004).

Seagrass preferentially grows around channels (Figure 45A,B,F) , but also on the edges of estuaries and embayments (Figure 45A,C,D,E). Seagrass grows around estuarine channels and not in these due to the more tranquil hydrodynamics (Van Katwijk and Hermus, 2000). This preference for more sheltered areas over estuary channels is visible in all our simulations as well.

Our simulations show that *Zostera* prefers the edges of the estuary just as in nature. Most maps clearly show that *Zostera* predominantly occurs as more continuous meadows, only figure 45C shows patchy vegetation patterns. This occurrence in continuous meadows might be caused either by its condition enhancing effects or because these areas are more suitable for *Zostera*. In our simulations

Zostera either forms dense meadows (in the case of uniform colonization) or a more patchy distribution (in the case of 10% random colonization). Rand (2000) have shown that *Zostera* spreads predominantly to neighbour areas, a pattern which we, especially for the 10% random colonization simulations do not reproduce. Bos and Van Katwijk (2007); Van Keulen et al. (2003) have shown that denser *Zostera* covers have a higher survivability rate when planted. The simulations with 10% random colonization show that areas which are characterized by a dense *Zostera* concentration after 30 years tend to be in the middle of larger *Zostera* areas, which shows a similar protective behaviour of *Zostera*.

The model is able to reproduce mud deposition and *Spartina* zonation patterns fairly well and thus these can yet be further investigated. *Zostera* has shown to occur adjacent to channels and in more tranquil areas but does not yet produce the pattern of continuous meadows and areas where *Zostera* does not develop at all.

5.4 Contribution to theory, practice and society

This research provides insight in the redistribution of mud under influence of vegetation. Through an increased understanding of this redistribution and its effect on the vegetation density it becomes possible to make better predictions on the effect of *Spartina* invasions. On the other hand the increased mud accumulation under influence of *Spartina* can be used to manage systems which experience hyper-turbidity like the ems estuary. Enhanced sedimentation of fines under influence of *Spartina* can probably reduce the turbidity. One of the causes of the hyper-turbidity in this estuary is the drag reduction due to mud accumulation in the channels which might be reduced as well when mud sedimentates predominantly in the marsh areas (van Maren et al., 2015).

After additional verification it becomes possible to investigate *Zostera* zonation patterns which helps in *Zostera* restoration attempts. In terms of scientific relevance it was well known that vegetation enhances mud deposition, but now it has been shown that vegetation can totally redistribute mud over the estuary. Also a two-directional interaction between the presence of vegetation and mud has been shown which is a new discovery which can lead to further research and which has to be taken into account in future research on either mud or vegetation distribution.

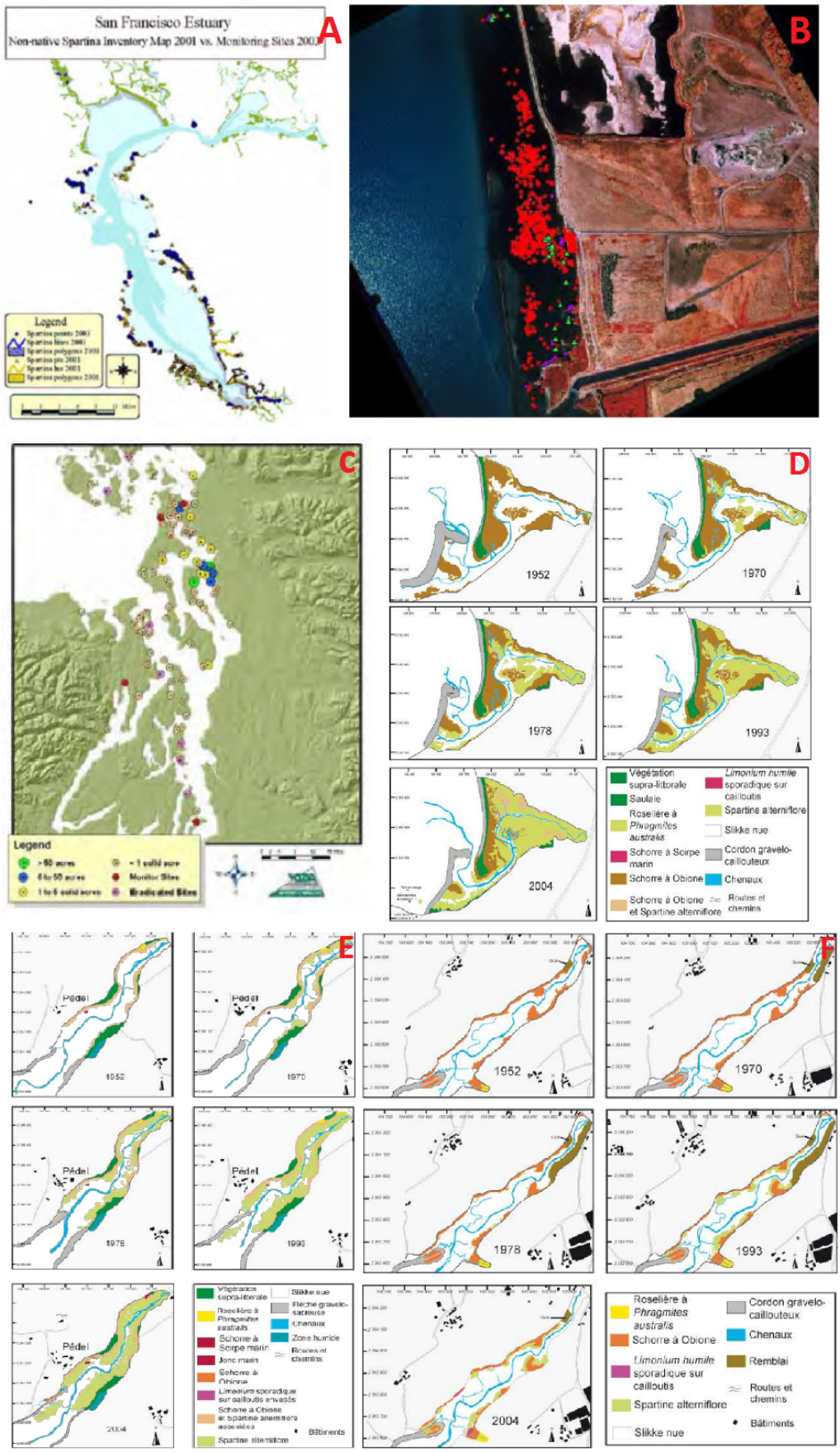

Figure 44: A) occurrences of *Spartina* indicated by dots in the San Francisco estuary (Zaremba et al., 2004), B) *S. alterniflora* spreading in one year (green to red) in San Francisco bay (Sloop et al., 2004), C) *Spartina* spreading indicated by the dots in Washington state estuary (MURPHY et al., 2004), D) *Spartina* cover in the Mengleuz estuary over the years, E) *Spartina* cover over the years in the site du Pédel estuary, F) *Spartina* cover in the Pont-Callec estuary over the years, D,E,F are all found in the Quimper province, France (Sparfel et al., 2005).

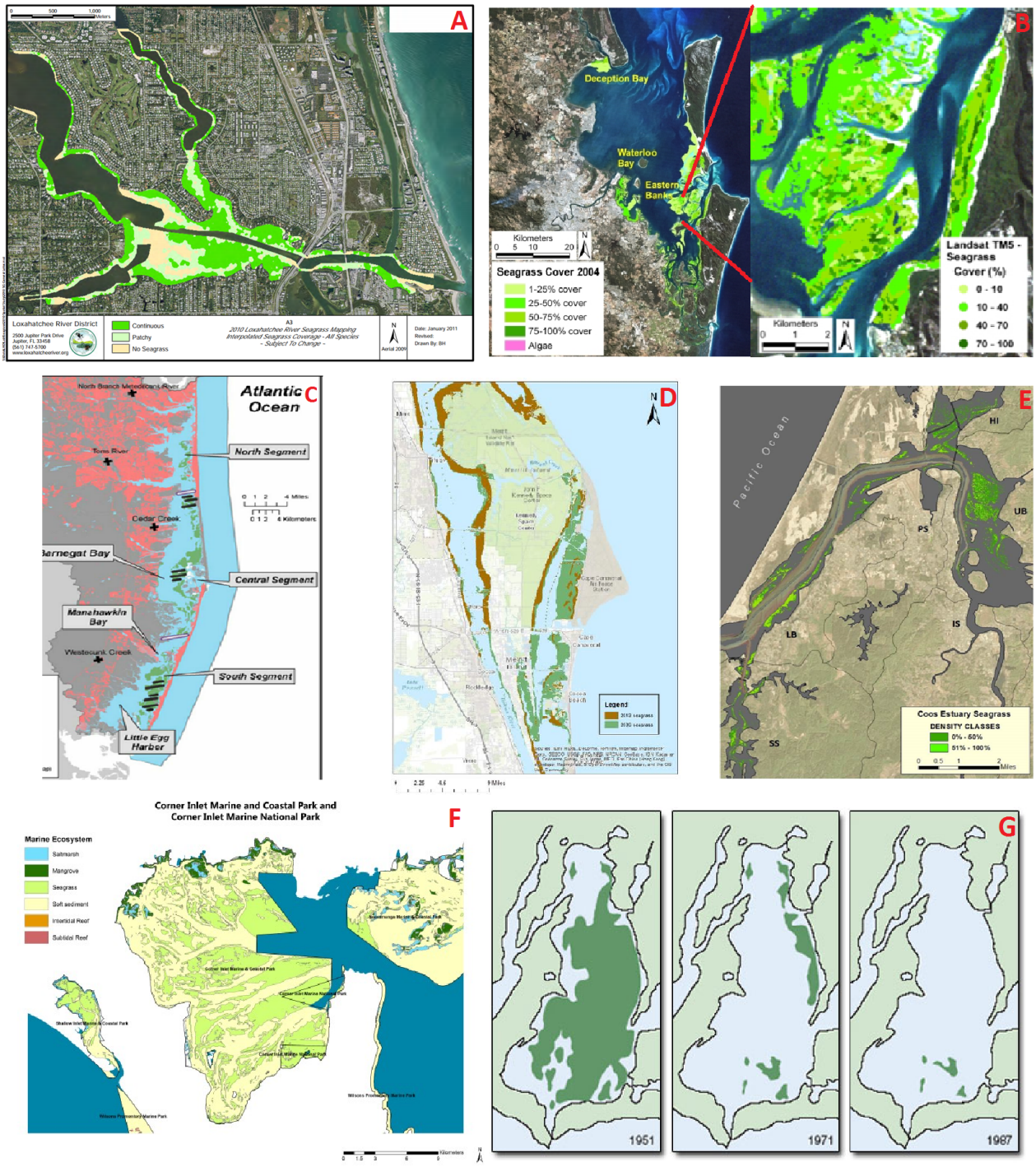

Figure 45: A) seagrass in the Loxahatchee river, Florida (Loxahatchee River Environmental Control District), B) seagrass spreading in Moreton Bay, Australia (ozcoasts.gov.au), C) seagrass spreading in Barnegat Bay (Fertig et al., 2014), D) seagrass in the Indian River Lagoon (St. Johns River Water Management District), E) seagrass in the Coos estuary (Clinton et al., 2007), F) seagrasses in Corner inlet Marine and National Park (www.enviroactive.com.au/), G) seagrass decline in Waquoit Bay (The Open University)

6 Conclusion

6.1 Model development

The first hydromorphodynamic estuary model with cohesive sediment and dynamic intertidal and subtidal vegetation ever was developed. This offers a lot of possibilities to research estuaries though there are three important limitations left: First, colonization patterns have shown to have significant influence, especially for submerged vegetation and the model does not contain a decent module for this yet. Secondly, seagrasses (and many other submerged vegetation species) are flexible and this flexibility cannot be modelled properly yet. Decreasing the maximum vegetation height has shown to help with the modelling but this is similar to the assumption that seagrass is always bending which is not true. Third, the mortality and growth timescales are different now which results in some strange behaviour due to eco-engineering effects of vegetation.

6.2 The effect of mud, *S. anglica*, and *Z. marina*

Mud decreases the braiding index of the estuary because it limits the lateral movement of estuarine channels. The decrease in braiding index happens mainly in the upper part of the estuary and is not as significant as in river and delta systems. Unlike in rivers and delta's mud does not drive an increase in channel depth because it does not confine them as much. This is because mud accumulates mainly on the estuary edges instead of in floodplains adjacent to the channels. When *Spartina* is added to the simulations the mud accumulation pattern follows the *Spartina* distribution. The effect which mud usually has on estuary morphodynamics can change under influence of *Spartina*, because the distribution pattern of mud changes and it acts as a morphodynamic catalyst for *Spartina*. It is, however, still unknown whether it enhances the morphological effects of *Spartina* because of its cohesiveness, because its transported in suspension or because there is just more sediment in the system.

Spartina grows in the intertidal area at the edges of the estuary and on shoals. It strongly increases the sediment accumulation in these areas, but can drive disappearance of its neighbour intertidal area because it increases the flow velocity at the patch edges. When the intertidal area, however, is naturally prone to erosion, *Spartina* can stabilize it and prevent erosion. *Spartina* adds additional flow resistance to the intertidal areas and therefore the flow velocity in these areas decreases. This decrease in flow velocity in the intertidal area, however, is compensated by an increased flow velocity in the areas beyond the extend of the marsh. If the marsh lies adjacent to the estuary channels these are deepened, but channels further away from the marsh edges are not influenced.

Zostera was expected to drive an increase in intertidal area because it grows in the subtidal areas close to the intertidal area where the light attenuation and water movement is little. The sedimentation is, however, not enhanced enough to elevate the *Zostera* patches into the intertidal area. The channels are deepened by *Zostera* because it forces the flow to go through the channels.

Finally a two-directional interaction between mud and vegetation was found. Neither vegetation nor mud distribution can be modelled reliably without taking the other into account in future research.

6.3 Comparison between model and field data

The modelled mud distribution resembles mud accumulation patterns which we observe in the Western scheldt and the Gironde estuary. The relative extent of the mud accumulations is largest in the upstream part of the estuary and mud accumulates on the estuary edges and on some of the tidal bars. Therefore the predictions with respect to mud distribution and its effects are likely to be realistic.

The spreading of *Spartina* is partly realistic. *Spartina* occupies the intertidal areas fringing the estuary as it does in nature, but it probably colonizes areas which are submerged for too long. This might be because grown *Spartina* can survive longer inundation than its seedlings which are also

more likely to become completely submerged. Its dynamics are too limited in our simulations as well but this is due to the simplified tides and lack of waves.

Zostera does not produce fully realistic patterns though there is limited field data available to compare with. It does grow adjacent to channels and not in them as it does in reality. The pattern of dense continuous meadows separated by areas without any *Zostera* is not yet reproduced though. A better colonization module might be able to solve this in the future.

7 Future work

More verification is required before the model produces fully reliable results, especially for submerged, flexible, vegetation. After verification, however, it offers a broad range of research possibilities. Here a few ideas for future research are presented which could be executed in a similar manner as the present research but which where not performed yet.

7.1 Model optimization

It was hypothesized that extreme conditions are of vital importance to maintain dynamic ecosystem development. Through including waves and different/more tidal components it becomes possible to test their influence on vegetation zonation. When this is combined with a more realistic colonization module it might be possible to obtain even more realistic results. A better colonization module would take the preferential spreading to neighbour areas into account, for example through a random 10% colonization and colonization to all cells adjacent to current vegetation patches. It can also be investigated what the effect is when substrate is taken into account in the colonization module. A preferential spreading to areas with a significant mud concentration in the toplayer could be programmed because *Spartina* preferentially colonizes muddy areas in nature. It would be interesting to see how the effect of *Spartina* on mud distribution changes when the presence of mud increases the likeliness of *Spartina* colonization.

7.2 Turbidity reduction

Spartina has shown to increase sedimentation of predominantly fines. Many areas around the world have problems with hyper-turbid waters due to anthropogenic alterations of estuaries. This model can be used to investigate the possibility of eco-engineering to reduce turbidity in the waters and bring the system back to natural conditions.

References

Allen, G. P. and Posamentier, H. W. (1993). Sequence stratigraphy and facies model of an incised valley fill: the gironde estuary, france. *Journal of Sedimentary Research*, 63(3).

Bakema, A. (1988). Empirische licht modellering voor een aantal nederlandse meren. *WL T387. Delft*.

Baptist, M., Babovic, V., Rodríguez Uthurburu, J., Keijzer, M., Uittenbogaard, R., Mynett, A., and Verwey, A. (2007). On inducing equations for vegetation resistance. *Journal of Hydraulic Research*, 45(4):435–450.

Barwis, J. H. (1977). Sedimentology of some south carolina tidal-creek point bars, and a comparison with their fluvial counterparts.

Bertoldi, W., Gurnell, A., Surian, N., Tockner, K., Zanoni, L., Ziliani, L., and Zolezzi, G. (2009). Understanding reference processes: linkages between river flows, sediment dynamics and vegetated landforms along the tagliamento river, italy. *River Research and Applications*, 25(5):501–516.

Bockelmann, A.-C. and Neuhaus, R. (1999). Competitive exclusion of elymus athericus from a high-stress habitat in a european salt marsh. *Journal of Ecology*, 87(3):503–513.

Bos, A. R. and Van Katwijk, M. M. (2007). Planting density, hydrodynamic exposure and mussel beds affect survival of transplanted intertidal eelgrass. *Marine Ecology Progress Series*, 336:121–129.

Bouma, H., De Jong, D., Twisk, F., and Wolfstein, K. (2007a). *Zoute wateren EcotopenStelsel (ZES. 1)*. Rijkswaterstaat, RIKZ.

Bouma, T., Van Duren, L., Temmerman, S., Claverie, T., Blanco-Garcia, A., Ysebaert, T., and Herman, P. (2007b). Spatial flow and sedimentation patterns within patches of epibenthic structures: Combining field, flume and modelling experiments. *Continental Shelf Research*, 27(8):1020–1045.

Bouma, T., Vries, M. D., Low, E., Kusters, L., Herman, P., Tanczos, I., Temmerman, S., Hesselink, A., Meire, P., and Van Regenmortel, S. (2005). Flow hydrodynamics on a mudflat and in salt marsh vegetation: identifying general relationships for habitat characterisations. *Hydrobiologia*, 540(1-3):259–274.

Braat, L. and Kleinhans, M. (2016). Effects of mud supply on large-scale estuarine morphology: Estuarine self-confinement by mud supply in long-term morphodynamic modelling. *In prog.*

Braat, L., Kleinhans, M., van Kessel, T., Wongsoredjo, S., and Bergsma, L. (2016). Effects of mud supply on large-scale estuarine morphology. *EGU General Assembly Conference Abstracts*, 18:5618.

Brown, C. E. and Pezeshki, S. R. (2007). Threshhold for recovery in the marsh halophyte spartina alterniflora grown under the combined effects of salinity and soil drying. *Journal of plant physiology*, 164(3):274–282.

Brown, J. and Davies, A. (2010). Flood/ebb tidal asymmetry in a shallow sandy estuary and the impact on net sand transport. *Geomorphology*, 114(3):431–439.

Clinton, P., Young, D., Specht, D., and Lee II, H. (2007). A guide to mapping intertidal eelgrass and nonvegetated habitats in estuaries of the pacific northwest usa. Technical report, Report EPA/600/R-07/062 (August 2007). US Environmental Protection Agency, Washington, DC, USA.

Coco, G., Zhou, Z., van Maanen, B., Olabarrieta, M., Tinoco, R., and Townend, I. (2013). Morphodynamics of tidal networks: advances and challenges. *Marine Geology*, 346:1–16.

Corenblit, D., Steiger, J., Gurnell, A. M., and Naiman, R. J. (2009). Plants intertwine fluvial landform dynamics with ecological succession and natural selection: a niche construction perspective for riparian systems. *Global Ecology and Biogeography*, 18(4):507–520.

D'Alpaos, A., Lanzoni, S., Mudd, S. M., and Fagherazzi, S. (2006). Modeling the influence of hydroperiod and vegetation on the cross-sectional formation of tidal channels. *Estuarine, Coastal and Shelf Science*, 69(3):311–324.

Dalrymple, R. W. and Choi, K. (2007). Morphologic and facies trends through the fluvial–marine transition in tide-dominated depositional systems: a schematic framework for environmental and sequence-stratigraphic interpretation. *Earth-Science Reviews*, 81(3):135–174.

Dalrymple, R. W., Zaitlin, B. A., and Boyd, R. (1992). Estuarine facies models: conceptual basis and stratigraphic implications: perspective. *Journal of Sedimentary Research*, 62(6).

Davidson, N., Laffoley, D. d., Doody, J., Way, L., Gordon, J., Key, R. e., Drake, C., Pienkowski, M., Mitchell, R., and Duff, K. (1991). Nature conservation and estuaries in great britain. *Nature Conservancy Council, Peterborough*, pages 1–76.

Den Hartog, C. (1970). The sea-grasses of the world.

Deng, Z., Deng, Z., An, S., Wang, Z., Liu, Y., Ouyang, Y., Zhou, C., Zhi, Y., and Li, H. (2009). Habitat choice and seed–seedling conflict of spartina alterniflora on the coast of china. *Hydrobiologia*, 630(1):287–297.

Dias, J. and Picado, A. (2011). Impact of morphologic anthropogenic and natural changes in estuarine tidal dynamics. *Journal of Coastal Research*, (64):1490.

Dijk, W., Teske, R., Lageweg, W., and Kleinhans, M. (2013a). Effects of vegetation distribution on experimental river channel dynamics. *Water Resources Research*, 49(11):7558–7574.

Dijk, W. M., Lageweg, W. I., and Kleinhans, M. G. (2013b). Formation of a cohesive floodplain in a dynamic experimental meandering river. *Earth Surface Processes and Landforms*, 38(13):1550–1565.

Donaldson, A. C. (1970). Holocene guadalupe delta of texas gulf coast.

Dyer, K. R. (1986). *Coastal and estuarine sediment dynamics*. John Wiley & Sons, Inc.

Dyer, K. R. (1995). Sediment transport processes in estuaries. *Developments in Sedimentology*, 53:423–449.

Edmonds, D. A. and Slingerland, R. L. (2010). Significant effect of sediment cohesion on delta morphology. *Nature Geoscience*, 3(2):105–109.

Fertig, B., Kennish, M. J., Sakowicz, G. P., and Reynolds, L. K. (2014). Mind the data gap: identifying and assessing drivers of changing eutrophication condition. *Estuaries and coasts*, 37(1):198–221.

Friedrichs, C. T. (2010). Barotropic tides in channelized estuaries. *Contemporary Issues in Estuarine Physics*, pages 27–61.

Friedrichs, C. T. and Aubrey, D. G. (1988). Non-linear tidal distortion in shallow well-mixed estuaries: a synthesis. *Estuarine, Coastal and Shelf Science*, 27(5):521–545.

Gacia, E., Granata, T., and Duarte, C. (1999). An approach to measurement of particle flux and sediment retention within seagrass (posidonia oceanica) meadows. *Aquatic Botany*, 65(1):255–268.

Gaines, S. D. and Denny, M. W. (1993). The largest, smallest, highest, lowest, longest, and shortest: extremes in ecology. *Ecology*, 74(6):1677–1692.

Ganthy, F., Soissons, L., Sauriau, P.-G., Verney, R., and Sottolichio, A. (2015). Effects of short flexible seagrass zostera noltei on flow, erosion and deposition processes determined using flume experiments. *Sedimentology*, 62(4):997–1023.

Graham, G. and Manning, A. (2007). Floc size and settling velocity within a spartina anglica canopy. *Continental Shelf Research*, 27(8):1060–1079.

Gurnell, A. M., Bertoldi, W., and Corenblit, D. (2012). Changing river channels: The roles of hydrological processes, plants and pioneer fluvial landforms in humid temperate, mixed load, gravel bed rivers. *Earth-Science Reviews*, 111(1):129–141.

Hammond, M. E., Malvarez, G. C., and Cooper, A. (2002). The distribution of spartina anglica on estuarine mudflats in relation to wave-related hydrodynamic parameters. *Journal of Coastal Research*, 36:352–355.

Hansen, D. V. and Rattray, M. (1966). New dimensions in estuary classification. *Limnology and Oceanography*, 11(3):319–326.

Hayes, M. O. (1980). General morphology and sediment patterns in tidal inlets. *Sedimentary geology*, 26(1-3):139–156.

Hayes, O., Cronin, L., et al. (1975). Morphology of sand accumulation in estuaries: An introduction to the sympos.

Heip, C., Goosen, N., Herman, P., Kromkamp, J., Middelburg, J., and Soetaert, K. (1995). Production and consumption of biological particles in temperate tidal estuaries. *Oceanography and marine biology: an annual review*.

Hey, R. D. and Thorne, C. R. (1986). Stable channels with mobile gravel beds. *Journal of Hydraulic Engineering*, 112(8):671–689.

Ibáñez, C., Morris, J. T., Mendelssohn, I. A., and Day, J. W. (2012). Coastal marshes. *Estuarine Ecology, Second Edition*, pages 129–163.

Järvelä, J. (2002). Flow resistance of flexible and stiff vegetation: a flume study with natural plants. *Journal of Hydrology*, 269(1):44–54.

Jones, C. G., Lawton, J. H., and Shachak, M. (1994). Organisms as ecosystem engineers. In *Ecosystem management*, pages 130–147. Springer.

Karrenberg, S., Edwards, P., and Kollmann, J. (2002). The life history of salicaceae living in the active zone of floodplains. *Freshwater Biology*, 47(4):733–748.

Kouwen, N., Unny, T., and Hill, H. M. (1969). Flow retardance in vegetated channels. *Journal of the Irrigation and Drainage Division*, 95(2):329–344.

Lawrence, D., Allen, J. R. L., and Havelock, G. (2004). Salt marsh morphodynamics: an investigation of tidal flows and marsh channel equilibrium. *Journal of Coastal Research*, pages 301–316.

Lee, W. G. and Partridge, T. R. (1983). Rates of spread of spartina anglica and sediment accretion in the new river estuary, invercargill, new zealand. *New Zealand Journal of Botany*, 21(3):231–236.

Leopold, L. B. and Maddock Jr, T. (1953). The hydraulic geometry of stream channels and some physiographic implications. Technical report.

Li, W.-Q., Xiao-Jing, L., Khan, M. A., Gul, B., et al. (2008). Relationship between soil characteristics and halophytic vegetation in coastal region of north china. *Pak J Bot*, 40(3):1081–1090.

Luhar, M. and Nepf, H. M. (2011). Flow-induced reconfiguration of buoyant and flexible aquatic vegetation. *Limnology and Oceanography*, 56(6):2003–2017.

Luhar, M. and Nepf, H. M. (2013). From the blade scale to the reach scale: A characterization of aquatic vegetative drag. *Advances in Water Resources*, 51:305–316.

Mackin, J. E. and Kennish, M. J. (1988). Ecology of estuaries, vol. 1: Physical and chemical aspects.

Marani, M., Lanzoni, S., Silvestri, S., and Rinaldo, A. (2004). Tidal landforms, patterns of halophytic vegetation and the fate of the lagoon of venice. *Journal of Marine Systems*, 51(1):191–210.

Masselink, G., Hughes, M., and Knight, J. (2014). *Introduction to coastal processes and geomorphology*. Routledge.

Meire, P., Ysebaert, T., Van Damme, S., Van den Bergh, E., Maris, T., and Struyf, E. (2005). The scheldt estuary: a description of a changing ecosystem. *Hydrobiologia*, 540(1-3):1–11.

Monge-Ganuzas, M., Cearreta, A., and Evans, G. (2013). Morphodynamic consequences of dredging and dumping activities along the lower oka estuary (urdaibai biosphere reserve, southeastern bay of biscay, spain). *Ocean & coastal management*, 77:40–49.

Moore, K. A., Wetzel, R. L., and Orth, R. J. (1997). Seasonal pulses of turbidity and their relations to eelgrass (zostera marina l.) survival in an estuary. *Journal of Experimental Marine Biology and Ecology*, 215(1):115–134.

Mudd, S. M., D'Alpaos, A., and Morris, J. T. (2010). How does vegetation affect sedimentation on tidal marshes? investigating particle capture and hydrodynamic controls on biologically mediated sedimentation. *Journal of Geophysical Research: Earth Surface*, 115(F3).

MURPHY, K., BROWN, W., and HEIMER, D. (2004). Acomprehensive look at the management of spartina in washington state. In *Conference on Invasive Spartina*.

Nehring, S. and Adsersen, H. (2006). Nobanis–invasive alien species fact sheet spartina anglica. *From: Online Database of the North European and Baltic Network on Invasive Alien Species–NOBANIS www. artportalen. se/nobanis, Date of access*, 3(02):2015.

Nicholas, A. P. (2013). Modelling the continuum of river channel patterns. *Earth Surface Processes and Landforms*, 38(10):1187–1196.

Olsen, J. L., Rouzé, P., Verhelst, B., Lin, Y.-C., Bayer, T., Collen, J., Dattolo, E., De Paoli, E., Dittami, S., Maumus, F., et al. (2016). The genome of the seagrass zostera marina reveals angiosperm adaptation to the sea. *Nature*, 530(7590):331–335.

Oorschot, M. v., Kleinhans, M., Geerling, G., and Middelkoop, H. (2015). Distinct patterns of interaction between vegetation and morphodynamics. *Earth Surface Processes and Landforms*.

Parker, G. (1979). Hydraulic geometry of active gravel rivers. *Journal of the Hydraulics Division*, 105(9):1185–1201.

Potter, I. C., Chuwen, B. M., Hoeksema, S. D., and Elliott, M. (2010). The concept of an estuary: a definition that incorporates systems which can become closed to the ocean and hypersaline. *Estuarine, Coastal and Shelf Science*, 87(3):497–500.

Pringle, A. (1993). Spartina anglica colonisation and physical effects in the tamar estuary, tasmania 1971-91. In *Papers and Proceedings of the Royal Society of Tasmania*, volume 127, pages 1–10.

Qin, L.-Z., Li, W.-T., Zhang, X., Zhang, P., and Qiao, W. (2016). Recovery of the eelgrass zostera marina following intense manila clam ruditapes philippinarum harvesting disturbance in china: The role and fate of seedlings. *Aquatic Botany*, 130:27–36.

Rand, T. A. (2000). Seed dispersal, habitat suitability and the distribution of halophytes across a salt marsh tidal gradient. *Journal of Ecology*, 88(4):608–621.

Reineck, H.-E. and Singh, I. B. (1980). Tidal flats. In *Depositional Sedimentary Environments*, pages 430–456. Springer.

Sand-Jensen, K., Pedersen, O., Binzer, T., and Borum, J. (2005). Contrasting oxygen dynamics in the freshwater isoetid lobelia dortmanna and the marine seagrass zostera marina. *Annals of Botany*, 96(4):613–623.

Schramkowski, G. P., Schuttelaars, H., and De Swart, H. E. (2004). Non-linear channel–shoal dynamics in long tidal embayments. *Ocean Dynamics*, 54(3-4):399–407.

Schuurman, F., Marra, W. A., and Kleinhans, M. G. (2013). Physics-based modeling of large braided sand-bed rivers: Bar pattern formation, dynamics, and sensitivity. *Journal of geophysical research: Earth Surface*, 118(4):2509–2527.

Schuurman, F., Shimizu, Y., Iwasaki, T., and Kleinhans, M. (2016). Dynamic meandering in response to upstream perturbations and floodplain formation. *Geomorphology*, 253:94–109.

Silvestri, S., Defina, A., and Marani, M. (2005). Tidal regime, salinity and salt marsh plant zonation. *Estuarine, coastal and shelf science*, 62(1):119–130.

Siniscalchi, F., Nikora, V. I., and Aberle, J. (2012). Plant patch hydrodynamics in streams: Mean flow, turbulence, and drag forces. *Water Resources Research*, 48(1).

Sloop, C. M., Ayres, D. R., and Strong, D. R. (2004). Invasive hybrid cordgrass (spartina alterniflora x foliosa) recruitment dynamics in open mudflats of san francisco bay. In *Conference on Invasive Spartina*.

Small, C. and Nicholls, R. J. (2003). A global analysis of human settlement in coastal zones. *Journal of Coastal Research*, pages 584–599.

Sparfel, L., Fichaut, B., and Suanez, S. (2005). Progression de la spartine (spartina alterniflora loisel) en rade de brest (finistère) entre 1952 et 2004: de la mesure à la réponse gestionnaire. *Norois. Environnement, aménagement, société*, (196):109–123.

Temmerman, S., Bouma, T., Van de Koppel, J., Van der Wal, D., De Vries, M., and Herman, P. (2007). Vegetation causes channel erosion in a tidal landscape. *Geology*, 35(7):631–634.

Thompson, J. D. (1991). The biology of an invasive plant. *Bioscience*, 41(6):393–401.

Ursino, N., Silvestri, S., and Marani, M. (2004). Subsurface flow and vegetation patterns in tidal environments. *Water Resources Research*, 40(5).

Van den Berg, J., Boersma, J., and Gelder, A. v. (2007). Diagnostic sedimentary structures of the fluvial-tidal transition zone–evidence from deposits of the rhine and meuse. *Netherlands Journal of Geosciences/Geologie en Mijnbouw*, 86(3).

Van Katwijk, M. and Hermus, D. (2000). Effects of water dynamics on zostera marina: transplantation experiments in the intertidal dutch wadden sea. *Marine Ecology Progress Series*, 208:107–118.

Van Katwijk, M., Hermus, D., De Jong, D., Asmus, R., and De Jonge, V. (2000). Habitat suitability of the wadden sea for restoration of zostera marina beds. *Helgoland Marine Research*, 54(2):117.

Van Keulen, M., Paling, E. I., and Walker, C. (2003). Effect of planting unit size and sediment stabilization on seagrass transplants in western australia. *Restoration Ecology*, 11(1):50–55.

Van Ledden, M., Wang, Z.-B., Winterwerp, H., and De Vriend, H. (2004). Sand–mud morphodynamics in a short tidal basin. *Ocean Dynamics*, 54(3-4):385–391.

van Lent, F. and Verschuure, J. M. (1994). Intraspecific variability of zostera marina l.(eelgrass) in the estuaries and lagoons of the southwestern netherlands. i. population dynamics. *Aquatic botany*, 48(1):31–58.

van Maren, D. S., Winterwerp, J. C., and Vroom, J. (2015). Fine sediment transport into the hyper-turbid lower ems river: the role of channel deepening and sediment-induced drag reduction. *Ocean Dynamics*, 65(4):589–605.

van Schaik AWJ, d. J. D. and van der Pluijm AM (1988). Vegetatie buitendijkse gebieden westerschelde. Technical report.

van Veen, J., van der Spek, A. J., Stive, M. J., and Zitman, T. (2005). Ebb and flood channel systems in the netherlands tidal waters 1. *Journal of Coastal Research*, pages 1107–1120.

van Zuidam, B., van Geest, G., Harezlak, V., and Noordhuis, R. (2014). Update kennisregels voor lichtklimaat, waterplanten en mosselen.

Vaughan, I., Diamond, M., Gurnell, A., Hall, K., Jenkins, A., Milner, N., Naylor, L., Sear, D., Woodward, G., and Ormerod, S. (2009). Integrating ecology with hydromorphology: a priority for river science and management. *Aquatic Conservation: Marine and Freshwater Ecosystems*, 19(1):113–125.

Waterwatch New South Wales, NSW, A. G. (2010). *Waterwatch Estuary Guide*. Department of Environment, Climate Change and Water NSW.

Widdows, J., Pope, N. D., and Brinsley, M. D. (2008). Effect of spartina anglica stems on near-bed hydrodynamics, sediment erodability and morphological changes on an intertidal mudflat. *Marine Ecology Progress Series*, 362:45–57.

Wijgergangs, L. and de Jong, D. (1999). *Een ecologisch profiel van zeegras en de verspreiding in Nederland*. Katholieke Universiteit.

Wijgergans, L. and de Jong, D. (1999). Een ecologisch profiel van zeegras. *En de verspreiding in Nederland. Rapportage*.

Wolanski, E., Boorman, L., Chícharo, L., Langlois-Saliou, E., Lara, R., Plater, A., Uncles, R., and Zalewski, M. (2004). Ecohydrology as a new tool for sustainable management of estuaries and coastal waters. *Wetlands Ecology and Management*, 12(4):235–276.

Woodroffe, C., Chappell, J., Thom, B., and Wallensky, E. (1989). Depositional model of a macrotidal estuary and floodplain, south alligator river, northern australia. *Sedimentology*, 36(5):737–756.

Wright, L., Coleman, J. M., and Thom, B. G. (1973). Processes of channel development in a high-tide-range environment: Cambridge gulf-ord river delta, western australia. *The Journal of Geology*, pages 15–41.

Zaremba, K., McGowan, M., and Ayres, D. (2004). Spread of invasive spartina in the san francisco estuary. In *Conference on Invasive Spartina*.

Zong, L. and Nepf, H. (2011). Spatial distribution of deposition within a patch of vegetation. *Water Resources Research*, 47(3).

Appendices

A Model recommendations

1. The river overflows its boundaries in the simulation without mud or vegetation on a different bathymetry when the matlab model is used (#11). When this simulation is run solely through Delft3D (which should be the exact same simulation) this does not happen. Apparently there is a problem with the river boundary in the simulations with matlab. This might be a problem with the way matlab handles the *bct file.

2. Changing hydrodynamics are essential to create truly dynamic vegetation development, which were not modelled now. The problem with multiple tidal components is that these are usually defined as a harmonic which is restarted every time the model is restarted (which is every 12 hours due to the vegetation model) because of this tidal periods longer than 12 hours cannot be defined as a harmonic. A water level or Neumann boundary could, however, be defined as a timeseries instead of harmonic or astronomic which does not have this problem.

3. The mortality is right now calculated as a fraction of the defined colonization density. This is done to avoid small concentrations of vegetation in cells which do not die. A better system would be to empty cells if their vegetation cover falls below a certain percentage of the colonization density. The current system does not work properly with small colonization densities. Think of a 5% colonization density: if plants colonize a tranquil area for several years covers can easily go up to 50%, afterwards it will take at least 10 years to empty the cell again once the cell becomes subject to significant stress.

4. The maximum inundation time of grown *Spartina* is 9 hours. Information on its maximum inundation time as a seedling was not found, but this is very important information for its zonation.

5. A colonization method should be developed which takes into account that *Zostera* and *Spartina* spread predominantly to neighbour areas. Also the assumption that all cells which are flooded end up with seedlings gives much more aggressive colonization results in estuaries than in rivers and is therefore not sufficient.

6. The discrepancy between the growth and mortality timescale in the model gives significant errors due to the eco-engineering effect of especially *Zostera*. When *Zostera* is supposed to die it will continue to grow till the end of the year and continue to decrease flow velocities and enhance light availability. These timescales should, therefore become the same.

B Delft3D files

*MDF file

```
Ident = #Delft3D-FLOW 3.56.29165#
Commnt =
Runtxt = #simplified estuary#
Filcco = #matlabgrid.grd#
Anglat = 0.0000000e+000
Grdang = 0.0000000e+000
Filgrd = #run1.enc#
MNKmax = 290 162 1
Thick = 1.0000000e+002
Commnt =
Fildep = #run1.dep#
Commnt =
Commnt = no. dry points: 0
Commnt = no. thin dams: 0
Commnt =
Itdate = #2000-01-01#
Tunit = #M#
Tstart = 0.0000000e+000
Tstop = 2.629440e+006
Dt = 0.2
Tzone = 0
Commnt =
Sub1 = # I#
Sub2 = # C #
Namc1 = #Sediment1 #
Namc2 = #Sediment2 #
Namc3 = #Sediment3 #
Commnt =
Wnsvwp = #N#
Wndint = #Y#
Commnt =
Filic = #matlabwl.ini#
Commnt =
Commnt = no. open boundaries: 6
Filbnd = #run1.bnd#
FilbcH = #run1.bch#
FilbcT = #run1.bct#
FilbcC = #run1.bcc#
Rettis = 0.0000000e+000
     0.0000000e+000
     0.0000000e+000
     0.0000000e+000
     0.0000000e+000
     0.0000000e+000
Rettib = 0.0000000e+000
     0.0000000e+000
```

```
    0.0000000e+000
    0.0000000e+000
    0.0000000e+000
    0.0000000e+000
Commnt =
Ag = 9.8100000e+000
Rhow = 1.0000000e+003
Tempw = 1.5000000e+001
Salw = 3.1000000e+001
Wstres = 6.30e-004      0.00e+000      7.23e-003      1.00e+002      7.23e-003      1.00e+002
Rhoa = 1.0000000e+000
Betac = 5.0000000e-001
Equili = #N#
Ktemp = 0
Fclou = 0.0000000e+000
Sarea = 0.0000000e+000
Temint = #Y#
Commnt =
Roumet = #C#
Ccofu = 5.0000000e+001
Ccofv = 5.0000000e+001
Xlo = 0.0000000e+000
Vicouv = 1.0000000e+000
Dicouv = 1.0000000e+001
Htur2d = #N#
Irov = 0
Filsed = #run1.sed#
Filmor = #run1.mor#
Commnt =
Iter = 2
Dryflp = #YES#
Dpsopt = #MAX#
Dpuopt = #MOR#
Dryflc = 8.0000000e-002
Dco = -9.9900000e+002
Tlfsmo = 0.0000000e+000
ThetQH = 0.0000000e+000
Forfuv = #Y#
Forfww = #Y#
Sigcor = #N#
Trasol = #Cyclic-method#
Momsol = #Cyclic#
Commnt =
Commnt = no. discharges: 0
Commnt = no. observation points: 11
Filsta = #run1.obs#
Commnt = no. drogues: 0
Commnt =
Commnt =
Commnt = no. cross sections: 16
```

```
Filcrs = #run1.crs#
Commnt =
SMhydr = #YYYYY#
SMderv = #YYYYYY#
SMproc = #YYYYYYYYYY#
PMhydr = #YYYYYY#
PMderv = #YYY#
PMproc = #YYYYYYYYYY#
SHhydr = #YYYY#
SHderv = #YYYYY#
SHproc = #YYYYYYYYYY#
SHflux = #YYYY#
PHhydr = #YYYYYY#
PHderv = #YYY#
PHproc = #YYYYYYYYYY#
PHflux = #YYYY#
Flmap = 0.0000000e+000      60      2.6251200e+006
Flhis = 0.0000000e+000      10      5.2720320e+006
Flpp = 0.0000000e+000       0       2.6251200e+006
Flrst = 1440
Commnt =
Online = #N#
trafrm = #eh.tra#
Trtrou = #Y#
Trtdef = #veg.trd#
Trtu = #veg.trv#
trtv = #veg.trv#
Chezy = #Y#
PmCrit = 0.4
Commnt =
```

*MOR file

[*MorphologyFileInformation*]
FileCreatedBy = Delft3D FLOW-GUI, Version: 3.56.29165
FileCreationDate = Thu Aug 11 2016, 09:39:15
FileVersion = 02.00
[*Morphology*]
EpsPar = false
IopKCW = 1
RDC = 0.01
RDW = 0.02
MorFac = 3.0000000e+001 [−]
MorStt = 1.4400000e+004 [*min*]
Thresh = 5.0000000e-002 [*m*]
MorUpd = true
EqmBc = true
DensIn = false
AksFac = 1.0000000e+000 [−]
RWave = 2.0000000e+000 [−]
AlfaBs = 1.0000000e+000 [−]
AlfaBn = 1.5000000e+000 [−]
Sus = 1.0000000e+000 [−]
Bed = 1.0000000e+000 [−]
SusW = 1.0000000e+000 [−]
BedW = 1.0000000e+000 [−]
SedThr = 5.0000000e-002 [*m*]
ThetSD = 5.0000000e-001 [−]
HMaxTH = 0.0000000e+000 [*m*]
FWFac = 1.0000000e+000 [−]
Espir = 1
ISlope = 3
AShld = 0.2
BShld = 0.5
[*Underlayer*]
IUnderLyR = 2
ExchLyr = false
TTLForm = 1
ThTrLyr = 0.1
NLaLyr = 0
NEuLyr = 50
ThLaLyr = 0.1
ThEuLyr = 0.1
IniComp = morlyr.inb
IDiffusion = 0
Flufflyr = 0
[*Output*]
Frac = true
AverageAtEachOutputTime= true

*SED file

Pmcrit = 0.4
[*SedimentFileInformation*]
FileCreatedBy = Delft3D FLOW-GUI, Version: 3.56.29165
FileCreationDate = Mon Feb 16 2015, 12:34:16
FileVersion = 02.00
[*SedimentOverall*]
Cref = 1.6000000e+003 [$kg/m3$]
IopSus = 0
[*Sediment*]
Name = #Sediment1#
SedTyp = sand
RhoSol = 2.6500000e+003 [$kg/m3$]
SedDia = 3.0000000e-004 [m]
CDryB = 1.6000000e+003 [$kg/m3$]
IniSedThick = 1.5000000e+001 [m]
FacDSS = 1.0000000e+000 [$-$]
[*Sediment*]
Name = #Sediment2#
SedTyp = mud
RhoSol = 2.6500000e+003 [$kg/m3$]
SalMax = 0.0000000e+000 [ppt]
WS0 = 2.5000000e-004 [m/s]
WSM = 2.5000000e-004 [m/s]
TcrSed = 1.0000000e+003 [$N/m2$]
TcrEro = 2.0000000e-001 [$N/m2$]
EroPar = 1.0000000e-004 [$kg/m2/s$]
CDryB = 1.6000000e+003 [$kg/m3$]
IniSedThick = 5.0000001e-002 [m]
FacDSS = 1.0000000e+000 [$-$]
[*Sediment*]
Name = #Sediment3#
SedTyp = mud
RhoSol = 2.6500000e+003 [$kg/m3$]
SalMax = 0.0000000e+000 [ppt]
WS0 = 2.5000000e-004 [m/s]
WSM = 2.5000000e-004 [m/s]
TcrSed = 1.0000000e+003 [$N/m2$]
TcrEro = 2.0000000e-001 [$N/m2$]
EroPar = 1.0000000e-004 [$kg/m2/s$]
CDryB = 1.6000000e+003 [$kg/m3$]
IniSedThick = 5.0000001e-002 [m]
FacDSS = 1.0000000e+000 [$-$]